

December 2014

# Modification of Pyrimidine and Purine Nucleotides By "Click" Chemistry: Design, Synthesis and Properties Study

Mohammad Mojibul Haque  
*University of Wisconsin-Milwaukee*

Follow this and additional works at: <https://dc.uwm.edu/etd>

 Part of the [Chemistry Commons](#)

---

## Recommended Citation

Haque, Mohammad Mojibul, "Modification of Pyrimidine and Purine Nucleotides By "Click" Chemistry: Design, Synthesis and Properties Study" (2014). *Theses and Dissertations*. 609.  
<https://dc.uwm.edu/etd/609>

This Dissertation is brought to you for free and open access by UWM Digital Commons. It has been accepted for inclusion in Theses and Dissertations by an authorized administrator of UWM Digital Commons. For more information, please contact [open-access@uwm.edu](mailto:open-access@uwm.edu).

MODIFICATION OF PYRIMIDINE AND PURINE NUCLEOTIDES BY “CLICK” CHEMISTRY:  
DESIGN, SYNTHESIS AND PROPERTIES STUDY

By

Mohammad Mojobul Haque

A Dissertation Submitted in  
Partial Fulfillment of the  
Requirements for the Degree of

Doctor of Philosophy

in Chemistry

at

The University of Wisconsin-Milwaukee

December 2014

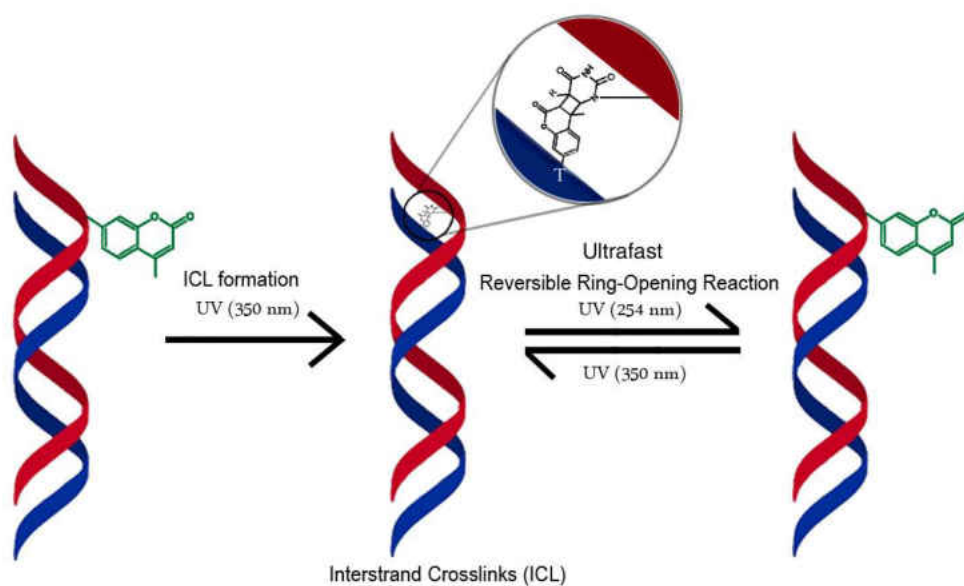
## ABSTRACT

### MODIFICATION OF PYRIMIDINE AND PURINE NUCLEOTIDES BY “CLICK” CHEMISTRY: DESIGN, SYNTHESIS AND PROPERTIES STUDY

By

Mohammad Mojibul Haque

The University of Wisconsin-Milwaukee, 2014  
Under the Supervision of Professor Xiaohua Peng



This dissertation consists of three main parts, totaling five chapters, and focuses on developing novel nucleosides via “click” chemistry and studying their potential biological

properties. Chapter three describes the synthesis and properties of coumarin-modified fluorescent DNAs. Coumarin-modified 2'-deoxythymidine was synthesized via "click" chemistry and incorporated into oligodeoxynucleotides (ODNs) which induce photoreversible interstrand cross-link (ICL) upon 350/254 nm photoirradiation. The irradiation at 350 nm induces DNA cross-linking with ODNs containing coumarin. The cross-linked DNA products formed from coumarin are not fluorescent. Further investigation showed that coumarin moiety undergoes the  $(2\pi+2\pi)$  photocycloaddition with 2'-deoxythymidine (dT), 2'-deoxycytidine (dC), and to a much lower extent, 2'-deoxyadenine (dA). As an additional ability, ICL material was observed to be reverted to their original single stranded ODN by a ring-opening reaction upon irradiation at 254 nm without the addition of any chemical reagents. After the successful discovery of the photo-reversible DNA cross-linking ability of coumarin-modified dT, coumarin was conjugated to dA and dC to examine the generality of this phenomena. This part is discussed in chapter four. In the fifth chapter, triazole- and phenyltriazole-modified dT were synthesized and incorporated into ODNs by solid phase DNA synthesis. Similar to the canonical nucleosides, the modified nucleoside scaffolds maintain Watson-Crick hydrogen bonding formation. The physico-chemical and biological properties of triazole-containing ODN duplexes were investigated.

To  
the people who work for truth  
and  
who struggle for their rights

## TABLE OF CONTENTS

CHAPTER	PAGE
1. Introduction.....	1
1.1. Modification in Base Parts.....	1
1.2. Modification ODN Analogs.....	6
1.3. Click Chemistry.....	9
1.4. DNA Interstrand Cross-Link(ICL).....	11
2. Subject of the Work.....	14
2.1. Photo-Switchable DNA Interstrand Cross-Link(ICL) Formation by Coumarin-Modified 2'-Deoxythymidine(dT).....	14
2.2. Synthesis of Coumarin-Modified 2'-Deoxycytosine(dC) and 2'- Deoxyadenosine(dA) by "Click" Chemistry.....	17
2.3. Modified 2'-Deoxythymidine(dT) and Oligodeoxynucleotide(ODN) Containing Triazole-and Phenyl-triazole; Synthesis and Properties.....	18
3. Photo-Switchable DNA Interstrand Cross-Link(ICL) Formation by Coumarin-Modified 2'-Deoxythymidine(dT).....	21
3.1. Background.....	21
3.2. Results and Discussion.....	26
3.2.1. Synthesis of Coumarin-Modified dT (1).....	26
3.2.2. Synthesis of the Phosphoramidite Derived from 1.....	27
3.2.3. Coumarin-Modified Derivatives of dT and Anticancer Activity Test.....	27
3.2.4. Bio-physical Properties Study of 1 in OBNs.....	29
3.2.4.1. Synthesis of Modified ODNs (7a-15a) Containing1.....	29
3.2.4.2. Coumarin-Induced ICL Formation and Analysis.....	36
3.2.4.3. Sequence Effect on Coumarin-Induced ICL.....	37
3.2.4.4. Properties Study of Coumarin-Induced ICL.....	39
3.2.5. Determination of ICL Site.....	41
3.2.5.1. Hydroxy Radical Cleavage Reaction for ICL Site Determination.....	44
3.2.5.2. LC-MS Analysis for Determining ICL Site via Enzymatic Digestion.....	45
3.2.6. Selected-ion Chromatogram (SIC) Analysis for ICL Structure Determination.....	45
3.2.7. Kinetic Study of ICL.....	47
3.2.8. Photocleavage Reaction of ICL Materials.....	49
3.2.9. Multiple Cycles Photoreversibility Test of Coumarin-Induced ICL.....	51
3.2.10. Kinetic Study of Photolytic Cleavage for ICL Materials.....	59
3.3. Experimental Parts.....	66

4. Synthesis of Coumarin-Modified 2'-Deoxycytosine(dC) and 2'-Deoxyadenosine(dA) by "Click" Chemistry.....	74
4.1. Background.....	74
4.2. Results and Discussion.....	75
4.2.1. Synthesis of Coumarin-Containing dA (10).....	75
4.2.2. Synthesis of Coumarin-Containing dC (11).....	79
4.3. Experimental Parts.....	80
5. Modified 2' Deoxythymidine (dT) and Oligadeoxynucleotide (ODN) Containing Triazole and Phenyltriazole: Synthesis and properties.....	86
5.1. Background.....	86
5.2. Results and Discussion.....	87
5.2.1. Synthesis of Triazole-Conjugated dT (5).....	87
5.2.2. Modification ODN Containing 5: Synthesis and Properties.....	89
5.2.2.1. Synthesis of Modified ODN Containing 5.....	89
5.2.2.2. ICL Study with Triazole-Modified dT.....	90
5.2.3. Synthesis Of Phenyltriazole Conjugated dT (6).....	92
5.2.4. Modified ODN Containing 6: Synthesis and Properties.....	93
5.2.4.1. Synthesis of Modified ODN Containing 6.....	93
5.2.4.2. ICL Study with Phenyltriazole Modified dT.....	94
5.2.5. Melting Temperature ( $t_m$ ) Study of Modified ODNs.....	95
5.3. Experimental Parts.....	96
6. References.....	144
7. List of Publications.....	155
8. Curriculum vitae.....	156

Attached manuscripts

## LIST OF FIGURES

Figure 1:	The monomeric unit of ODN .....	1
Figure 2:	Complementary base pairs. dR= deoxyribose.....	2
Figure 3:	Comparison of wavelengths and quantum yields.....	3
Figure 4:	Photoadduct formation of psoralen under UVA-irradiation.....	23
Figure 5:	The structure of ODN single strands and ICL .....	25
Figure 6:	UV emission spectra of ODN 6a and ODN <b>7a</b> .....	33
Figure 7:	PAGE analysis of ICL formation for ODN duplex-6 and duplex <b>7</b> .....	37
Figure 8:	PAGE analysis of ICL formation for duplexes <b>6-11</b> .....	38
Figure 9:	PAGE analysis of ICL formation for duplexes <b>12-15</b> .....	39
Figure 10:	UV spectra of ODN <b>6a</b> , ODN <b>7a</b> , and ICL .....	40
Figure 11:	PAGE analysis of ICL materials after piperidine treatment.....	41
Figure 12:	Selectivity of ICL formation .....	41
Figure 13:	Hydroxy radical cleavage analysis for duplex <b>7</b> .....	43
Figure 14:	Histogram diagram of duplex <b>7</b> .....	44
Figure 15:	LC-MS spectra of dinucleosides from enzymatically digested ICL .....	45
Figure 16:	Fragmented ions of dT- <b>1</b> from enzymatically digested ICL .....	46
Figure 17:	Fragmented ions of dU- <b>1</b> from enzymatically digested ICL.....	47
Figure 18:	Kinetics of coumarin induced ICL growth.....	48
Figure 19:	PAGE analysis of photoreversible ICL reaction .....	50
Figure 20:	MALDI-TOF MS spectra of single stranded ODNs cleaved from ICL .....	51



Figure 21: PAGE analysis of multiple cycles ICL photoreversibility study for duplex <b>10</b> .....	52
Figure 22: PAGE analysis of multiple cycles ICL photoreversibility study for duplex <b>13</b> .....	54
Figure 23: PAGE analysis of multiple cycles ICL photoreversibility study for duplex <b>15</b> .....	55
Figure 24: PAGE analysis of multiple cycles ICL photoreversibility study for duplex <b>12</b> .....	57
Figure 25: The ratio of area of peaks for the fragmentations of ICL cleavage.....	68
Figure 26: PAGE analysis of photolytic cleavage of ICL from duplex <b>10</b> .....	60
Figure 27: Photolytic cleavage growth of ICL from duplex <b>10</b> .....	61
Figure 28: PAGE analysis of photolytic cleavage of ICL from duplex <b>13</b> .....	62
Figure 29: Photolytic cleavage growth of ICL from duplex <b>13</b> .....	63
Figure 30: PAGE analysis of photolytic cleavage of ICL from duplex <b>15</b> .....	64
Figure 31: Photolytic cleavage growth of ICL from duplex <b>15</b> .....	65
Figure 32: PAGE analysis of photolytic cleavage of ICL from duplex <b>12</b> .....	65
Figure 33: Photolytic cleavage growth of ICL from duplex <b>12</b> .....	65
Figure 34: Synthesis of coumarin modified dA .....	77
Figure 35: PAGE analysis of ICL formation for duplex 6 and duplex <b>20</b> .....	91
Figure 36: `PAGE analysis of ICL formation for duplex 6 and duplex <b>21</b> .....	94

## LIST OF TABLES

Table 1	List of coumarin modified ODNs; <b>1</b> = dT (Cm).....	30
Table 2	List of complementary strand ODNs .....	31
Table 3	MALDI-MS analysis of synthesized ODNs.....	33
Table 4	List of coumarin modified ODN duplexes.....	35
Table 5	Synthesized ODNs and duplexes .....	90
Table 6	Percentage of ICL formation under variable pH for duplex <b>20</b> .....	91
Table 7	Synthesized ODNs and duplexes .....	93
Table 8	Percentage of ICL formation under variable pH for duplex <b>21</b> .....	94
Table 9	Melting temperature (MT) study of modified ODN duplexes.....	96

## ACKNOWLEDGMENTS

All praise and thanks due to Allah, for giving me the strength and ability to complete this exceptionally solid research work. In particular, I would acknowledge the exemplary work and professionalism of Dr. Xiaohua Peng, an outstanding scholar and supervisor in her mentorship of these research projects. Dr. Peng has done great efforts to see that this project was a success. She generously shared her expertise with great effort and fostered in me a greater understanding to make this bio-organic research project successful. I am honored to have had the privilege to be encouraged and trained under her direction, which was invaluable, consistent, and caring during the last 5 years. I carry deep respect, admiration, and appreciation from the core of my heart for Dr. Peng.

Besides my advisor, I would like to thank the rest of my thesis committee: Professor Alexander A. Arnold, Professor M. Mahmud Hossain, Professor A. Andy Pacheco, and Professor Nicholas Silvaggi for their encouragement, insightful comments, and hard questions. What a joy and challenge it has been. I admire their talents and appreciate their generosity in sharing them. My sincere thanks also go to Dr. Yinsheng Wang from University of California Riverside for offering us such sincere collaboration opportunities and allowing me to lead one of the successful projects.

I thank my fellow lab mates in our Group: Wenbing Chen, Huabing Sun, Yibin Wang, Jayne Owens, Chay Yeo Tai, Bruce Lee, Colin Brook, and other members of the Peng group for their friendship and support. I also would like to express my gratitude to

the faculty members and staffs of the Department of Chemistry and Biochemistry at the University of Wisconsin-Milwaukee.

Last but not the least, I would like to thank my family for their constant encouragement and support especially my wife, I could not have accomplished my dream without her restless inspiration.

# Chapter 1

## Introduction

DNA is one of the most versatile molecules discovered to date. Current studies on the properties of modified DNAs showed that they led to many great discoveries in modern biological and medicinal field, such as new drug and biosensors discovery [1]. The DNA polymer consists of three components: (1) a pentose, (2) a nitrogenous base including purines and pyrimidines, and (3) a phosphodiester backbone (Figure 1). Modifications can be made to these three parts. The nitrogenous base moieties were selected in this research for modification with designed functional groups (Figure 1).

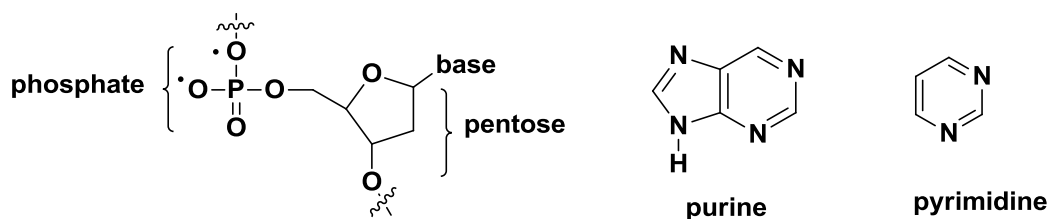


**Figure 1.** The monomeric unit of DNA

### 1.1 DNA Modification

In natural DNA, the 2'-deoxynucleotides are distinguished by the four nitrogen bases: the purines adenine (A) and guanine (G), and the pyrimidines cytosine (C) and thymine (T). These four nucleobases show specific base recognition by forming Watson-Crick base pair, namely A always pairing with T and C pairing with G (Figure 2). The 2'-deoxynucleosides themselves are responsible for holding the DNA duplex together by

forming hydrogen bonding and  $\pi$ - $\pi$  stacking. Hydrogen bonding interactions occur between complementary base pairs. dA forms a bidendate base pair with dT while dG forms a tridendate base pair with dC (Figure 2). The Watson-Crick base pair plays a critical role for the fidelity of DNA replication and transcription. Modification in the base moieties without affecting Watson-Crick base pair formation is highly important for maintaining their recognition property while also introducing new biological application.

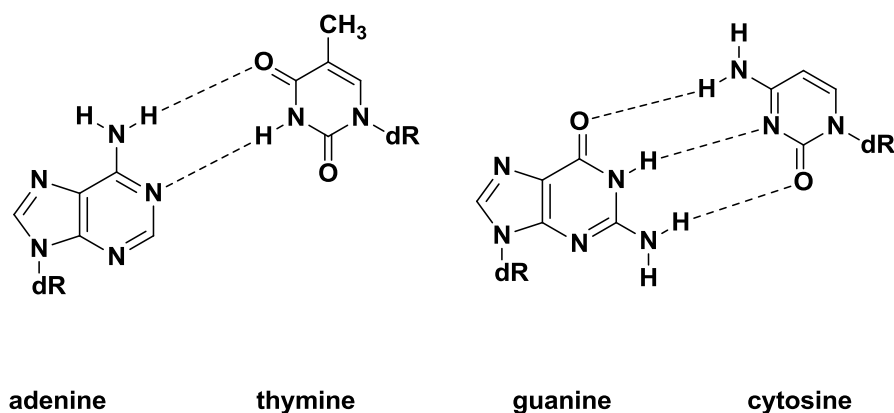


**Figure 2.** Complementary base pairs. dR= deoxyribose

Modifying the nucleobases of 2'-deoxynucleosides with heterocyclic molecules are incredibly important for biological and medicinal chemistry, which is the main focus of this research. Heterocyclic molecules have UV absorption at longer wavelengths than the natural nucleobase moieties, which is important to introduce new photophysical properties. For example, indole and benzoxazole both have longer wavelengths of absorption and significantly higher quantum yields than their purine counterparts (Figure 3). Therefore 2'-deoxynucleosides were expected to show the significant

photophysical properties after processing with heterocyclic molecules and other functional groups.

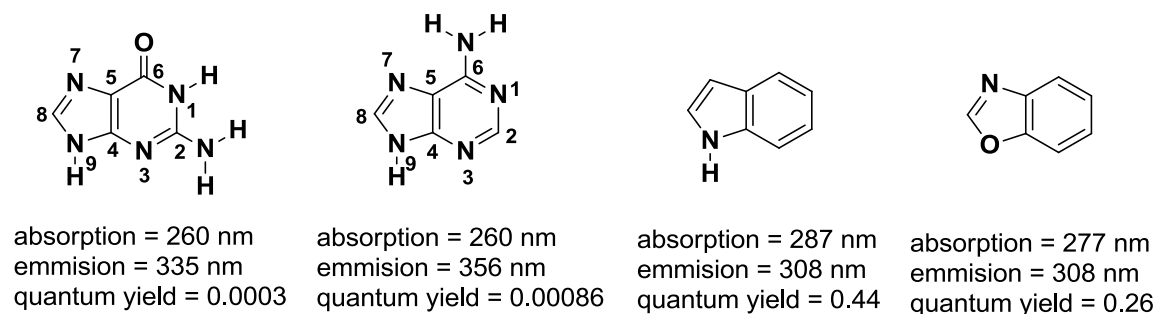


**Figure 3** Comparison of wavelengths and quantum yields

On behalf of modifying nucleotides and studying their photophysical properties, the following characteristics represent the desired attributes of newly designed nucleosides: (a) an emission band in the visible range, (b) a high structural similarity to the native nucleobases to mimic their size and shape, as well as hybridization and recognition properties, (c) the ability to form Watson-Crick base pairs and recognition properties and Hoogsteen face (a heteroatom at the position equivalent to the N7 position of the purines) should preferably be present for purine analogs, (d) absorption spectrum with minimal overlap with the absorption spectrum of the natural bases, (e) a respectable emission quantum efficiency.

In the past few decades, considerable advances have been made in the field of synthetically modified nucleosides and nucleotides depending on the type and nature of the functional group. The modification on nucleobase moieties plays a significant role

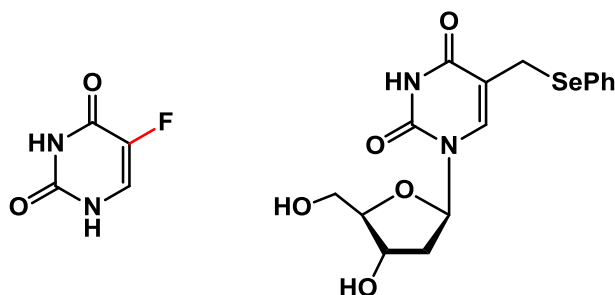
on several important cellular processes surrounding the DNA such as replication, transcription, and translation [2]. These modified nucleosides have been incorporated into oligodeoxynucleotides (ODNs). Several routes are potential for the modifications at the base unit of purine and pyrimidine including base substitution in which a designed functional group replaces the heterocycle of nucleoside analogs and extended base analogs in which a new functional group is attached through a linker to the heterocycle. Among those various processes, extending the conjugation of nucleotides with a naturally occurring heterocycle [3] has many valuable interactions and is an important tool for the study of the chemical reactivity and function of DNA and expanding its biological application.

Nucleotides could be modified within the sugar moiety, phosphodiester backbone, and in the nucleobase in presynthetic modification. Altering at the 2' or 3' position of sugar unit is a viable option for the multipurpose study and these modified analogs are more closely mimic the behavior of their parent nucleotides than do pyrimidine and purine modified analogs. Hiratsuka and Uchida were the first to introduce a sugar-modified nucleotide, 2',3'-O-2,4,6-trinitrocyclohexadienylidene, which exists as an equilibrium mixture depending on the pH of the solution [4]. Hiratsuka then introduced the 2',3'-O-anthraniloyl and 2',3'-O-methylantraniloyl derivatives. In addition, base modification is also significant as it could be presynthetic and postsynthetic. Presynthetic modification in base moieties has a wide variety of application such as DNA functionalization [5] and DNA methylation that involves the addition of a methyl group to different nucleotides by methyl transferase (MTase) [6].



DNA methylation is essential for growth and development for gene expression in plants [7-10].

Modification at the 5-position of thymidine is particularly important because it leads to distinctive application in nucleic acid. For example, 5-fluorouracil has been used for cancer treatment by inhibiting the synthesis of 2'-deoxythymidine because the carbon-fluorine bond is extremely stable and prevents the addition of a methyl group in the 5-position. The failure to synthesize the thymidine nucleotide results in little or no production of DNA. Another example of 5-position modification is phenylselenenyl-substituted derivatives of dT that produces interstrand cross-links in duplex DNA when oxidized by  $\text{NaIO}_4$  [11].

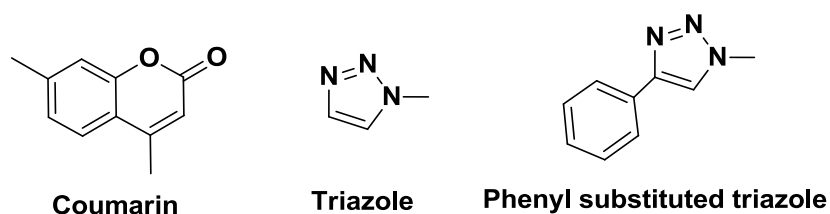


**Scheme 1.** Modification of ODN nucleotides at the 5-position of thymine.

Based on these criteria, we sought to design and synthesize novel nucleosides where different functional groups or heterocycles are conjugated with nucleosides at the 5-position of pyrimidines or 6-position of purines, incorporate them into ODNs, and study their photophysical behavior within an oligomeric duplex.

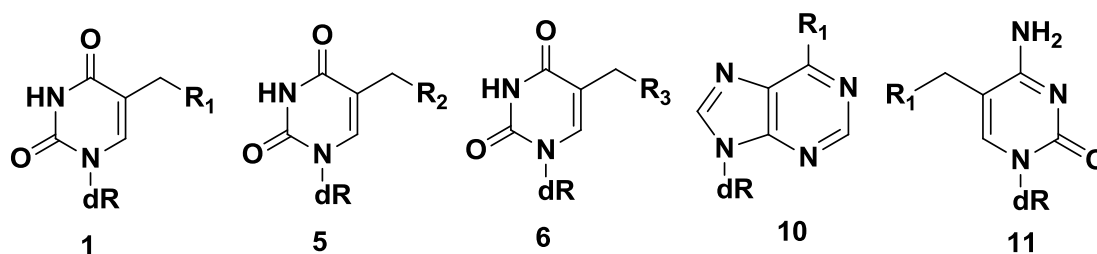
## 1.2 Modified ODN Analogs

Among the great varieties of heterocyclic molecules, coumarin, triazole, and phenyl-triazole are chosen to conjugate with 2'-deoxynucleosides (Scheme 2). Coumarins comprise a very large class of compounds among the plant kingdom [12-14], with a wide range of responses and sensitive detection for cysteine (Cys) over homocysteine (Hcy) and glutathione (GSH) [15], unique photophysical, and spectroscopic properties. It has also been used quite effectively as a probe of the physical, structural, and chemical properties of a wide range of heterogeneous host systems. Another aspect of coumarin being chosen is that coumarin and its derivatives show sufficient fluorescence in the visible light range to be used in laser dyes and organic light-emitting diodes (LEDs) [16-20]. It shows fluorescence and phosphorescence spectra when irradiated at 320 nm. Researchers have studied the photophysics of coumarin compounds since the 1940s due in part to the tunability of their absorbance and fluorescence [21-28]. Fluorescence-based methods have become instrumental in advancing high throughput screening techniques, particularly in the context of drug discovery [29]. The ideal fluorophore would display, for example, the shifting wavelength of absorbance, emission, or excitation upon changes in its physical environment.



**Scheme 2.** Selected heterocyclic molecules for ODNmodification.

Coumarin interaction in DNA is very much significant because coumarin-induced spectroscopic methods have been used to characterize the DNA and helps to analyze the information and their mechanisms in a very effective way when a coumarin-probe is incorporated into DNA at a specific site [30, 31]. For example, coumarin-modified 2'-deoxynucleoside analogs are powerful tools for the investigation of nucleic acid structure if they are sensitive to their local environment, demonstrating changes in the fluorescent properties when induced by changes in polarity or pH. The applications of coumarin in the field of nucleic acid research are also significant. The important applications are DNA detection [32], producing fluorescence-labelled DNA nucleosides [33], and functionalization of DNA with coumarin [34]. They maintain the hybridization properties of the parent nucleosides. In this research, coumarin and other heterocyclic groups are introduced to nucleobase analogs through a triazole linker (Scheme 3).



**R<sub>1</sub>, R<sub>2</sub>, and R<sub>3</sub> = various substituents and dR= deoxyribose**

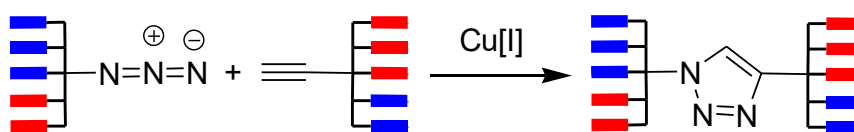
**Scheme 3.** Modified 2'-deoxynucleoside analogues (dR= deoxyribose)

Nowdays, photo-switchable compounds are becoming increasingly popular for a series of biological applications based on the reversible photo-control of structure and function of biomolecules. The biological activities of those compounds are altered by light-triggering [35]. Among the many applications of photo-switchable compounds, biocatalysis [36, 37], ion transport [38, 39], cell adhesion [40], and protein folding [41, 42] are vital. For instance chemical modification of nucleotides, peptides, proteins, and lipids with azobenzenes have been investigated as photo-switchable chromophores [43, 44]. Photoactivity of coumarin has also been the great interest for the researcher. For example, it was discovered by Ciamician and Silber in 1902 that coumarin significantly undergoes photodimerization under sunlight [45]. Coumarin dimer forms via the  $[2\pi s+2\pi s]$  cycloaddition of a cyclobutane ring under different reaction conditions by photoirradiation. However, photoactivity of coumarin in DNA is still unknown. Thus, we developed a strategy for the incorporation of coumarin into ODN and studied the photo-physical activity of coumarin-incorporated DNA.

Triazoles belong to a class of compounds called azoles. Five-membered aromatic ring azoles contain one nitrogen atom and any other heteroatoms of nitrogen, sulfur, or oxygen. Its continued use is increasing exponentially due to its reliability, non-toxicity, water solubility, regiospecificity, readily available starting materials as well as a tolerance to a wide variety of functional groups [46]. Triazoles have a versatile impact on industrial research and production such as hydraulic fluids, agrochemicals (fungicides), photochemical products [47, 48], and drug discovery research such as being used as reducing tumor cell proliferation drugs for cancer treatment [49].

### 1.3 “Click” Chemistry

“Click” chemistry was employed to conjugate selected compounds with nucleosides (Scheme 4). This method was first introduced by Barry Sharpless in 1999 at the 217<sup>th</sup> American Chemical Society annual meeting. Since then, it has been widely used for being both versatile and inexpensive [50, 51]. This reaction is more commonly known as a 1,3-dipolar cycloaddition [52, 53]; two  $\pi$ -electrons are supplied by the alkyne and four are supplied by the dipolar compound. Since this method forms a cyclic triazole (Scheme 4) from an alkyne and an azide, this type of reaction was classified as a Copper-(I) catalyzed Azide-Alkyne Cycloaddition (CuAAC) [54]. This is the most prominent example of “click” chemistry [55, 56] and takes place with a wide variety of conditions and works efficiently in many organic solvents as well as aqueous media to generate a stable, stereospecific, and easily purified product.



**Scheme 4.** Cu[I]-catalyzed azides-alkynes cycloadditions (CuAAC)

This reaction is clean, fast, high-yielding, bioorthogonal, and highly tolerant of a variety of functional group. That is why “click” chemistry has been significant in its application to the nucleic acid field and is a powerful tool for DNA modification by promoting the ability for researchers to incorporate the procedure into biological systems.

The modified ODN products are very stable under these reaction conditions due to the formation of a fairly rigid triazole linker. “Click” reaction is very useful for the labeling of ODN with fluorophores [57-59] under mild conditions which has wide application in the emerging field of cell biology and functional proteomics.

In addition to fluorophore labeling of DNA, the “click” reaction has been widely applied for preparing various functionalized ODNs, such as dumbbell ODNs, small-molecule DNA hybrids, and other modified ODNs [60-63]. This strategy uses the stable and easily prepared ODN precursors for preparing Dumbbell ODNs with an extra functional group, which enables us to functionalize DNA and RNA with appropriate properties for development of ODN therapeutics. Among the many other applications; DNA conjugation [64, 65], DNA nanomaterials, drug discovery], labeling [66, 67], ligation [68, 69], cross-linking [70, 71], and the formation of triplex are magnificent.

#### 1.4 DNA Interstrand Cross-link (ICL)

The separation of the two strands of a DNA double helix is essential for cellular processes such as replication and transcription. ICLs are formed by covalently linking two DNA complementary strands together, physically preventing the double helix from opening, which can block DNA replication and transcription therefore leading to DNA mutations and/or cell death. Certain agents including bifunctional alkylating agents, platinum compounds, and psoralen can produce covalent adducts with DNA bases on both strands of DNA, leading ultimately to the formation of ICLs. In general, small molecules and modified ODNs that cross-link DNA are potentially useful tools for mechanistic studies, in biotechnology applications [72-76], in therapeutic applications [77, 78]. In addition, chemical agents capable of inducing ICLs have been developed for many biological applications, such as for DNA damage and repair studies [79-83], for nucleic acid detection [84,85], for targeting telomeric G-quadruplex structures [86, 87], and most importantly for the construction of DNA nanomaterials [88] as DNA has the potential to be a remarkably useful technological material.

Typically manipulating DNA nanostructures is challenging, via external force and repeated thermal changes, to control the positioning of various nano-components with nanometre-scale precision. Cross-linking of DNA strands is effective to stabilize DNA nanostructures, because of the extremely tight space on the nanostructures where DNA strands are entangled tightly and intricately. DNA cross-linking has been demonstrated as a scaffold for the assembly of organic and inorganic nanomaterials [89-94] which

could play a significant role on the next-generation nanofabrication and can be used as a possible wire for transporting electrical signals [95]. DNA reveals excellent abilities for site-selective immobilization and ordering of metal nanoparticles in one to three dimensions [96-100]. DNA also can form complexes with functional nanomaterials by linking DNA with single-wall carbon nanotubes (SWCNTs), which can then be used as nanoscale electrical contacts for probing electron transport in DNA.

Several chemical methods have been developed for inducing ICL formation, such as photoirradiation, oxidation, reduction, fluoride induction, and  $H_2O_2$  induction [101]. Even though these conventional methods are effective for achieving ICL they are often difficult to control and typically employ chain-like reactions species such as radicals or cations because these reactions often require the use of an initiator and the addition of thermal energy to initiate ICL. Therefore photoirradiation was used to form ICL which was developed by Plambeck in the 1950's. Photoirradiation is a non-invasive method with high spatio-temporal resolution and offers the option of orthogonality. Most of the photoirradiated ICL materials could be cleaved to single strands with low wavelength UV light. Many modified nucleosides can induce DNA ICL formation upon photo irradiation, which has found wide applications in producing photoresists, printing plates, inks, coatings, adhesives, biological and biomedical applications. Photo-cross-linking is also applied in the fields of tissue engineering scaffolds and drug discovery.

Photo-cross-linking with coumarin does not involve any additional molecule because coumarin is first introduced into the DNA strand, and therefore it may be a promising method to tightly stabilize DNA nanostructures with small deformations.



Coumarin introduced in the modified ODN binds to an adjacent pyrimidine base in the complementary strand via 350 nm UV irradiation. When the bonding partner is a thymine base, the efficiency of photo-cross-linking with coumarin is considerably higher, about 87% in the various sequence sets. Thus, the DNA photo-cross-linking using coumarin has great potential for tightly stabilizing DNA nanostructures with high yield without large structural deformations.

The bases in a DNA duplex must have van der Waals interactions and the bonds involved must have molecular orbitals that overlap for the generation of ICL. Since all bases absorb specific UV light and ICL takes place under photolytic irradiation on functional subunits under native conditions, UV light induction was chosen for photo-crosslinking. The spectral properties of DNAs arise from the bases by absorbing UV light maximally around 260 nm. The absorption of a photon by the base causes them to enter an excited state which transforms the electronic structure and chemical properties and cause ICL of DNA bases to other nucleotides. Another important aspect of UV is under the low-intensity of UV irradiation conditions. The most common types of photoproducts formed are cyclobutane dimers and pyrimidine 4-6 dimers. The formation of cyclobutane dimer involves two covalent bonds between the C5 and C6 atoms of pyrimidines and between the N7 and C8 atoms of purines. In this research, switching wavelength UV photoirradiation was applied for the coumarin induced photo-reversible ICL study in DNA.

## Chapter 2

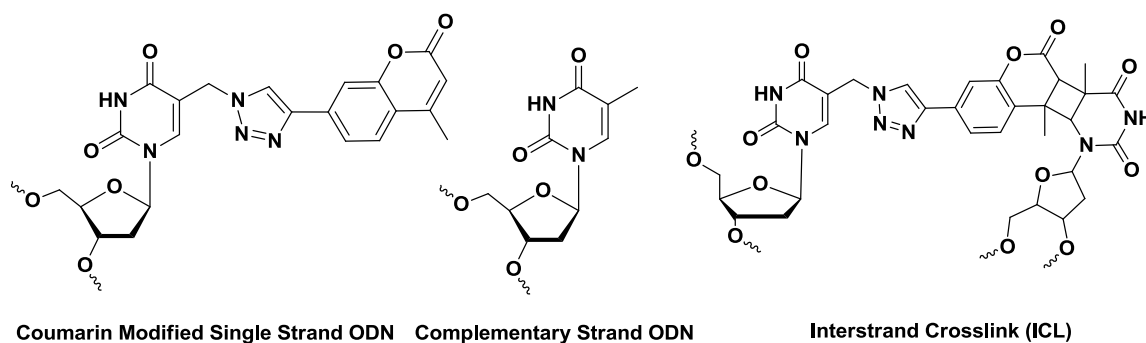
### Subject of the work

#### 2.1 Photo-Switchable DNA Interstrand Cross-Link (ICL) Formation by Coumarin-Modified 2'-Deoxythymidine (dT)

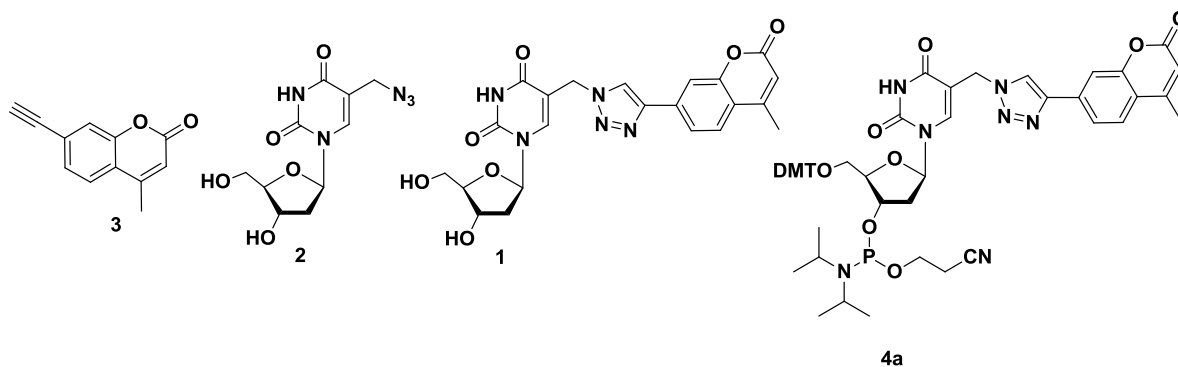
Photo-switchable compounds find many biological applications because of their photolytic reversibility of both structure and function. Coumarin derivatives show many advantages such as high fluorescence quantum yield, large Stokes shift, excellent photostability and low toxicity. They have been widely used in the fields of biology, medicine, and cosmetics. They have also been used as fluorescent chemosensors for DNA, RNA, and protein detection. However, there is no report about the photo reactivity of coumarin with DNA. Our attention was drawn to coumarin-DNA photo activity as this will provide new insights into the biochemical properties of coumarins and the possible toxicity. Based on the idea that if a compound absorbs at a higher energy then it will show emission and relaxation at a corresponding higher energy. We reasoned that because coumarin absorbs energy at a longer wavelength than ODN ( $\lambda_{\text{abs}} = 275 \text{ nm}$  and  $260 \text{ nm}$  respectively), it may exhibit emission at a longer wavelength than DNA. For this reason, coumarin-conjugated nucleosides were designed, incorporated into DNA and the photophysical properties were investigated upon UV irradiation. The primary focus of this chapter involves the study of coumarin's photoreactivity with DNA.

Coumarin-conjugated dT was synthesized and incorporated into ODN and its photophysical activity was studied. Coumarin-induced ICL was formed by UV irradiation

at 350 nm. The ICL site in coumarin-incorporated ODN was determined by hydroxyl radical cleavage of gel-purified ICL. LC-Mass study was employed followed by selected ion chromatogram of ICL materials to determine the structure of ICL. The coumarin-induced ICL significantly cleaves back to its original single strands by UV light irradiation at a lower wavelength. The  $^{32}\text{P}$ -ATP labelled ICL and single stranded ODNs were identified on the basis of their electrophoretic mobility in 20% denaturing PAGE.



The coumarin modified dT (**1**) was synthesized by “click” reaction between the azide-modified dT (**2**) and alkyne-modified coumarin (**3**) [66]. For solid phase synthesis of ODN containing **1**, the corresponding phosphoramidite **4a** was prepared. The 4, 4'-dimethoxytriphenylmethyl (DMT) residue was introduced for protecting 5'-OH functional group of compound **1**. The DMT-derivative was converted into the phosphoramidite **4a** with standard synthesis method.



In order to study the potential biological properties of coumarin and the effect of coumarin on DNA, a series of ODN (**6a-15a**) were synthesized by solid phase synthesis using the protocol of phosphoramidite chemistry. Complementary strands were also synthesized following the same procedure. The ODN duplexes were formed by hybridization between coumarin modified ODNs and the complementary strands. The ODN duplex was photo-irradiated at 350 nm for 50 minutes using a Rayonet Photochemical Chamber Reactor (Model RPR-100), thus forming an ICL. A wavelength of 350 nm was chosen because near-UV light (>300 nm) is compatible with living cells and is almost completely non-absorbed by most biological molecules with the exception of coumarin-modified ODNs. The specific wavelength was chosen because coumarin moiety excites to singlet and triplet excitation states upon irradiation with 350-nm UV light to form cyclobutane. Several duplexes of ODN were designed using coumarin-incorporated ODN with different opposing sequences and flanking sequences for broad analysis of both the ICL reaction site and possible mechanisms. Selectivity study and mass spectra analysis indicated that coumarin induced ICL formation via a  $(2\pi+2\pi)$  photodimerization reaction when irradiated in the Ultraviolet-A (UVA) region. To analyze

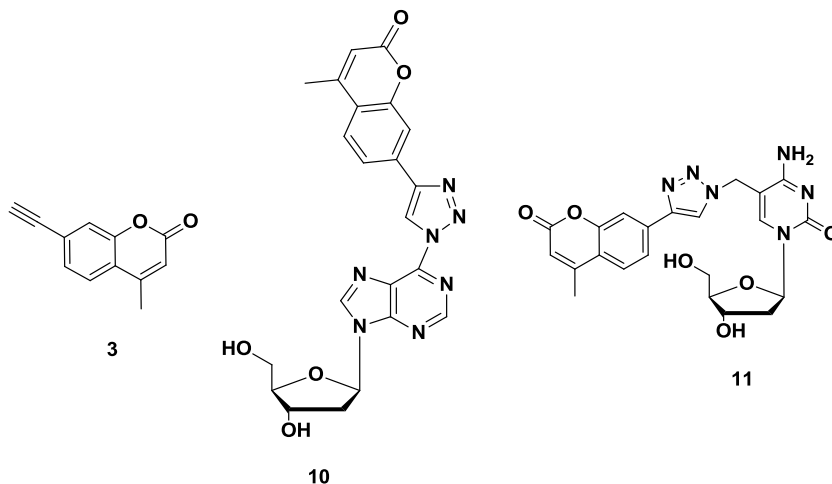
the photo-reversibility of ICL materials, the ICL materials were photoirradiated at a wavelength of 254 nm; the cyclobutane ring in ICL was cleaved and reverted to its initial single stranded ODN structures which were confirmed by MALDI-Mass analysis.

So far, neither unsubstituted nor substituted pyrimidines have ever been applied as components of coumarin photoswitches ICL. This feature would be one of the important milestones for the photo activity of DNA. Ten distinct complete cycles of photoreversible reaction were investigated to verify the ratification of this exceptional photoswitchability.

## **2.2 Synthesis of Coumarin-Modified 2'-Deoxycytosine (dC) and 2'-Deoxyadenosine (dA) by "Click" Chemistry**

Modified purine and pyrimidine nucleotides show distinct properties as active biological agents. Coumarins and their derivatives are of great interest in the field of medicinal chemistry due to widespread pharmacological properties of coumarin and the possibility to screen them as several novel therapeutic agents. Moreover, coumarin fluorescence can and has been proven as a tremendously effective probe of the physical, structural and chemical properties of a wide range of heterogeneous host systems including: molecular hosts, micelles, polymers, and porous, glassy, and crystalline solids. Potential ICL property of coumarin-modified pyrimidine which has recently been reported [102] and has been explained in the previous chapter of this thesis. In addition, coumarin-conjugated dT derivative **4** showed some anticancer activity from screening in 60 human cancer cell lines. Therefore, there is a certain need to expand the modification

of dA and dC with coumarin, which might result in important biomolecules with interesting biological properties and lead essential applications.



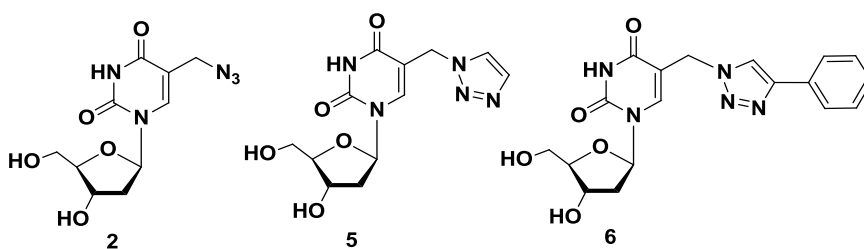
In order for conjugation of coumarin into dA and dC, Cu-mediated azide-alkyne “click” ligation was undertaken between alkyne modified coumarin **3** and azide modified dA and dC, leading to 6-(4-methylchromen-2-one-1,2,3-triazol-1-yl)-9-[2-deoxy-β-D-ribofuranosyl]adenosine (**10**) and 5-(4-methylchromen-2-one-1,2,3-triazol-1-yl)methyl-2'-deoxycytosine (**11**).

### 2.3 Modified 2'-Deoxythymidine (dT) and Oligodeoxynucleotide (ODN) Containing Triazole and Phenyl-triazole: Synthesis and Properties

Heterocyclic compounds have great importance in a wide variety of fields ranging from industrial to pharmaceutical chemistry. The ever-increasing demand for novel biologically active compound as well as widespread applications of 1,2,3-triazoles result in a continuous search for generating analogues of 1,2,3-triazoles. Considering the broad spectrum of activities that triazoles exhibit; 1,2,3-triazole and its substituted triazole conjugated dT were synthesized as well as their physico-chemical and biological

characteristics were examined. Conjugation of 1,2,3-triazole ( $pK_a = 9.3$ ) and phenyl substituted 1,2,3-triazole into dT ( $pK_a = 9.8$ ) moiety were performed through a few synthetic steps. 5-(1,2,3-Triazol-1-yl)methyl-2'-deoxyuridine (**5**) and 5-(4-phenyl-1,2,3-triazol-1-yl)methyl-2'-deoxyuridine (**6**) were easily obtained by using the copper-catalyzed alkyne-azide “click” cycloaddition reaction.

For solid phase synthesis of ODN containing **5** and **6**, the corresponding phosphoramidite **5d** and **6d** were prepared. The DMT residue was introduced in the 5'-OH function leading to the DMT derivatives (**5c** and **6c**), which were converted to the phosphoramidites (**5d** and **6d**). In order for further analysis of the effect of triazole and phenyl-triazole on DNA, ODN-**107** and ODN-**15** were synthesized by solid phase synthesis using standard phosphoramidite chemistry protocol. Complementary strands were also synthesized following the same procedure.



The modified ODN duplexes were found significantly stabilized with the replacement of triazole and phenyl-triazole at 5-position of dT. Stability of ODN duplex was enhanced by modified nucleosides in a basic medium with higher pH value. The strongest stacking and most pronounced positive influence on thermal stability was found for the dT analogue at pH 8.

ICL formation was analyzed with triazole and phenyl-triazole modified ODN duplexes **20** and **21** upon UV photo-irradiation at 350 nm for 2 hours. The details analysis of ICL reaction under different pH showed that the highest cross-linking yield was observed in acidic condition at lower pH values.



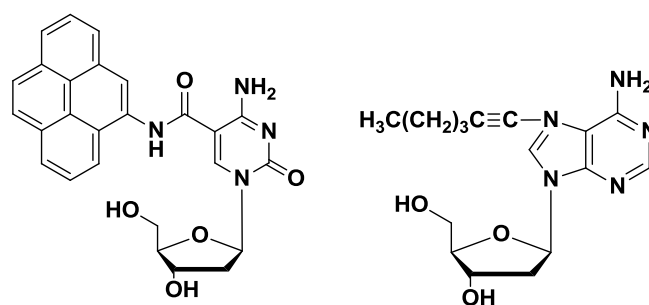
## Chapter 3

### Photo-Switchable DNA Interstrand Cross-Link (ICL) Formation by Coumarin-Modified 2'-Deoxythymidine (dT)

#### 3.1. Background

Coumarin and coumarin-related compounds come from a wide variety of natural sources. These have been used as medicines since ancient era in Egypt and many other fields [103-110]. They have shown a significant therapeutic potential for many years in chemical biology research including anti-tumour effects, disease prevention, growth modulation, and anti-oxidant properties. Coumarins are also highly researched today due to their physiological, pharmacological [111], anti-tumour activity [112] and exhibited cytotoxic activity [113] but they also deserve further study to produce successful outcomes.

In addition, the strongly fluorescent coumarin shows fluorescence and phosphorescence in the visible light range. Conjugation of fluorescent molecules to nucleosides is the great interest for nucleic acid chemistry. Netzel and coworkers utilized pyrene conjugates (Scheme 5) to study the redox processes in DNA oligomers and duplexes at specific base sites [114]. Seela and coworkers also reported enhanced fluorescent properties with an ethynyl linker at the 7-position of deaza-adenosine [115].



**Scheme 5.** Pyrene-extended dT and ethynyl-extended dA.

Modification of nucleosides in DNA are significantly important in nucleic acid chemistry research, for instance, modified nucleosides construct DNA-based reversible photoswitches and photo-manipulation of DNA. Photo-inducible quinone methide formation from biphenyl or binol quaternary ammonium salts was reported recently by Freccero, Zhou and their coworkers [116-118]. Quinone methides are highly reactive electrophiles which efficiently form ICL in DNA double stranded duplex. They also reported the formation of vinylidene-quinone methides from 2-alkynylphenols [119]. Psoralens are also an excellent group of naturally-occurring photoreactive products also known as “fuoro-coumarin,” which have been used as probes of nucleic acid structure and function. They have also been used for therapeutic gene modulation and the study of DNA damage and repair [120-122]. UVA-activated (320-400 nm) psoralen can effectively generate up to 40% ICL in duplex and triplex DNA [123] (Figure 4). The cytotoxic psoralen-induced ICLs induce unwinding of the DNA duplex and significantly block the replication and transcription to damage the cell.

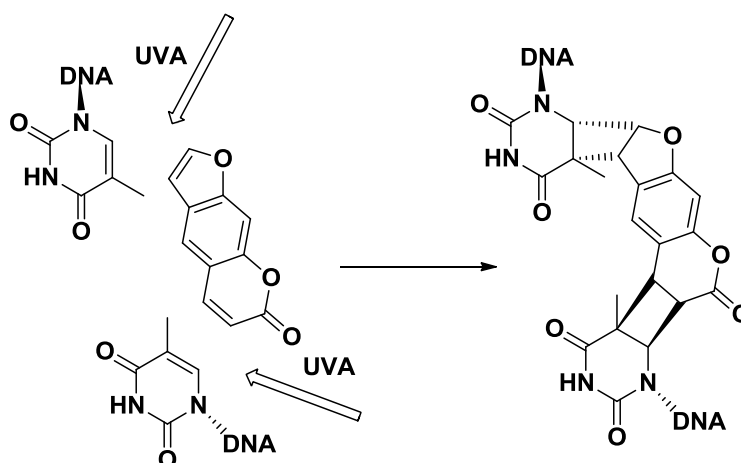
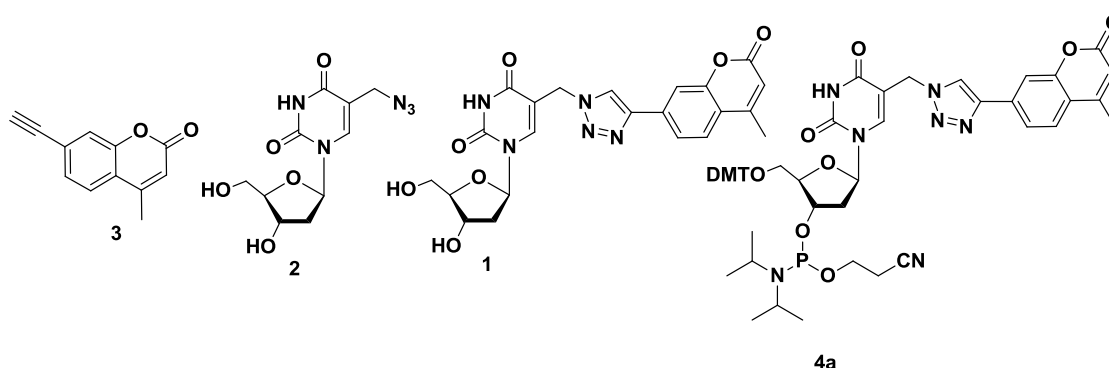


**Figure 4.** Photoadduct formation of psoralen under UVA-irradiation

Coumarin is structurally related to psoralen; only one furan ring addition to coumarin can form psoralen. Coumarin has excellent photostability and low toxicity, has been widely used in the fields of biology, medicine, cosmetics, and as fluorescent chemosensors for DNA, RNA, and protein detection [124, 125]. Photoactivity of coumarin is also significant, such as photodimerization of coumarin was discovered by Ciamician and Silber in 1902, in which sunlight was used to irradiate and synthesize dimerized coumarin product. Schenck and coworkers used  $^1\text{H}$  NMR spectroscopy to determine the structure of possible dimers that were produced from the irradiation of coumarin at different reaction conditions. In the 1970s, they concluded that the dimer was formed via the  $[2\pi\text{s}+2\pi\text{s}]$  cycloaddition formation of a cyclobutane ring. As far concerned, there is no report about the photo-physical activity of coumarin with DNA. Therefore, in order to determine the photo-physical properties of coumarins in DNA,

coumarin conjugated dT was designed and investigated for the first time photo-switchable ICL formation in DNA upon UVA irradiation.

In this project, coumarin was conjugated to dT by Cu-catalyzed azide-alkyne cycloaddition “click” reaction using azide-modified dT (**2**) and an alkyne-modified coumarin (**3**). Compound **1** was converted to its phosphoramidite building block **4a** (Scheme 6) under standard conditions after DMT residue was introduced in 5'OH function. ODNs containing **1** were synthesized via automated solid-phase synthesis using **4a** and their structure was confirmed by MALDI-TOF-MS analysis.



**Scheme 6.** The structure of coumarin-modified dT

In order to study the biological properties of coumarin and the effect of coumarin in DNA, a series of ODNs were synthesized using protocol of phosphoramidite chemistry by solid phase DNA synthesizer. Complementary strands were also synthesized following the same procedure. ODN duplex was formed by hybridization between coumarin modified ODN and complementary strands. ICL was formed by the photo-irradiation of ODN duplex at 350 nm for 50 min (Figure 5). Photo-irradiation was

employed which has several advantages over thermal or redox induced ICL formation procedure such as speed, low cost of materials and energy, and the ability to selectively cure systems as well as solvent-free formulations [126-133]. In addition, unlike many photo-initiated reactions these photo-crosslinking reactions via  $[2\pi+2\pi]$  cycloaddition do not suffer by oxygen inhibition. Broad analysis of ICL reaction was performed with different opposite sequences and flanking sequences effect for the determination of selectivity of ICL site. The ICL site in modified ODN was confirmed by hydroxyl radical cleavage experiment of gel-purified ICL. The structure of ICL was determined by LC-MS/MS analysis of selected-ion chromatogram (SIC). Further analysis showed that ICL materials were again photo-reversed to its initial single strands by UV-irradiation at 254 nm (Figure 5).

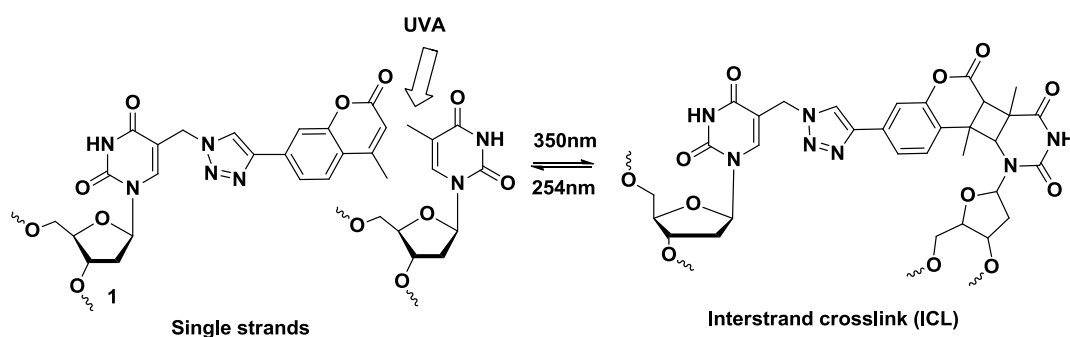


**Figure 5.** The structure of ODN single strands and ICL

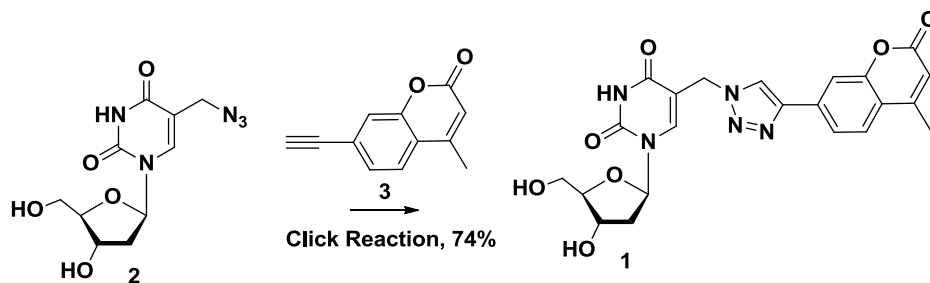
The photochromic behavior of these compounds was observed via gel electrophoresis analysis followed by UV photo-irradiation at variable wavelengths. Ten distinct

absorption bands were investigated to verify the ratification of this exceptional photoswitchability. This feature is certainly the important milestone for the photoswitchable DNA study in nucleic acid research.

## 3.2 Results and Discussions

### 3.2.1 Synthesis of Coumarin-Modified dT (1)

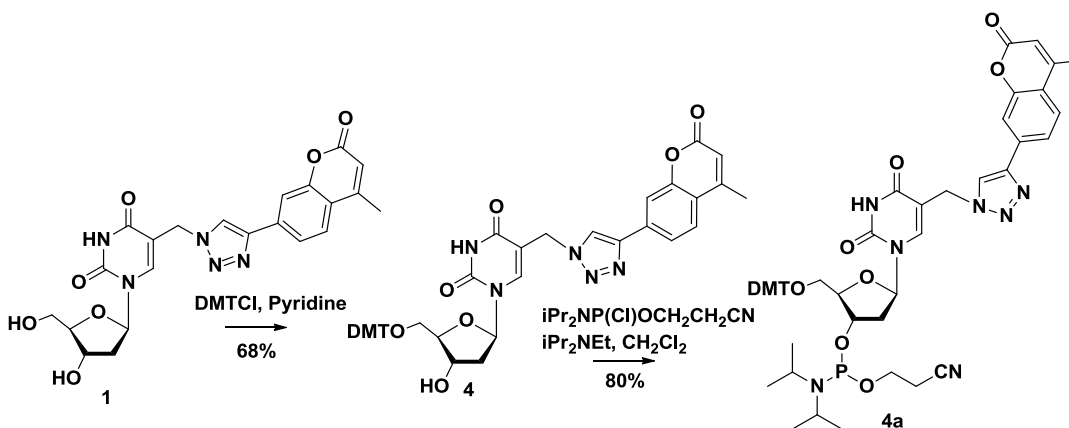
For our preliminary investigation we choose to synthesize coumarin-modified dT (1) (Scheme 7). First, 7-ethynyl-4-methyl-chromen-2-one (3) and 5-azidomethyl-2'-deoxyuridine (2) were synthesized by following the known procedure [134]. "Click" reaction was performed between alkyne-modified coumarin 3 and azide-modified dT 2 under the catalysis of sodium ascorbate and copper sulphate in water solution to produce 5-(4-methylchromen-2-one-1,2,3-triazol-1-yl)methyl-2'-deoxyuridine (1) in 74% yield.



**Scheme 7.** Synthesis of coumarin-conjugated dT

### 3.2.2 Synthesis of the Phosphoramidite Derived from 1

For studying the photophysical characteristics of coumarin in DNA, solid phase synthesis was used to synthesize ODNs containing compound **1**, the corresponding phosphoramidite (**4a**) was synthesized from coumarin conjugated nucleoside **1** (Scheme 8). At first, DMT residue was introduced in 5'OH functional group of **1** with 68% yield. The DMT derivative **4** was converted into the phosphoramidite (**4a**) in 80% yield by phosphorylation under Ar atmosphere using diisopropylethylamine and 2-cyanoethyl-*N,N*-diisopropylchlorophosphoramidite.

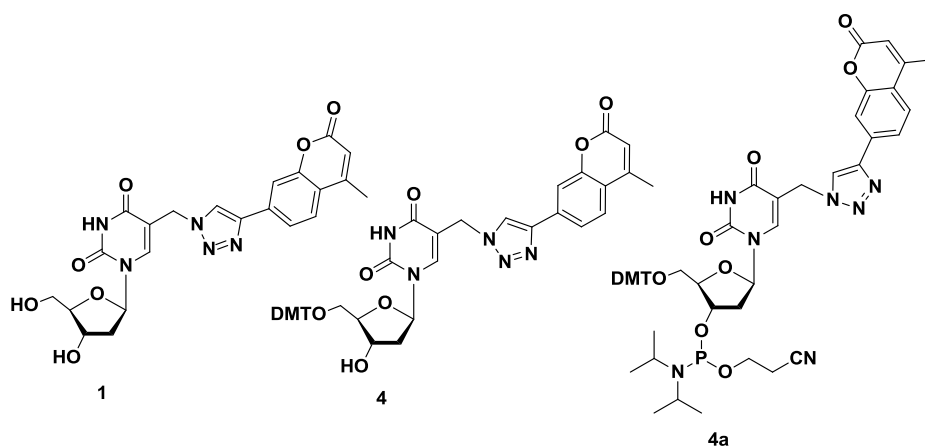


**Scheme 8.** Synthesis of phosphoramidite derived from **1**

### 3.2.3 Coumarin-Modified Derivatives of dT and Anticancer Activity Test

Modified nucleosides attract great attention because of their biological activities such as antiviral [135-137] and anticancer activities [138, 139]. Coumarin was chosen for the modification because it acts as an anti-inflammatory, antibacterial, antifungal,

antiviral, anticancer, antitubercular, anticonvulsant, antiadipogenic, antihyperglycemic, antioxidant, and contains neuroprotective properties. Bacteriostatic and anti-tumor activity of coumarin make it attractive for further backbone derivatisation and this further validates that coumarin has great potential for use in/as a therapeutic agent. For instance, Weber [140] and co-workers have shown that coumarin and its metabolite 7-hydroxycoumarin have antitumor activity against several human tumor cell lines. Much research also showed that both coumarin and their derivatives have been investigated as potential inhibitors of cellular proliferation in various carcinoma cell lines [141, 142]. Moreover, 4-hydroxycoumarin and 7-hydroxycoumarin inhibited cell proliferation in gastric carcinoma cell lines [143]. Therefore, coumarin-modified dT nucleosides have been synthesized for the purpose of investigating anticancer activity against the 60 human cancer cell. Compound **4** was identified as potential anticancer active analog among the coumarin-modified analogs **1**, **4**, and **4a** (Scheme 9).



**Scheme 9.** Coumarin-modified dT



### 3.2.4 Bio-physical Properties Study of **1** in ODNs

#### 3.2.4.1 Synthesis of Modified ODNs (**7a-15a**) Containing **1**

Synthesis of fluorescent ODNs is one of the great important attractions in nucleic acid research. Different research groups have already been using fluorescent probes to investigate the nucleic acid structure, dynamics, and recognition. To accomplish coumarin incorporated ODN **7a-15a** (Table-1), Automated DNA synthesizer was used to incorporate phosphoramidite building block **4a** via protocol of standard solid phase phosphoramidite chemistry. The average coupling yield was above 75%. After cleavage from the solid support, ODNs were deprotected with an ultra-mild deprotection condition (25% aq. NH<sub>3</sub>, 1 h, room temperature). Complementary strands were also synthesized following the same procedure. Purification of crude ODNs were accomplished by 20% polyacrylamide gel electrophoresis and sequence of ODNs were confirmed by MALDI mass.

**Table 1.** List of coumarin-modified ODNs (**1** = dT (Cm))

ID	ODN Sequences
<b>7a</b>	5'-dAGATGGAT <b>1</b> TAGGTAC
<b>12a</b>	5'-dAGATTTTT <b>1</b> TTTGTAC
<b>13a</b>	5'-dAGATTTAA <b>1</b> AAAGTAC
<b>14a</b>	5'-dAGATTTCC <b>1</b> CCCGTAC
<b>15a</b>	5'-dAGATTTGG <b>1</b> GGGGTAC

**Table 2.** List of Complementary Strand ODNs.

ID	ODN Sequences
<b>6a</b>	5'-dAGATGGATTTAGGTAC
<b>6b</b>	3'-dTCTACCTAAATCCATG
<b>9b</b>	3'-dTCTACCTACATCCATG
<b>10b</b>	3'-dTCTACCTATATCCATG
<b>11b</b>	3'-dTCTACCTAGATCCATG
<b>12b</b>	3'-dTCTAAAAAAAAAACATG
<b>13b</b>	3'-dTCTAATTTTTTTCATG
<b>14b</b>	3'-dTCTAAGGGGGGGCATG
<b>15b</b>	3'-dTCTAACCCCCCCCATG

*Fluorescence study of coumarin-incorporated ODN:* To verify the integrity and composition of the coumarin-containing ODNs, fluorescence spectroscopy was used as an alternative method for investigating the structure and properties of ODN. Characterization and information of ODN can be obtained with the use of spectroscopic methods in which a fluorescent probe is incorporated into ODN at a specific site. The presence of fluorescence signal from modified ODN molecules offers the advantage over the non-fluorescent signals from natural or non-modified ODN. Therefore for the determination of coumarin-modified dT (**1**) was incorporated into single strand ODN and was studied and was observed to be strongly fluorescent as emission spectrum displays a maximum at 410 nm compared to non-modified ODN (Figure 6). The fluorescent activity of modified ODN proved the presence of coumarin in synthesized ODN and coumarin modified dT (**1**) was incorporated successfully. This experiment also confirmed that the coumarin modified nucleoside is stable toward multiple cycles of ODN synthesis. In addition to fluorescence measurement, MALDI mass spectroscopy was used to characterize the modified ODNs. Mass spectrum identified the same mass as the calculated one (Table 3), which also proved that ODN was modified successfully with coumarin by incorporating coumarin conjugated dT (**1**) into synthesized ODN via solid phase DNA synthesizer. The reaction mixture for the experiment contained 5.0  $\mu$ M DNA, 100 mM NaCl, and 10 mM phosphate buffer (pH 7.0).

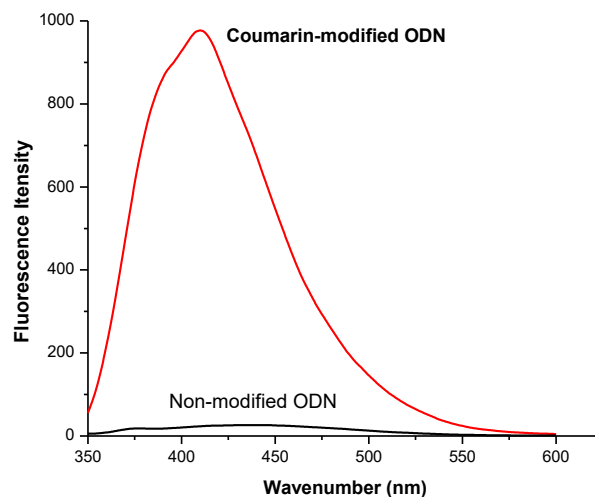


**Figure 6.** UV emission spectra of coumarin modified ODN (5  $\mu$ M,  $\lambda_{\text{ex}}$  = 350 nm, slit width = 15 nm;  $\lambda_{\text{em}}$  = 410 nm, slit width = 2.5 nm).

**Table 3.** MALDI-MS analysis of synthesized ODNs.

ODN ID	ODN Sequences	MALDI-MS Analysis	
		Calculated	Found
<b>7a</b>	5'-dAGATGGAT <b>1</b> TAGGTAC	5187.4	5187.0
<b>12a</b>	5'-dAGATTTTT <b>1</b> TTTGTAC	5091.3	5091.0
<b>13a</b>	5'-dAGATTA <b>1</b> AAAGTAC	5147.4	5147.5
<b>14a</b>	5'-dAGAT <b>1</b> CCCCGTAC	5003.3	5003.3
<b>15a</b>	5'-dAGAT <b>1</b> GGGGTAC	5243.4	5243.3

*Hybridization of ODN single strands* – Modified single stranded ODNs were hybridized with complementary strands following the standard procedure (Table 4). After quantification, radiolabeling of modified ODNs was carried out according to the standard protocols with [ $\gamma$ -<sup>32</sup>P] ATP. The [ $\gamma$ -<sup>32</sup>P] ATP-labelled ODNs were mixed with 1.5 equiv of their complements ° at room temperature in a buffer of 100  $\mu$ M potassium phosphate, pH 7.0, and 1M NaCl, then heated to 65°C followed by slow-cooling to room temperature overnight.

**Table 4.** List of coumarin-modified ODN duplexes

ODN duplexes	Sequences
<b>6</b>	5'-dAGATGGAT <b>T</b> TAGGTAC ( <b>6a</b> ) 3'-dTCTACCTAAATCCATG ( <b>6b</b> )
<b>7</b>	5'-dAGATGGAT <b>1</b> TAGGTAC ( <b>7a</b> ) 3'-dTCTACCTAA <b>A</b> ATCCATG ( <b>6b</b> )
<b>9</b>	5'-dAGATGGAT <b>1</b> TAGGTAC ( <b>7a</b> ) 3'-dTCTACCTA <b>C</b> ATCCATG ( <b>9b</b> )
<b>10</b>	5'-dAGATGGAT <b>1</b> TAGGTAC ( <b>7a</b> ) 3'-dTCTACCTA <b>T</b> ATCCATG ( <b>10b</b> )
<b>11</b>	5'-dAGATGGAT <b>1</b> TAGGTAC ( <b>7a</b> ) 3'-dTCTACCTA <b>G</b> ATCCATG ( <b>11b</b> )
<b>12</b>	5'-dAGATTTTT <b>1</b> TTTGTAC ( <b>12a</b> ) 3'-dTCT <b>AAAAAAAAA</b> CATG ( <b>12b</b> )
<b>13</b>	5'-dAGATTAAA <b>1</b> AAAGTAC ( <b>13a</b> ) 3'-dTCTAA <b>TTTTTTT</b> CATG ( <b>13b</b> )
<b>14</b>	5'-dAGATTCCC <b>1</b> CCCGTAC ( <b>14a</b> ) 3'-dTCTAAG <b>GGGGGGG</b> CATG ( <b>14b</b> )
<b>15</b>	5'-dAGATTGGG <b>1</b> GGGGTAC ( <b>15a</b> ) 3'-dTCTAA <b>CCCCCCC</b> CATG ( <b>15b</b> )

### 3.2.4.2 Coumarin-Induced ICL Formation and Analysis

Photoirradiation usually forms ICL that result from a cyclic covalent bond between unsaturated bonds of two different compounds such as coumarin, cinnamate, and maleimides [144-148]. They undergo a  $[2\pi+2\pi]$  cycloaddition when exposed to long wavelength UV photoirradiation. Coumarin derivatives undergo a photodimerization reaction under the ultraviolet-A (UVA) region irradiation [149-151]. UVA wavelength of 350 nm was used which is compatible with living cells and the coumarin moiety can be excited in this irradiation to form singlet and triplet excitation states to generate ICL materials.

For the ICL formation study, coumarin-functionalized ODNs were labelled with [ $\gamma$ - $^{32}\text{P}$ ] ATP at the 5' position of modified ODN and hybridized with complementary strand. The hybridized ODN duplexes were photo-irradiated at 350 nm for 50 min using a Rayonet Photochemical Chamber Reactor (Model RPR-100). As we expected, a new band of ICL product was observed with the duplex **7** in the PAGE analysis after UV-irradiation. The migration of new band of ICL was severely retarded for duplex **7** relative to non-modified and unreacted ODN duplex **6** after UV photo-irradiation which is indicative of ICL formation (Figure 7). Single-stranded ODN was identified on the basis of their faster electrophoretic mobility.



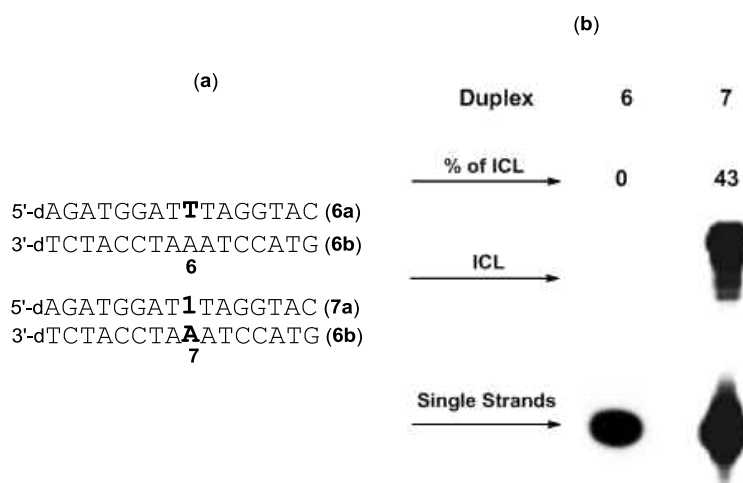


**Figure 7.** PAGE analysis of ICL formation for ODN **duplex-6** and **duplex-7**

### 3.2.4.3 Sequence Effect on Coumarin-induced ICL

In order to determine the selectivity of coumarin-induced ICL, the reactivity patterns of coumarin were further investigated with the coumarin-modified ODN duplexes **6-11**, which contain coumarin-modified ODNs hybridized with opposing sequence complementary of coumarin with dA, dC, dT, and dG in complementary strands. Lanes 6-9 are for duplexes **6-11** respectively, where in lanes 7-9, coumarin modified dT (**1**) is opposite to four different nucleosides. Decreased ICL yield was observed in the order of dT (**10**, 69%) > dC (**9**, 55%) > dA (**7**, 43%) > dG (**11**, 24%) (Figure 8). This result indicates that **1** has a higher reactivity towards pyrimidines than purines.

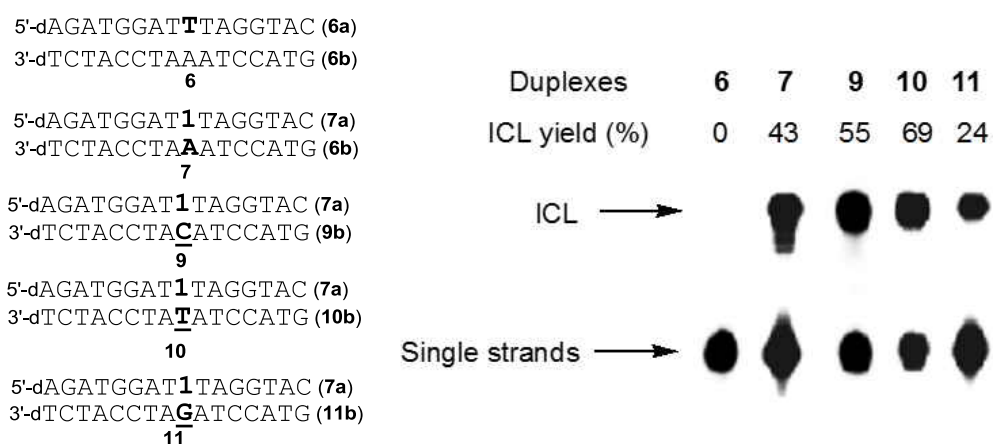


**Figure 8.** PAGE analysis of ICL formation from duplexes 6-11

In order to fully investigate the reactivity of **1** towards the four canonical nucleosides, several variations in the complementary sequence around the central coumarin were used for this further study. DNA duplexes **12-15** with only dA, dT, dG, or dC surrounding the ICL site were used and the ICL efficiency was examined (Figure 9). All the substrates used were annealed to the complementary ODNs to generate duplexes. Among these duplexes, the highest ICL yield was observed with duplex **13** (dT, 87%), while no ICL was found with duplex **14** (dG) (Figure 9). Although duplexes **12** (dA) and **15** (dC) resulted in about 4% and 7% ICL respectively, the reaction of dC or dA with **1** is much slower than that of dT with **1**. All these results supported that coumarin has much higher selectivity with dT than with dC and dA.

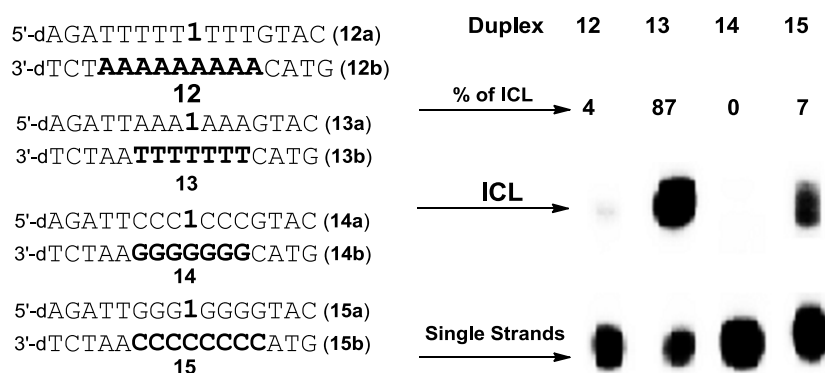
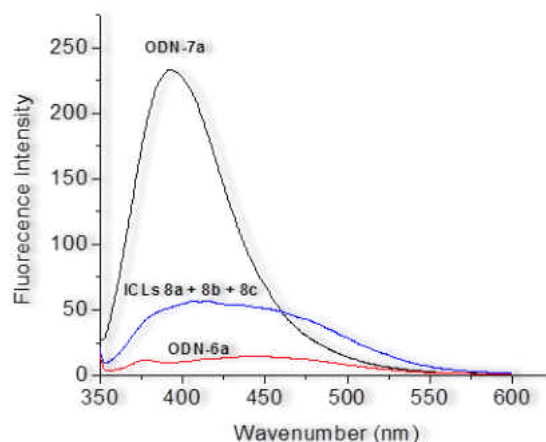


Figure 9. PAGE analysis of ICL formation with duplexes 12-15

#### 3.2.4.4 Properties Study of Coumarin-induced ICL

Fluorescence intensity was sharply dropped for the cross-linked coumarin-DNA adduct (Figure 10). As the unsaturated bonds of coumarin and dT were converted to the cyclobutane to form the ICL between two ODN single strands, the extended conjugation of the coumarin moiety was decreased, and the wavelength of absorbance was reduced from 350 nm to 254 nm. The reaction mixture contained 5.0  $\mu$ M DNA, 100 mM NaCl, and 10 mM phosphate buffer (pH 7.0). This suggests that the ICL formation may lead to the destruction of the conjugation system of coumarin moiety. This property allows rapid, direct, and efficient monitoring of the DNA cross-linking process on time via a non-invasive method instead of employing a traditionally-used harmful  $^{32}$ P-labelling method in biochemical research. The novel method could be introduced as an effective way in biology for DNA cross-linking study and allow real-time detection without disrupting native cell environment.



**Figure 10.** Fluorescence emission spectra of 10  $\mu$ M ODN **6a**, ODN **7a** and ICL products in 100 mM NaCl and 10 mM pH 7 phosphate buffer solution ( $\lambda_{\text{ex}} = 350$  nm, slit width = 10 nm;  $\lambda_{\text{em}} = 392$  nm, slit width = 10 nm).

*Stability study of ICL product* - Investigation was performed to confirm the stability of ICL materials after separation from cross-linking reaction mixture. The ICL was purified by 20% denaturing PAGE after UV irradiation at 350 nm for 50 min. The isolated and dried ICL products obtained from duplexes **7-12** were dissolved in 1.0 M piperidine (20  $\mu$ L) and incubated at 90  $^{\circ}$ C for 30 min. The samples were subjected to electrophoresis on a 20% denaturing polyacrylamide gel (Figure 11). Lane 1, the isolated ICL was used as control; Lane 2, single stranded (SS) ODN **7a** was used as control; Lanes 3-8 for piperidine treatment of ICL products at 90  $^{\circ}$ C for 30 min (lane 3: ICL product formed from duplex **7**; lane 4: ICL product formed from duplex **8**; lane 5: ICL product formed from duplex **9**; lane 6: ICL product formed from duplex **10**; lane 7: ICL product formed from duplex **11**; Lane 8, the ICL products formed from duplex **12**).



### 3.2.5.1 Hydroxy Radical Cleavage Reaction for ICL Site Determination

Hydroxy radical cleavage experiment was performed to investigate the cross-linking site in coumarin-modified ODN. The ICL product was isolated for this experiment from UV-treated ODN duplex **7**. G+A sequence reaction and Fe(II)-EDTA cleavage reactions of the separated  $^{32}\text{P}$ -labelled cross-linked product ( $0.1\mu\text{M}$ ) were performed in a buffer and  $\text{H}_2\text{O}_2$  for 3 min at room temperature and then quenched with 100 mM thiourea ( $10\ \mu\text{L}$ ). Samples were lyophilized and incubated with 1M piperidine ( $20\ \mu\text{L}$ ) at  $90\ ^\circ\text{C}$  for 30 min, dissolved in  $20\ \mu\text{L}$   $\text{H}_2\text{O}$ , 90% formamide loading buffer (1:1) and subjected to 20% denaturing PAGE analysis. In figure 13A: **7a** was radiolabeled at 3'-terminus: lane 1, G+A sequencing; lane 2, Fe-EDTA reaction of **7a**; lane 3, piperidine treatment of ICL isolated from UV irradiation of **7a** and **6b** at  $90\ ^\circ\text{C}$  for 30 min; and in figure 13B: **7a** was radiolabeled at 5'-terminus. Lane 1, G+A sequencing; lane 2, Fe-EDTA reaction of **7a**; lane 3, Piperidine treatment of ICL isolated from UV irradiation of **7a** and **6b** at  $90\ ^\circ\text{C}$  for 30 min. Both figure 13A and B indicated that ICL was formed at the 9<sup>th</sup> position which is coumarin-modified dT (**1**) of ODN **7a**.

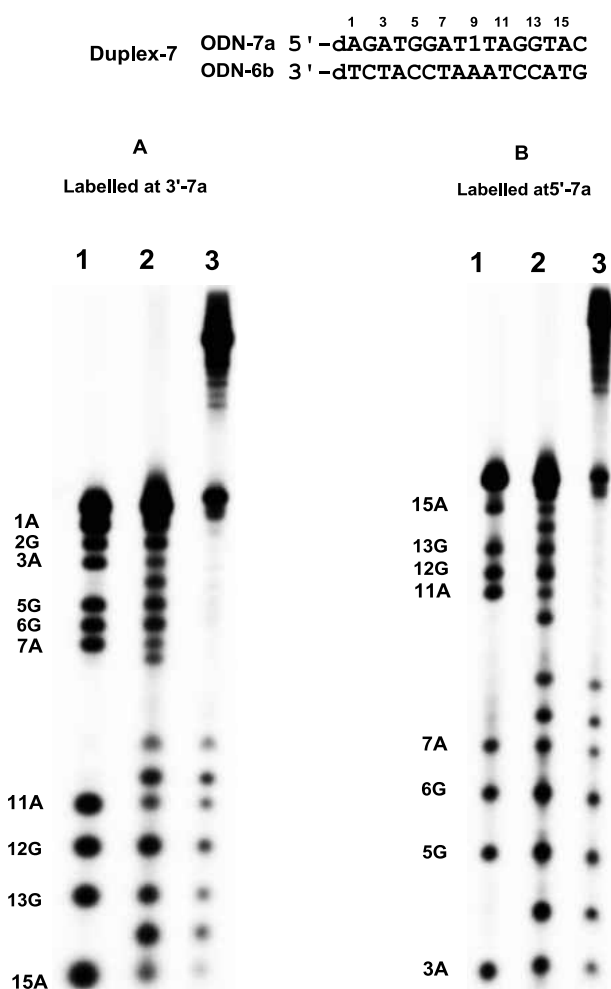


**Figure 13.** Hydroxy radical cleavage analysis for duplex 7

*Histogram diagram of Fe (ii) EDTA cleavage:* To substantiate the results of hydroxy radical cleavage reaction, histogram diagram experiment was performed for the determination of the ICL site at the coumarin-modified ODN via hydroxy radical cleavage of the ICL product isolated from UV-treated ODN duplex 7. This experiment determines the covalent bonding of ICL site of modified ODN with the complementary strand. ICL cleavage of Fe-EDTA product was observed in figure 14A and 14B at the 9<sup>th</sup> position which is coumarin-modified dT (1) of ODN 7a in duplex 7.

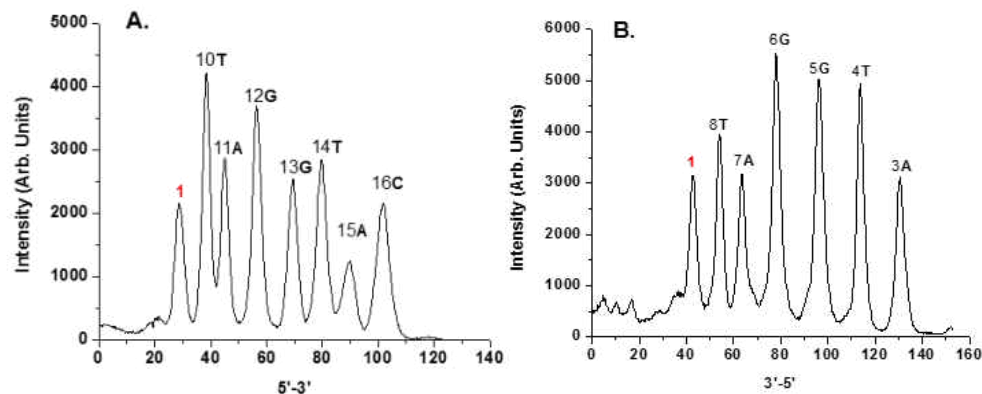


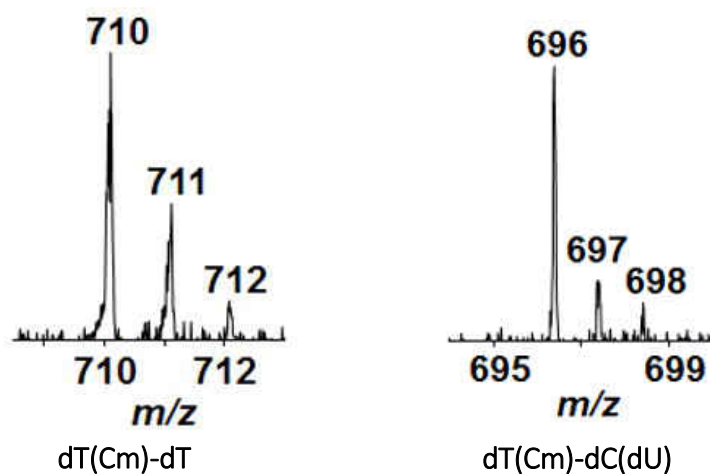
Figure 14. Histogram diagram of duplex 7.

### 3.2.5.2 LC-MS Analysis for Determining ICL Site via Enzymatic Digestion

ICL occurred mainly with **1** in coumarin-modified ODN **7a** that was determined by footprinting of hydroxyl radical reaction and histogram diagram experiment of gel-purified ICL. However, the exact ICL site in the complementary strand might be multiple. To exploit this further, LC-MS and MS/MS was used to determine the identities of the nucleobase(s) in the opposite strand that is(are) cross-linked with the coumarin-modified dT moiety. Isolated ICL from duplexes **7** and **9** with a cocktail of four enzymes to release the ICL as a dinucleoside remnant and subjected the resulting mixture to LC-MS and MS/MS analyses. The instrument was set up for monitoring the fragmentation of the dinucleoside remnant of putative ICL products as  $[M+H]^+$  ions in the positive-ion mode. As we expected, LC-MS/MS results revealed in the digestion mixture as dinucleosides, in which the coumarin-derived dT is conjugated to complementary strand with a dT and to dC, detected as the deaminated product dU (dC moiety was converted



to a dU). Expected LC-MS spectra of dimers dT-**1** (A) and dC (dU) - **1** (B) were found from the digestion mixture of ICL products (Figure 15)



(A) MW Calculated: 710 g/mole, Found: 710, (B) MW Calculated: 696 g/mole, Found: 696

**Figure 15.** LC-MS spectra of dinucleosides obtained from enzymatically digested ICL

### 3.2.6 Selected-ion Chromatogram (SIC) Analysis for ICL Structure Determination

Previous analysis have shown that ICL took place between nucleoside **1** in coumarin-modified ODN and dT and dC in the complementary strand and all ICL products were stable to heating in phosphate buffer or 1.0 M piperidine. It was also determined that dT had a much higher reactivity than dC towards the coumarin moiety. Several research group investigated that psoralen reacts with pyrimidine bases of dT and dC via [2+2] cycloaddition reaction involving either the 3, 4-double bond of the pyrone ring or the 4',5'-double bond of the furan ring which yields a "furan-side mono adduct"

[152]. Psoralens react primarily with dT in DNA and uridine in RNA although a minor reaction with cytosine also occurs [153]. Similarly, LC-Mass analysis of selected ions after neutral loss of a 2-deoxyribose by enzymatic digestion of coumarin induced ICL product confirmed that upon exposure to 350 nm of UV light, coumarin undergoes [2+2] cycloaddition reaction similarly with its neighboring dT and dC to give ICL products. *LC-Mass analysis of major fragmentation; (dT-1)* - The MS/MS analysis for monitoring the  $[M+H]^+$  ion of dT-1 revealed two major peaks  $m/z$  710 (17)  $\rightarrow$  594 (21) transition, which monitors the neutral loss of a 2-deoxyribose (Figure 16). Product ions of  $m/z$  470 (22) and 478 (23) were also found in the MS/MS due to neutral losses of 2-deoxyribose by enzymatic digestion of ICL product.

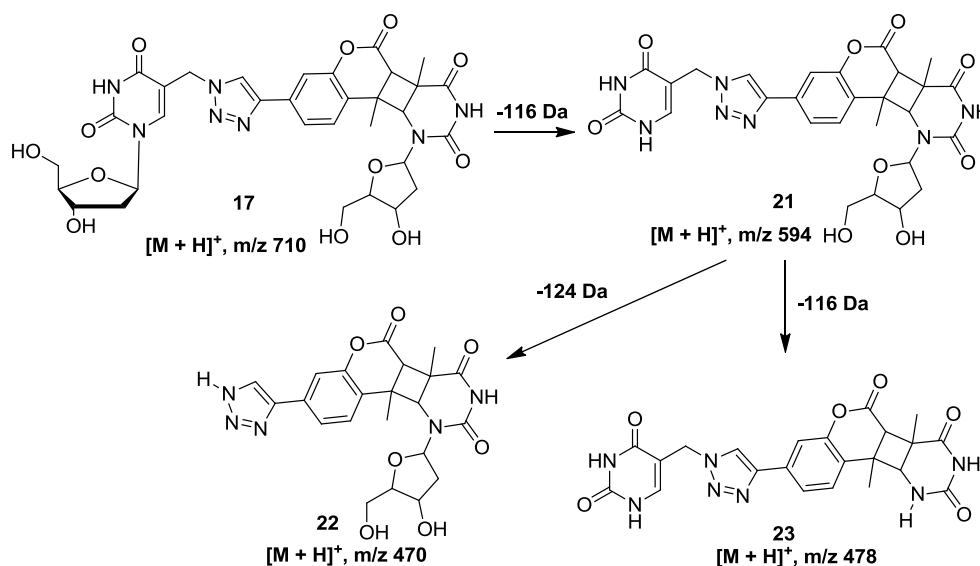


**Figure 16.** Fragmented ions of dT-1 from enzymatically digested ICL

*LC-Mass Analysis of major fragmentation; dU-1* - The MS/MS analysis for the selected-ion chromatogram (SIC) of monitoring the  $[M+H]^+$  ion of dU-1 revealed two

major peaks  $m/z$  696 (16)  $\rightarrow$  580 (18) transition, which monitors the neutral loss of a 2-deoxyribose (Figure 17). Product ions of  $m/z$  456 (19) and 464 (20) were also found in the MS/MS due to neutral losses of 2-deoxyribose by enzymatic digestion of ICL product.

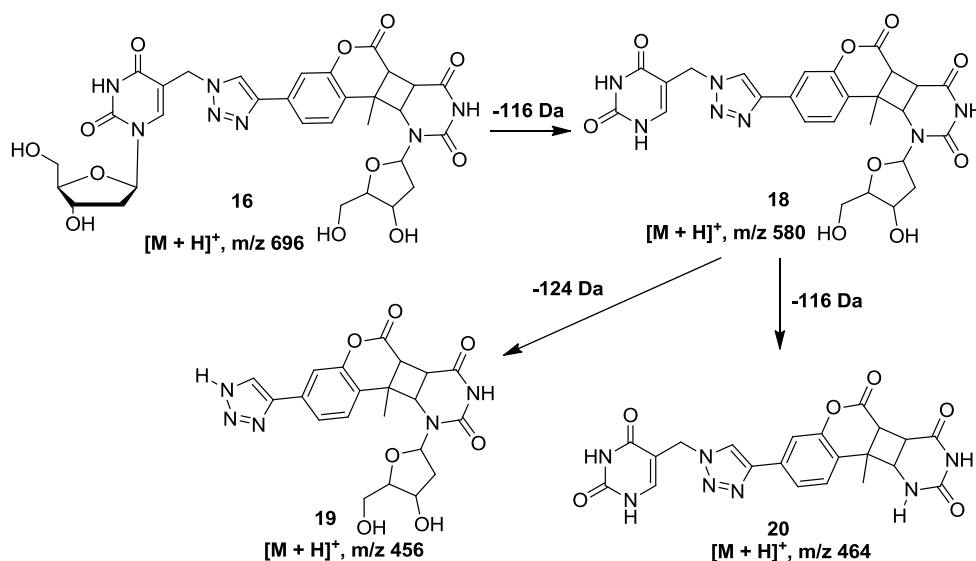


**Figure 17.** Major ion fragmentations for dU-1 from enzymatically digested ICL

### 3.2.7 Kinetic Study of ICL

To further substantiate the reactivity of coumarin in ODN towards dT and dC and dA, kinetics of ICL formation was analyzed. ICL formation was studied over different course of time. The final volume of  $^{32}\text{P}$ -labeled ODN duplex aliquots was 20  $\mu\text{L}$ . 1M NaCl, 10 mM potassium phosphate, pH=7 were mixed and UV irradiated at the prescribed times and immediately quenched by 90% formamide loading buffer, and stored at  $-20^\circ\text{C}$

until subjected to 20% denaturing PAGE analysis. dT was found more reactive ( $k_{dT} = 3.5 \pm 0.5 \times 10^{-3}$  (Figure 18) than dC ( $k_{dC} = 1.2 \pm 0.2 \times 10^{-3}$ ) and dA ( $k_{dA} = 0.8 \pm 0.2 \times 10^{-3}$ ) towards coumarin moiety, which supports our previous experimental results.

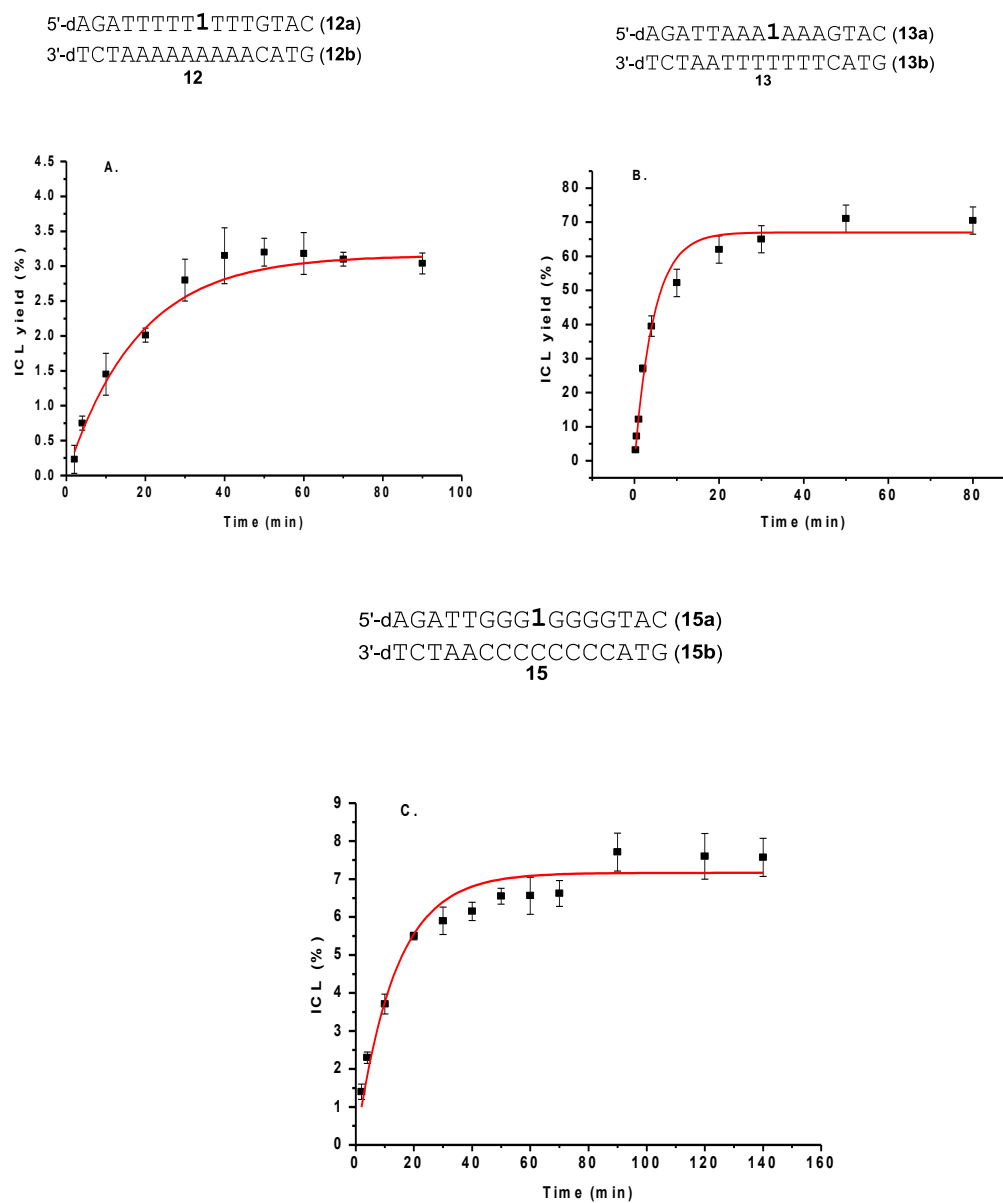


**Figure 18.** Kinetics of coumarin-induced ICL growth

### 3.2.8 Photocleavage Reaction of ICL Materials

*Photoreactivity of ICL materials* - Several researches showed that photocleavage allows photocross-linking materials revert to their original structure [154-158]. Cyclobutane rings that are derived from  $\alpha$ -truxilate,  $\beta$ - or  $\delta$ - truxinates, and the cyclobutane ring formed between coumarin and dT dimers reverse upon irradiation near 250 nm. Coumarin groups were utilized to form cyclobutane in the mid 1960s at the first time by photoirradiation and at the late 1980s they were utilized for their reversibility [159-161]. Here, coumarin-induced ICL of ODN was further evaluated to determine the effect of UV light irradiation at lower wavelength. Interestingly ICL of ODN duplexes reverted to the original single stranded ODNs as anticipated, where cyclobutane ring structure between ODN strands opens to unsaturated bonds. Cleavage of the ICL products to two single stranded ODNs was ultrafast and 90% cleavage was completed within 60 S. 2.14  $\mu$ M ICL solutions were used for this highly reversible study of coumarin-induced ICL. The reactions were quenched by an equal volume of 90% formamide stop/loading buffer, and phosphorimage autoradiogram of 20% denaturing PAGE was used to analyze the photoreversible reaction (Figure 19). lane 1, ICL as control; lane 2, SS as control, lane 3, ICL formation reaction by irradiation of duplex **7** at 350 nm with 50 min; lane 4, reverse reaction by irradiation at 254 nm for 6 min for cleavage of ICL to single-stranded ODN.

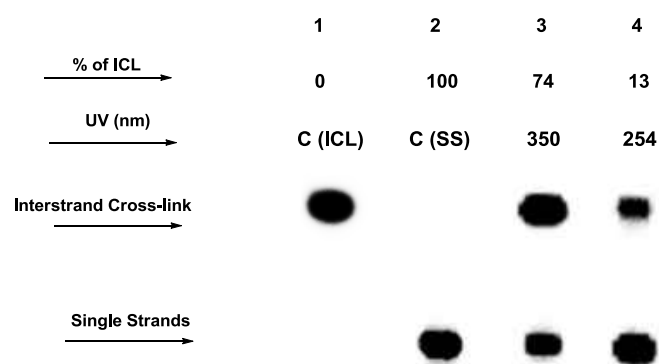


**Figure 19.** PAGE analysis photoreversible ICL reaction

*MALDI-mass analysis of ICL cleavage to single strands* - Cleavage of the ICL products into two single stranded ODNs was ultrafast and almost completed within 60 sec by 254 nm irradiation. This process was also confirmed by MALDI-TOF-MS analysis, where both coumarin-modified ODN and the complementary strand were confirmed. For this analysis isolated ICL from duplex **7** was further irradiated at 254 nm for 6 min. The detected masses of two ODNs are 5185 Da and 4800 Da, which are identical to the coumarin-modified ODN **7a** (Cal.: 5186.4 Da) and the complementary strand **6b** (Cal.: 4800.2 Da) (Figure 20).

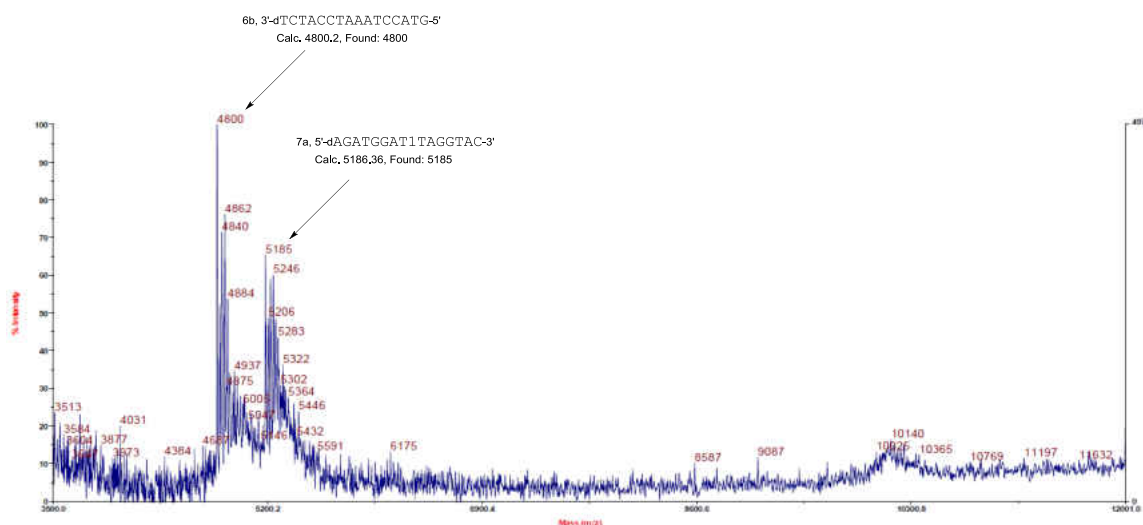


**Figure 20.** MALDI-TOF MS spectra of single stranded ODNs cleaved from ICL

### 3.2.9 Multiple Cycle Photoreversibility Test of Coumarin Induced ICL

The photoswitchability of the ICL induced by coumarin-modified dT (**1**) was investigated in previous experiments. To analyze the constancy of photoswitchability, the reversibility of ICL was examined by multiple cycles with duplexes **10**, **12**, **13**, and **15**. *Five cycle photoreversibility study of coumarin-induced ICL of duplex 10* – To analyze the multiple cycle photoswitchability, duplex **10** was photoirradiated at 350 nm to generate ICL, and the ICL solution was again irradiated by lower wavelength UV light 254 nm for 6 min to make a cycle. Four more consecutive cycles were completed by irradiation repeatedly. The reaction mixtures were collected each time and was quenched by an equal volume of 90% formamide stop/loading buffer and then electrophoresed on a 20% denaturing polyacrylamide gel at 1200 V for approximately 2.5 h. Single-stranded ODN and ICL were identified on the basis of their electrophoretic mobility. The ICL

product of duplex **10** was analyzed as successfully reverted to single stranded ODNs upon 254 nm irradiation. Therefore duplex 10 is reversible upon switching wavelength of UV photoirradiation.

ICL formation and cleaving to single stranded ODN are shown in figure 21 for 5 cycles. Where in Lane 1, single stranded ODN **7a** was run as constant; Lane 2, UV irradiation of duplex **10** at 350 nm for 50 min to form ICL; Lane 3, UV irradiation at 254 nm for 6 min to cleave the ICL product leading to single stranded ODN; Lane 4, UV irradiation at 350 nm for 50 min to form ICL; Lane 5, UV irradiation at 254 nm for 6 min to form reversed single strand ODN. Lane 6; UV irradiation at 350 nm for 50 min to form ICL; Lane 7, UV irradiation at 254 nm for 6 min to form reversed single strand ODN; Lane 8, UV irradiation at 350 nm for 50 min to form ICL; Lane 9, UV irradiation at 254 nm for 6 min to form reversed single strand ODN; Lane 10, UV irradiation at 350 nm for 50 min to form ICL; Lane 11, UV irradiation at 254 nm for 6 min to form reversed single strand ODN; Lane 12, UV irradiation at 350 nm for 50 min to form ICL.

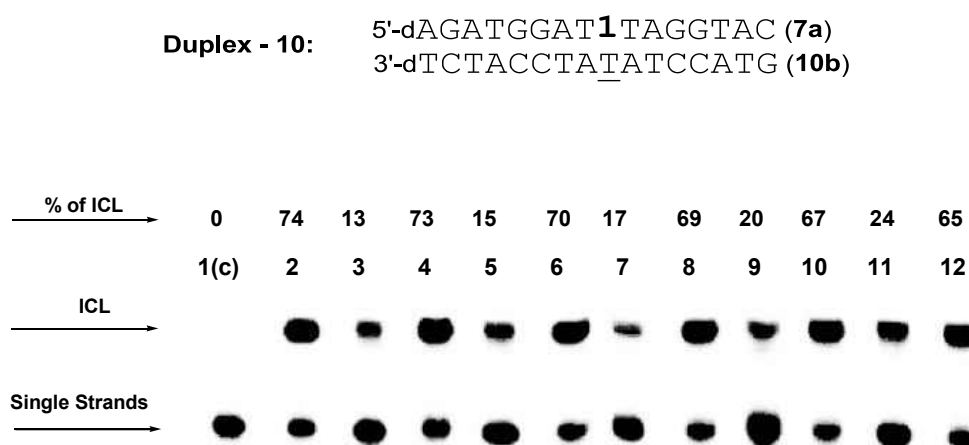


**Figure 21.** PAGE analysis of multiple cycles ICL photoreversibility study with duplex-10



In order to see the generalitiy of the phtoreversibility of ICLs formed from coumarin and dT, we investigated the photoproperties of the ICL formed with other independent DNA duplexes **13**, **15**, and **12**. This process was repeated for 5 cycles.

*Fivecycle photoreversibility study of coumarin-induced ICL of duplex-13:* - To analyze the multiple cycle photoswitchability, duplex **13** was photoirradiated at 350 nm to generate ICL, and the ICL solution was again irradiated by lower wavelength UV light (254 nm) for 6 min to make a cycle. Four more consecutive cycles were completed by irradiation repeatedly. Similar to duplex **10**, the ICL products generated from duplex **13** by 350 nm irradiation were also reverted to single stranded ODNs upon 254 nm irradiation. Therefore ICL formation from duplex **13** is also reversible upon switching wavelength of UV photoirradiation.

The reaction mixtures were collected each time and was quenched by an equal volume of 90% formamide stop/loading buffer and then electrophoresed on a 20% denaturing polyacrylamide gel at 1200 V for approximately 2.5 h. Single-stranded ODN and ICL were identified on the basis of their electrophoretic mobility.

In figure 22; Lane 1, single strand ODN **13a**; Lane 2, UV irradiation of duplex **13** at 350 nm for 50 min to form ICL; Lane 3, UV irradiation at 254 nm for 6 min to cleave the ICL product leading to single strand ODN; Lane 4, UV irradiation at 350 nm for 50 min to form ICL; Lane 5, UV irradiation at 254 nm for 6 min to form reversed single strand ODN. Lane 6; UV irradiation at 350 nm for 50 min to form ICL; Lane 7, UV irradiation at 254 nm

for 6 min to form reversed single strand ODN; Lane 8, UV irradiation at 350 nm for 50 min to form ICL; Lane 9, UV irradiation at 254 nm for 6 min to form reversed single strand ODN; Lane 10, UV irradiation at 350 nm for 50 min to form ICL; Lane 11, UV irradiation at 254 nm for 6 min to form reversed single strand ODNs.

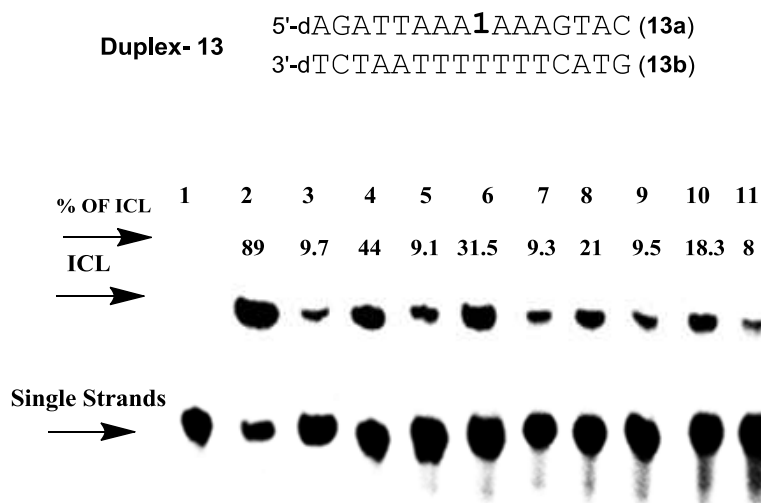


**Figure 22.** PAGE analysis of multiple cycles ICL photoreversibility study for duplex-13

*Fourcycle photoreversibility study of coumarin-induced ICL of duplex 15-* To analyze the multiple cycle photoswitchability, duplex **15** was photoirradiated at 350 nm to generate ICL, and the ICL solution was again irradiated by lower wavelength UV light 254 nm for 6 min to make a cycle. Three more consecutive cycles were completed by irradiation repeatedly. The ICL products generated from duplex **15** by 350 nm irradiation were reverted to single stranded ODNs upon 254 nm irradiation, which is similar to duplex **10**.

The reaction mixtures were collected each time and was quenched by an equal volume of 90% formamide stop/loading buffer and then electrophoresed on a 20% denaturing polyacrylamide gel at 1200 V for approximately 2.5 h. Single-stranded ODN and ICL were identified on the basis of their electrophoretic mobility.

In figure 22; Lane 1, single strand ODN **15a**; Lane 2, UV irradiation of duplex **15** at 350 nm for 50 min to form ICL; Lane 3, UV irradiation at 254 nm for 6 min to cleave the ICL product leading to single strand ODN; Lane 4, UV irradiation at 350 nm for 50 min to form ICL; Lane 5, UV irradiation at 254 nm for 6 min to form reversed single strand ODN. Lane 6; UV irradiation at 350 nm for 50 min to form ICL; Lane 7, UV irradiation at 254 nm for 6 min to form reversed single strand ODN; Lane 8, UV irradiation at 350 nm for 50 min to form ICL; Lane 9, UV irradiation at 254 nm for 6 min to form reversed single strand ODN.

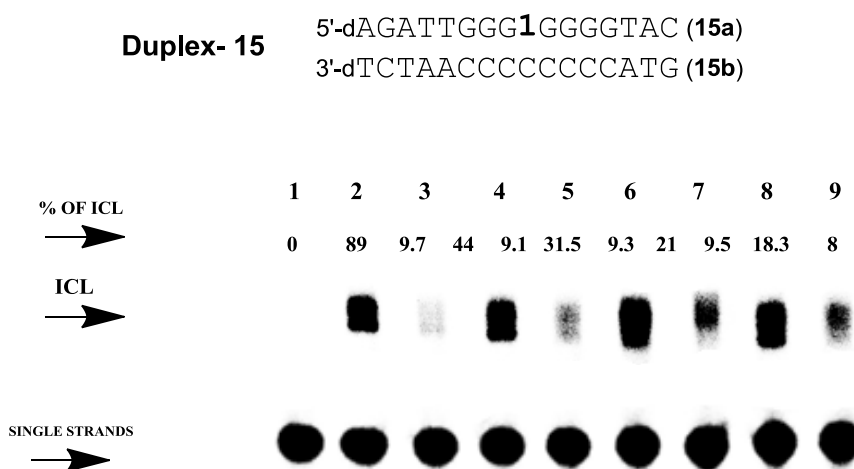


**Figure 23.** PAGE analysis of multiple cycles ICL photoreversibility study for duplex-15

*Fivecycle photoreversibility study of coumarin-induced ICL of duplex12*—To

analyze the multiple cycle photoswitchability, duplex **12** was photoirradiated at 350 nm to generate ICL, and the ICL solution was again irradiated by lower wavelength UV light 254 nm for 6 min to make a cycle. Four more consecutive cycles were completed by irradiation repeatedly. Different from duplex **10**, the ICL products generated from duplex **12** by 350 nm irradiation were not cleaved to single-stranded ODN upon 254 nm irradiation (Figure 24). Therefore the ICLs formed between **1-dA** in duplex **12** is not reversible upon switching wavelength of UV photoirradiation.

The reaction mixtures were collected each time and was quenched by an equal volume of 90% formamide stop/loading buffer and then electrophoresed on a 20% denaturing polyacrylamide gel at 1200 V for approximately 2.5 h. Single-stranded ODN and ICL were identified on the basis of their electrophoretic mobility. In figure 24; Lane 1, single strand ODN **12a**; Lane 2, UV irradiation of duplex **12** at 350 nm for 50 min to form ICL; Lane 3, UV irradiation at 254 nm for 6 min to cleave the ICL product leading to single strand ODN; Lane 4, UV irradiation at 350 nm for 50 min to form ICL; Lane 5, UV irradiation at 254 nm for 6 min to form reversed single strand ODN. Lane 6; UV irradiation at 350 nm for 50 min to form ICL; Lane 7, UV irradiation at 254 nm for 6 min to form reversed single strand ODN; Lane 8, UV irradiation at 350 nm for 50 min to form ICL; Lane 9, UV irradiation at 254 nm for 6 min to form reversed single strand ODN; Lane 10, UV irradiation at 350 nm for 50 min to form ICL; Lane 11, UV irradiation at 254 nm for 6 min to form reversed single strand ODNs.

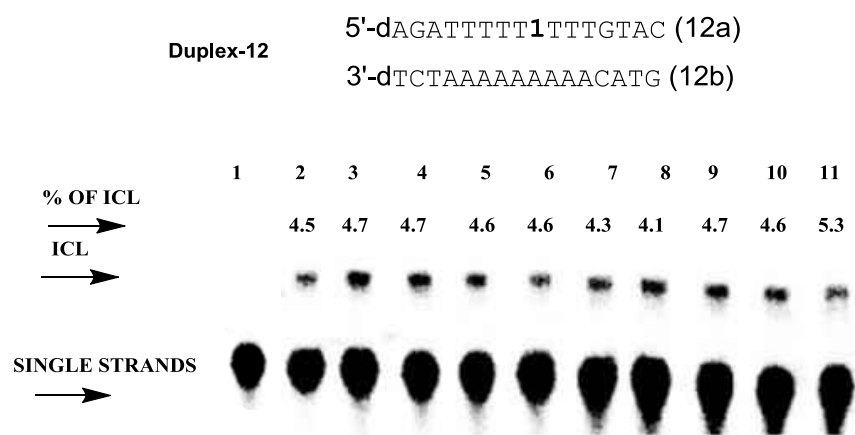


**Figure 24.** PAGE analysis of multiple cycles ICL photoreversibility study for duplex-12

*Overall discussion* - Multiple cycle photoreversibility analysis (Figures 21, 22, 23, and 24) confirmed that the ICL products formed from duplexes **10** and **13** (dT-1, ICL) and **15** (dC-1, ICL) via 350 nm irradiation were reversible by switching wavelength 350 nm and 254 nm photoirradiation while ICL products generated from duplex **12** (dA-1, ICL) was not cleaved to single strands by irradiation at 254 nm.

*Selected-ion chromatograms (SICs) for the 10 cycles reversibility study* -To further substantiate the finding of potential ICL reversibility of dT-1 and dC-1 and non-reversibility dA-1, Selected-ion chromatograms (SICs) analysis was performed for 10 cycles reversible reaction of ODN duplexes. The ICLs products of duplex **10** were isolated after irradiation at 350 nm (ICL-1), one cycle of 350 nm/254 nm irradiation (ICL-2), and those formed after 10 cycles of 350 nm/254 nm irradiation (ICL-20). Then isolated ICL products were digested with enzymes to release the ICL as a dinucleoside remnant and

subjected the resulting mixture to LC-MS and MS/MS analyses as described above. The ratios of area of peaks found were plotted in the SICs for monitoring the loss of a 2-deoxyribose from the  $[M+H]^+$  ions of dC-1 (as deaminated form,  $m/z$  696  $\rightarrow$  580 transition), dT-1 ( $m/z$  710  $\rightarrow$  594 transition), and dA-1 adducts ( $m/z$  710  $\rightarrow$  594 transition) versus that for the  $[M+H]^+$  ion of dA (Figure 25). The signals for the dT-1 and dU-1 cross-links were decreased from ICL-1 to ICL-2 and ICL-20, whereas a significant elevation of dA-1 signal was observed from ICL-1 and ICL-2 to ICL-20. These results suggested that the formation of dC-1 and dT-1, but not that of dA-1 is reversible. In this context, it is worth noting that, owing to the differences in ionization efficiencies for these dinucleosides (dA-1, due to the higher proton affinity of adenine than uracil or thymine, is expected to have much better ionization efficiency than dT-1 and dU-1 in the positive-ion mode),

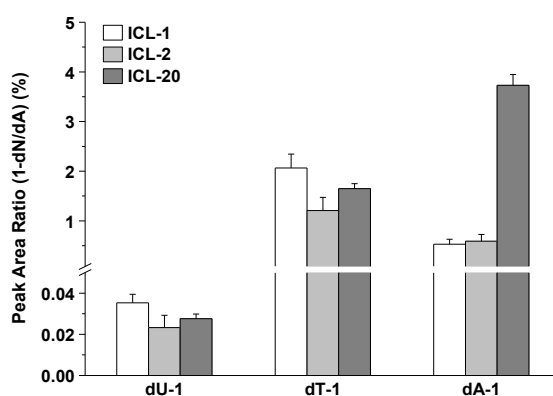


**Figure 25.** The ratio of area of peaks for the fragmentations of ICL cleavage

### 3.2.10 Kinetic Study of Photolytic Cleavage for ICL Materials

Clear indication about degree of reversibility was not found until this experiment because the peak area ratios displayed in figure 25 do not reflect the relative levels of dT-1, dU-1 and dA-1 ICL formation. Therefore kinetics were studied for the cleavage of ICL materials of duplexes **10**, **13**, **15**, and **12** upon UV-irradiation at 254 nm (the rate constant was calculated based on disappearance of the ICL products). Cleavage of ICL product into two single stranded ODNs were ultrafast and 90% of cleavage were completed within 60 s by 254 nm irradiation. However, the kinetic study of cleavage was studied over a longer time period. After each time, the irradiation reaction was quenched by an equal volume of 90% formamide stop/loading buffer, and then analyzed by electrophoresis on a 20% denaturing polyacrylamide gel at 1200 V for approximately 2.5 h. ICLs have been identified on the basis of their electrophoretic mobility and the analysis of the percentage of the ICL cleavage was accomplished.

*Photolytic cleavage of coumarin-induced ICL materials from duplex **10*** – Cleavage of ICL product of duplex **10** into two single stranded ODNs were investigated. Ultrafast cleavage was observed and 90% of ICLs were completely cleaved to single stranded ODN within 60 s by 254 nm irradiation. The kinetic study of cleavage was studied over a longer time period. The cleavage of coumarin-induced ICL product from duplex **10** into two single stranded ODNs upon 254 nm irradiation were analyzed by PAGE (Figures 26 and 27).

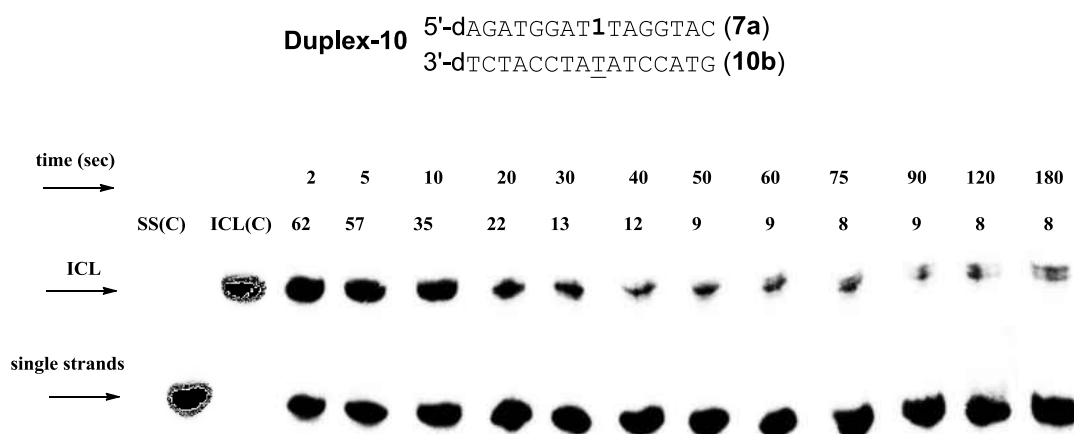


**Figure 26.** PAGE analysis of photolytic cleavage of ICL from duplex-10

Lane 1; SS as control, lane 2; ICL as control, lane 3; ICLs were irradiated at 254 nm for 2 sec, lane 4; ICLs were irradiated at 254 nm for 5 sec, lane 5; ICLs were irradiated at 254 nm for 10 sec, lane 6; ICLs were irradiated at 254 nm for 20 sec, lane 7; ICLs were irradiated at 254 nm for 30 sec, lane 8; ICLs were irradiated at 254 nm for 40 sec, lane 9; ICLs were irradiated at 254 nm for 50 sec, lane 10; ICLs were irradiated at 254 nm for 60 sec, lane 11; ICLs were irradiated at 254 nm for 75 sec, lane 12; ICLs were irradiated at 254 nm for 90 sec, lane 13; ICLs were irradiated at 254 nm for 120 sec, lane 14; ICLs were irradiated at 254 nm for 180 sec.



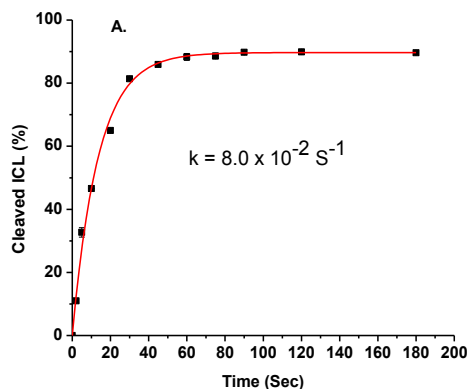


**Figure 27.** Photolytic cleavage growth of ICL from duplex-10

*Photolytic cleavage of coumarin-induced ICL materials for duplex 13* - Cleavage of ICL product of duplex **13** into two single stranded ODNs were investigated. Similar to the ICLs formed with duplex **10**, an ultrafast cleavage was observed with 90% of cleavage within 60 s upon 254 nm irradiation. The kinetic study of cleavage was studied over a longer time period and analyzed by PAGE (Figures 28 and 29).

ICLs have been identified on the basis of their electrophoretic mobility and the analysis of the percentage of the ICL cleavage (Figures 28 and 29). lane 1; SS as control, lane 2; ICL as control, lane 3; ICLs were irradiated at 254 nm for 0 sec, lane 4; ICLs was irradiated at 254 nm for 2 sec, lane 5; ICLs was irradiated at 254 nm for 5 sec, lane 6; ICLs was irradiated at 254 nm for 10 sec, lane 7; ICLs was irradiated at 254 nm for 20 sec, lane 8; ICLs was irradiated at 254 nm for 40 sec, lane 9; ICLs was irradiated at 254 nm for 50 sec, lane 10; ICLs was irradiated at 254 nm for 80 sec, lane 11; ICLs was irradiated at 254 nm for 120 sec, lane 12; ICLs was irradiated at 254 nm for 240 sec.

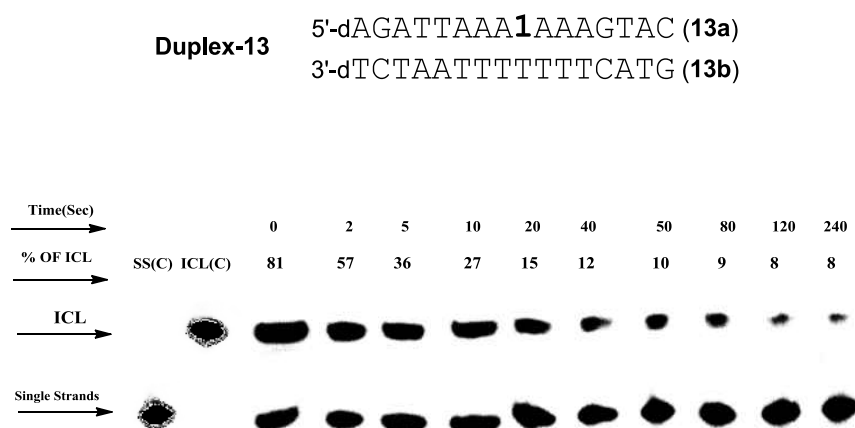


**Figure 28.** PAGE analysis of photolytic cleavage of ICL from duplex-13

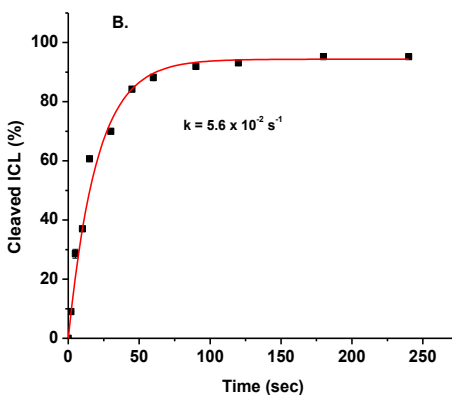


**Figure 29.** Photolytic cleavage growth of ICL from duplex-13

*Photolytic cleavage of coumarin-induced ICL materials for duplex 15* - Cleavage reaction of ICL products formed from duplex **15** was investigated as well. The kinetic study was studied over a longer time period and analyzed by PAGE analysis. Similar results as duplexes **10** and **13** were observed with duplex **15**. 90% of ICL products were completely cleaved to single stranded ODN within 60 s by 254 nm irradiation.

ICLs have been identified on the basis of their electrophoretic mobility and the analysis of the percent of ICL cleavage (Figures 30 and 31). lane 1-3; ICL as control; lane 4-6, ICLs was irradiated at 254 nm for 2 sec, lane 7-9; ICLs was irradiated at 254 nm for 4 sec, lane 10-12; ICLs was irradiated at 254 nm for 8 sec, lane 13-15; ICLs was irradiated at 254 nm for 15 sec, lane 16-18; ICLs was irradiated at 254 nm for 30 sec, lane 19-21 ; ICLs was irradiated at 254 nm for 60 sec, lane 22-24; ICLs was irradiated at 254 nm for 120 sec, lane 25-27; ICLs was irradiated at 254 nm for 300 sec

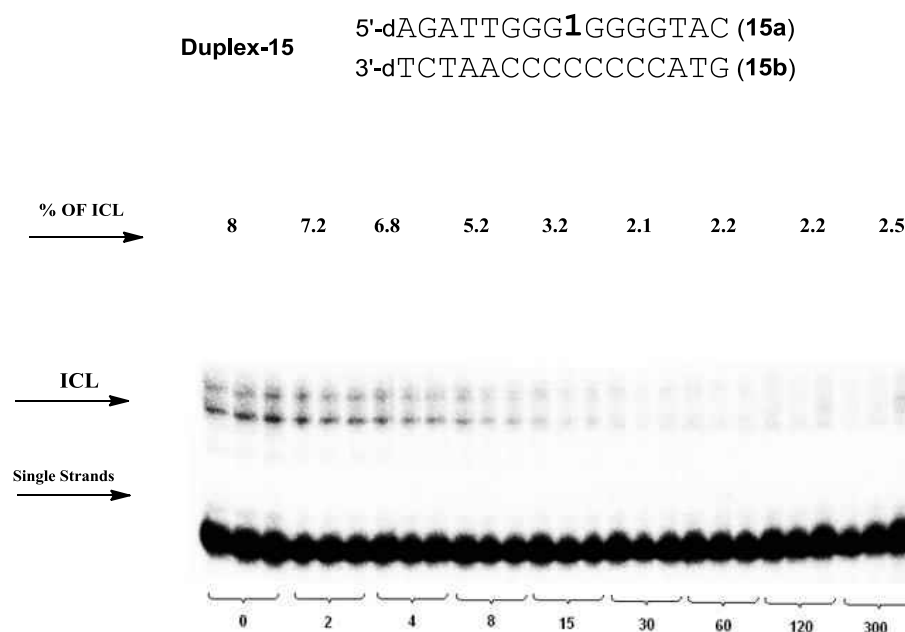


**Figure 30.** PAGE analysis of photolytic cleavage of ICL from duplex-15

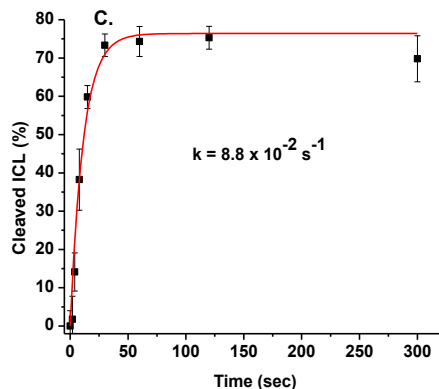


**Figure 31.** Photolytic cleavage growth of ICL from duplex-15

*Photolytic cleavage of coumarin induced ICL materials for duplex 12* – Different from duplexes **10**, **13**, and **15**, the ICL products formed with duplex **12** were stable to 250 nm irradiation. No cleavage was observed by irradiation at 250 nm for 15 min (Figure 32 and 33).

ICLs have been identified on the basis of their electrophoretic mobility and the analysis of the percent of ICL cleavage (Figures 32 and 33). lane 1; SS as control; lane 2; ICLs was irradiated at 254 nm for .25 min, lane 3; ICLs was irradiated at 254 nm for .5 min, lane 4; ICLs was irradiated at 254 nm for 1 min, lane 5; ICLs was irradiated at 254 nm for 2 min, lane 6; ICLs was irradiated at 254 nm for 3 min, lane 7; ICLs was irradiated at 254 nm for 4 min, lane 8; ICLs was irradiated at 254 nm for 5 min, lane 9; ICLs was irradiated at 254 nm for 6 min, lane 10; ICLs was irradiated at 254 nm for 7 min, lane 11; ICLs was irradiated at 254 nm for 8 min, lane 12; ICLs was irradiated at 254 nm for 12 min, lane 13; ICLs was irradiated at 254 nm for 15 min.



**Figure 32.** PAGE analysis of photolytic cleavage of ICL from duplex-12

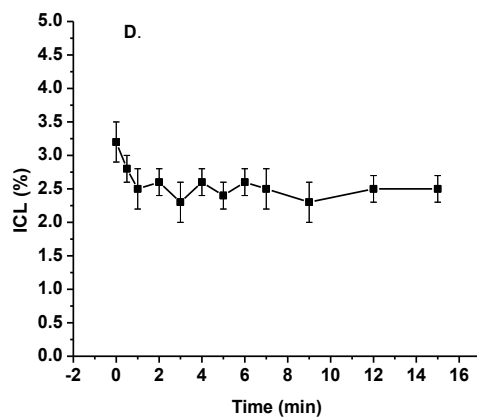


**Figure 33.** Photolytic cleavage growth of ICL from duplex-12

*Overall discussion* - Kinetic study of ICL photo-cleavage also showed that the ICLs formed from duplexes **13** (dT-1 cross-linking) and **15** (dC-1 cross-linking) via 350 nm irradiation were reversible by 254 nm irradiation, while ICL products generated from duplex **12** (dA-1 cross-linking) was not cleaved by irradiation at 254 nm. The photo-cleavage reaction of the ICL products formed with duplexes **13** and **15** is ultrafast and

complete within 90 s and 50 s, respectively (duplex **13**:  $k_{dT-1-cleave} = 5.0 \pm 0.9 \times 10^{-2} \text{ s}^{-1}$ ,  $t_{1/2} = 13.0 \text{ s}$ ; duplex **15**:  $k_{dC-1-cleave} = 8.8 \pm 0.4 \times 10^{-2} \text{ s}^{-1}$ ,  $t_{1/2} = 8.0 \text{ s}$ ). These data was consistent with the previous results obtained from LC-MS and MS/MS analysis.

### 3.3 Experimental Parts

#### Materials and methods:

Unless otherwise specified, all chemicals were purchased from Sigma-Aldrich or Fisher Scientific. Water was purified with a Milli-Q purification system. ODNs were synthesized via standard automated DNA synthesis techniques using an Applied biosystems model 394 instrument. The pac-dA and <sup>i</sup>Pr-Pac-dG phosphoramidites were employed for the synthesis of coumarin-dT containing ODNs. 28% NH<sub>3</sub> (aq) was used for the deprotection of the nucleobases and phosphate moieties at room temperature for 30 min. ODNs were subjected to 20% denaturing PAGE analysis for purification. The <sup>32</sup>P-labelled ODN (1.0 μM) was annealed with 1.5 equiv. of the complementary strand by heating to 65 °C for 3 min in a buffer containing 10 mM potassium phosphate, 100 mM NaCl, and pH 7.0 followed by a slow-cooling to room temperature overnight.

Radiolabeling was carried out according to the standard protocols.  $\gamma$ -<sup>32</sup>P-ATP and  $\alpha$ -<sup>32</sup>P-ATP was purchased from Perkin-Elmer Life Sciences. Quantification of radiolabeled ODNs was carried out using a Molecular Dynamics Phosphorimager equipped with ImageQuant Version 5.2 software. DNA duplexes were irradiated with 350 nm UV light. ICL was isolated and analyzed by enzymatic digestion reaction.

$^1\text{H-NMR}$  and  $^{13}\text{C-NMR}$  spectra were recorded on Bruker DRX 300 spectrometer operating at room temperature. Chemical shifts are reported in parts per million (ppm) relative to the residual solvent peak. Multiplicities are reported as singlet (s), doublet (d), doublet of doublets (dd), triplet (t) or multiplet (m). Enzymatic digestion of ICL and high resolution mass spectrometry were performed at the Department of Chemistry, University of California-Riverside.

*Solid-phase syntheses of ODN* - The ODNs were synthesized on automated DNA synthesizer in a CPG solid supports. Modified nucleotide **1** at concentration of  $154 \text{ mmol L}^{-1}$  in dry MeCN were coupled and commercial dA, dG, dC, and dT building blocks were used as phosphoramidites, which gave a 100% coupling efficiency. 1mL  $\text{NH}_3(\text{aq})$  solution was added for base deprotection followed by a 0.5 h occasional shaking and later dried. Crude ODNs were purified by gel electrophoresis.

*ODN Synthesis and Characterization* - ODNs were synthesized using standard solid-phase phosphoramidite chemistry. The coupling efficiency of the incorporation of the thieno-dT-containing nucleoside into the ODN was 75%. Purification was accomplished by preparative 20% of polyacrylamide gel electrophoresis. To verify the integrity and composition of the dT coumarin (**1**) -containing strand ODN **7a-15a**, the ODN was analyzed in spectroscopic emission spectrum study and MALDI-TOF analysis. In mass analysis, the sequence was determined by the total mass of the DNA molecule with coumarin.

*Desalination of ODN*- The largest band of ODN from gel electrophoresis was cut out of several bands and then grinded and centrifuged. Centrifuged ODN was used for

desalination by following procedure. First, the column was activated by running with 10mL MeCN, 10 mL H<sub>2</sub>O, and 3mL NH<sub>4</sub>OAC. Then the centrifuged ODN was slowly ran followed by a 30mL H<sub>2</sub>O and 3mL of MeOH and H<sub>2</sub>O mixture (3:2). The elute was collected into 3x1 small vials and were evaporated in a speed vacuum drier. After desalination, the ODN was dried and the concentration was determined.

*Preparation of DNA cross-linked products for LC-MS analysis* - The ICL reactions were performed using 10 μM coumarin-containing ODNs, which were annealed with 1.0 equiv. of the complementary strands by heating to 80 °C for 3 min in a buffer containing 10 mM pH 7 potassium phosphate buffer and 100 mM NaCl, followed by slowly cooling to room temperature overnight. The DNA duplexes were irradiated for 50 min with the UV light at 350 nm for the desired time to make sure that the reactions are completed. ICL products were isolated by 20% PAGE and Isolated ICLs were treated with a cocktail of four enzymes to release the ICL as a dinucleoside remnant and subjected the resulting mixture to LC-MS and MS/MS analyses. The instrument was set up for monitoring the fragmentation of the dinucleoside remnant of putative ICL products as [M+H]<sup>+</sup> ions in the positive-ion mode.

*Determination of DNA duplexes' thermal stability* - The melting temperature of coumarin containing ODN duplexes were performed by a Varian CARY-100 BIO UV-VIS spectrophotometer with the Cary Win UV Thermal program using a 1.0 cm path-length cell. All measurements were carried out in 10 mM potassium phosphate buffer (pH 7), 100 μM ethylenediaminetetraacetic acid (EDTA), and 100 mM NaCl, with 4 μM + 4 μM single strand concentration. Samples were heated at 1 °C min<sup>-1</sup> from 20 °C to 80 °C and



the absorbance of ODN at 260 nm was measured at 1.0 °C steps. At least two independent samples have been tested to get the melting temperatures of ODN duplexes.

*PAGE analysis of interstrand cross-link formation and kinetic study using 32P-labelling method* - ODNs (0.1 μM) without coumarin were 5'-32P-labeled and hybridized with 1.5 equiv. of the complementary strands in 100 mM NaCl and 10 mM potassium phosphate (pH 7). The ODN duplexes were irradiated at 350 nm to form ICLs (a control reaction was carried out without photoirradiation). Aliquots were taken at the prescribed time and immediately quenched with the equal volume of 95% formamide loading buffer, and stored at -20 °C until subjecting to 20% denaturing PAGE analysis. For kinetics study, three independent samples were used with the same procedures mentioned above.

*G+A sequencing* - after separation of ICL product, the reaction mixtures (0.35 μM ODN duplex, 20 μL) were co-precipitated with calf thymus DNA (2.5 mg/mL, 5 μL) and NaOAc (3 M, 5 μL) in the presence of EtOH (90 μL) at -80°C for 30 min and followed by centrifugation for 5 min at 15000rpm. The supernatant was removed, and the pellet was washed with cold 75% EtOH and lyophilized for 30 min in a Centrivap Concentrator of LABCONCO at 37°C. The dried ODN fragments were dissolved in H<sub>2</sub>O (30 μL) and incubated with piperidine (2 M, 10 μL) at 90°C for 30 min. The samples were then subjected to electrophoresis on a 20% denaturing polyacrylamide gel.

*Hydroxyl radical reaction (Fe (ii) EDTA reaction)* - The ICL was purified by 20% denaturing PAGE. The band containing cross-linked product was cut, crushed, and

eluted with 200 mM NaCl and 20 mM EDTA (2.0 mL). The crude product was further purified by C18 column eluting with H<sub>2</sub>O (3 × 1.0 mL) followed by MeOH:H<sub>2</sub>O (3:2, 1.0 mL). Fe(II)·EDTA cleavage reactions of <sup>32</sup>P-labelled oligonucleotide (0.1 μM) were performed in a buffer containing 50 μM (NH<sub>4</sub>)<sub>2</sub>Fe(SO<sub>4</sub>)<sub>2</sub>, 100 μM EDTA, 5 mM sodium ascorbate, 0.5 M NaCl, 50 mM sodium phosphate (pH 7.0) and 1 mM H<sub>2</sub>O<sub>2</sub> for 3 min at room temperature (total substrate volume of 20 μL). It was then quenched with 100 mM thiourea (10 μL). Samples were lyophilized, dissolved in 20 μL H<sub>2</sub>O: 90% formamide loading buffer (1:1), and subjected to 20% denaturing PAGE analysis.

*Enzymatic digestion of ICL mixture* - The isolated ICL products (50 pmol) were digested with nuclease P1 (0.5 unit) and phosphodiesterase 2 (0.005 unit) in a buffer (pH 5.6) containing 30 mM sodium acetate, 1.0 mM zinc acetate, and 1 mM *erythro*-9-(2-hydroxy-3-nonyl)adenine (EHNA) at 37°C for 48 h. Alkaline phosphatase (0.5 unit) and phosphodiesterase 1 (0.001 unit) were subsequently added to the digestion mixture and the reaction continued for 2 h in a 50-mM Tris-HCl buffer (pH 8.9). The enzymes were removed by chloroform extraction at the end of enzymatic digestion. The digestion products were then analyzed by LC-MS/MS/MS with an Agilent 1200 capillary HPLC pump (Agilent Technologies, Santa Clara, CA) and an LTQ linear ion-trap mass spectrometer (Thermo Fisher Scientific). A 0.5 × 250 mm Zorbax SB-C18 column (5 μm in particle size, Agilent Technologies) was used. A solution of 0.1% (v/v) formic acid in water (solution A) and a solution of 0.1% (v/v) formic acid in methanol (solution B) were employed as mobile phase at a flow rate of 8.0 μL/min. A gradient of 5 min 0-20% B and 25 min 20-70% B were used for the separation. The instrument was set up for

monitoring the fragmentation of the  $[M+H]^+$  ions of putative ICL products in the positive-ion mode.

*PAGE analysis of photo-induced (254 nm) cleavage reactions of DNA ICL products and kinetic study* - The cleavage reactions of ICL product were carried out with photoirradiation at 254 nm using two independent samples. Aliquots were taken at the prescribed time and immediately quenched with the equal volume of 95% formamide loading buffer, and stored at  $-20\text{ }^{\circ}\text{C}$  until subjected to 20% denaturing PAGE analysis.

**5-(4-Methylchromen-2-one-1,2,3-triazol-1-yl)methyl-2'-deoxyuridine (1).** To a solution of 7-ethynyl-4-methyl-chromen-2-one (**3**, 200 mg, 1.08 mmol) and 5-azido methyl-2'-deoxyuridine (**2**) (270 mg, 0.954 mmol) in MeOH (8 mL), a 0.296 M aqueous solution of Na-ascorbate (6 mL) was added followed by a 0.368 M aqueous solution of  $\text{Cu}_2\text{SO}_4$  (3.6 mL). After one hour, TLC confirmed completion of the reaction. The reaction mixture was evaporated to dryness and subjected to flash chromatography (DCM/MeOH, 20:1-7:1) yielding compound **1** (329 mg, 74%) as a white foam.  $^1\text{H}$  NMR (DMSO-*d*<sub>6</sub>, 300 MHz):  $\delta$  11.60 (s, NH), 8.69 (s, 1H), 8.23 (s, 1H), 7.91-7.90 (d,  $J = 3$  Hz, 1 H), 7.88-7.87 (d,  $J = 3$  Hz, 1H), 7.82 (s, 1H), 6.39 (s, 1H), 6.19-6.15 (t,  $J = 12$  Hz, 1H), 5.29-5.27 (m, 1H), 5.26 (s, 2H), 5.06-5.03 (t,  $J = 9$  Hz, 1H), 4.28-4.25 (m, 1H), 3.81-3.80 (d,  $J = 3$  Hz, 1H), 3.62-3.56 (d,  $J = 18$ , 2H), 3.33 (s, 3H), 2.19-2.15 (t,  $J = 12$  Hz, 2H);  $^{13}\text{C}$  NMR (DMSO-*d*<sub>6</sub>, 300 MHz):  $\delta$  163.05, 160.23, 153.98, 153.50, 150.74, 145.07, 141.89, 134.77, 126.59, 123.17, 121.43, 119.45, 114.51, 112.75, 107.52, 88.04, 85.02, 70.62, 61.64, 47.03, 22.98, 18.52; MALDI-MS  $[\text{MH}^+]$  calcd. for  $\text{C}_{22}\text{H}_{21}\text{N}_5\text{O}_7$ , 468.1519; found, 468.1515.

**5'-O-(4,4'-Dimethoxytriphenylmethyl)-5-(4-methylchromen-2-one-1,2,3-triazol-1-yl)methyl-2'-deoxyuridine (4).** Compound **1** (0.3 g, 0.64 mmol) was co-evaporated with anhydrous pyridine (3×5 mL) and then dissolved in pyridine (5 mL). To the solution, 4, 4'-dimethoxytriphenylmethyl chloride (0.304 g, 0.90 mmol) was added in two portions and the reaction mixture was stirred at r. t. for 8 h. The reaction was quenched by addition of MeOH and was concentrated *in vacuo*. The crude product was purified by flash chromatography (CH<sub>2</sub>Cl<sub>2</sub>/MeOH/Et<sub>3</sub>N = 96/3/1) to give **4** (0.345 g, 68%) as a off-white solid. <sup>1</sup>H NMR (CDCl<sub>3</sub>, 300 MHz): δ 7.92-7.60 (m, 4H), 7.47-6.87 (m, 15H), 6.47-6.43 (t, *J* = 12 Hz, 1H), 4.83 (s, 2H), 4.43-4.38 (t, *J* = 15 Hz, 1H), 4.18-4.17 (d, *J* = 3 Hz, 1H), 4.15-4.01 (s, 3H), 3.48-4.39 (m, *J* = 27 Hz, 1H), 2.74 (s, 6H), 2.72-2.67 (d, *J* = 15 Hz, 2H), 2.44-2.38 (t, *J* = 18 Hz, 2H); <sup>13</sup>C NMR (CDCl<sub>3</sub>, 300 MHz): δ 164.58, 161.45, 158.76, 158.73, 153.85, 152.88, 149.92, 145.96, 144.50, 141.54, 135.47, 135.23, 134.70, 130.25, 130.15, 128.17, 128.15, 127.18, 124.99, 122.29, 121.68, 119.30, 114.49, 113.91, 113.44, 108.18, 87.08, 86.89, 85.96, 77.47, 77.25, 76.62, 72.29, 63.62, 55.27, 46.18, 46.06, 42.18, 29.70, 18.66, 10.67, 1.02; MALDI-MS [MNa<sup>+</sup>] calcd. for C<sub>43</sub>H<sub>39</sub>N<sub>5</sub>O<sub>9</sub>, 792.2645; found, 792.2624.

**5'-O-(4,4'-Dimethoxytriphenylmethyl)-5-(4-methylchromen-2-one-1,2,3-triazol-1-yl)methyl-2'-deoxyuridine-3'-(2-cyanoethyl)-*N,N*-diisopropylphosphoramidite (4a).** Compound **4** (0.2 g, 0.25 mmol) was dissolved in anhydrous CH<sub>2</sub>Cl<sub>2</sub> (5 mL) under Ar atmosphere. Diisopropylethylamine (96 μL, 0.55 mmol) and 2-cyanoethyl-*N,N*-diisopropylchlorophosphoramidite (96 μL, 0.43 mmol) was added. The reaction mixture was stirred at r.t. for 30 min, diluted with CH<sub>2</sub>Cl<sub>2</sub> (30 mL), washed with 5% aqueous NaHCO<sub>3</sub> solution, followed by brine. The organic solution was dried over anhydrous

Na<sub>2</sub>SO<sub>4</sub>, filtered, and concentrated. The residue was submitted to flash chromatography (EtOAc/CH<sub>2</sub>Cl<sub>2</sub>/Et<sub>3</sub>N = 66/33/1) to yield product **4a** (0.200 g, 80%) as a white foam. <sup>31</sup>P NMR (CDCl<sub>3</sub>, 300 MHz): δ 150.0, 150.2.

## Chapter 4

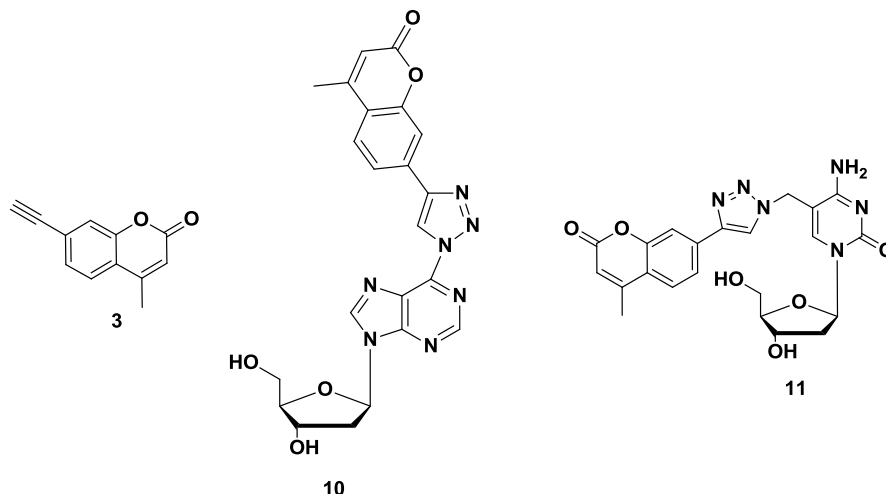
### Synthesis of Coumarin-Modified 2'-Deoxycytosine (dC) and 2'-Deoxyadenosine (dA) by "Click" Chemistry

#### 4.1 Background

Modification of nucleosides are extremely important for versatile fields of medicinal chemistry and chemical biology research. The "click" reaction is very useful for conjugating or functionalizing the nucleotide molecule under mild conditions and has wide applications in the emerging field of cell biology and functional proteomics. The enhancement of fluorescent properties within purine and pyrimidine nucleoside scaffolds is extremely important and versatile, and has wide biological applications. Many intense research work was done to discover fluorescent base analogs using stilbene, terphenyl, pyrene, phenanthrene, terthiophene, and benzoterthiophene [162]. Some groups have replaced the natural base with coumarin dye [136, 164], tethered stilbene [165], and pteridine dyes [166] which exhibit the aforementioned fluorescent moiety. Fluorophores also have been widely studied and reviewed for labeling of DNA [167-172].

Still there is a need for development and synthesis of newly modified fluorescent nucleosides that can act as novel analogs and act as precisely advantageous reporter probes with other exceptional biological properties in the ODN environment. Here, we performed an extended conjugation of coumarin to dA and dC. Cu-mediated azide-alkyne "click" reaction was undertaken smoothly between alkyne modified coumarin

derivative **3** and the azide modified dC and dA with excellent yields to form compounds **10** and **11**.



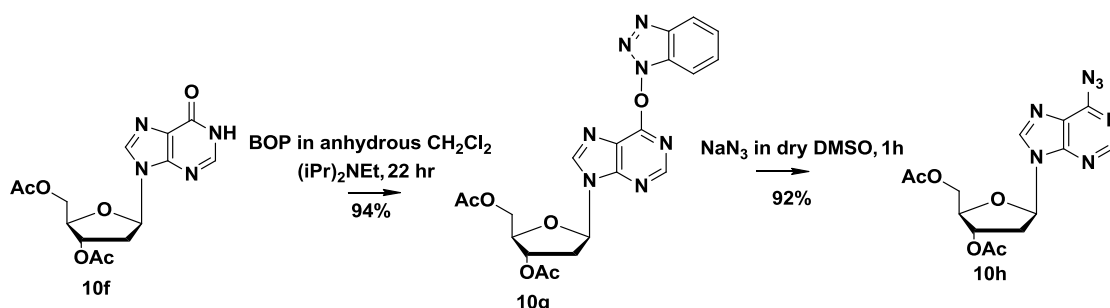
## 4.2 Results and discussion

### 4.2.1 Synthesis of Coumarin-Containing dA (**10**)

On behalf of conjugation of coumarin at the 6-position of dA via a triazole, “click” chemistry procedure was followed after modification of dA with azide. Initially two different routes were employed depending on protection of extremely nucleophilic 3' and 5'OH functional groups for the modification reactions; (i) introduction of base labile acetate-protecting group at the 3'- and 5'- OH group of dA precursor then conversion to coumarin-conjugated dA (Scheme 10 and Figure 34) and (ii) introduction of acid labile silyl group at the 3'- and 5'- OH group of dA precursor then conversion to coumarin-conjugated dA (Scheme 11 and 12)

*Synthesis of 6-azido-3', 5'-di-O-(tert-butyl dimethylsilyl)-9-[2-deoxy-β-D-ribofuranosyl]adenosine (**10h**)* – For the first route synthesis, dA was used as a starting material.

Deamination reaction was taken place with  $\text{NaNO}_2$  in glacial acetic acid to form **10a**, product **10a** was used for acetate protection reaction with acetic anhydride in pyridine solution giving **10f** following the known procedure [350](Scheme 10). Compound **10f** was reacted with (Benzotriazol-1-yloxy)tris(dimethylamino)phosphonium hexafluorophosphate (BOP) under the catalysis of  $(i\text{Pr})_2\text{NEt}$  in anhydrous  $\text{CH}_2\text{Cl}_2$  to give **10g** with 94% yield. Subsequent reaction with sodium azide in anhydrous DMSO results acetate-protected azide modified dA (**10h**) with 92% yield (Scheme 10). Similar NMR of **10h** was found to previously published NMR of same compound [350].



**Scheme 10.** Synthesis of azide modified dA

*“Click” reaction and deprotection of acetate group* -The next stage involved the azide-alkyne ligation reaction of coumarin using the optimized conditions of “click” reaction ( $\text{CuSO}_4/\text{Na-ascorbate}$  in  $\text{CH}_2\text{Cl}_2/\text{H}_2\text{O}$ ). Successful ligation was taken place by “click” reaction of coumarin 7-Ethynyl-4-methyl-chromen-2-one (**3**) and **10h** to form **10i** in 76% yield. Deprotection reaction of compound **10i** was run with aqueous  $\text{NH}_3$  in dioxane solution. The deprotection reaction did not go well and desired product was not obtained. Compound **10** was decomposed after three days as shown in TLC (Figure 34).



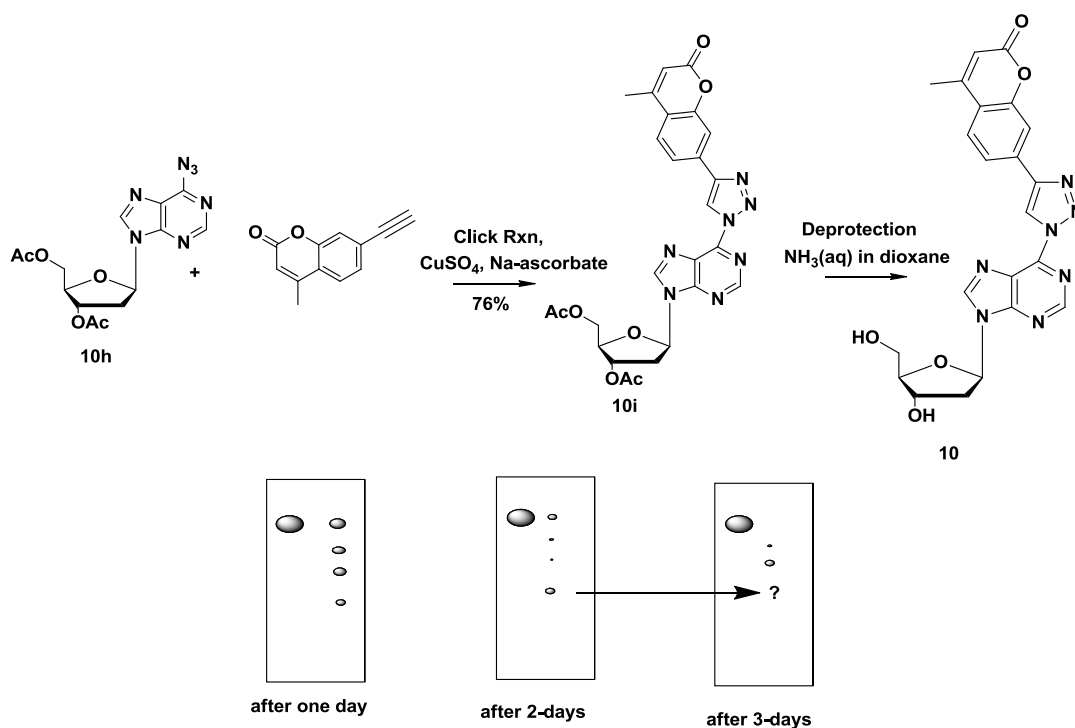
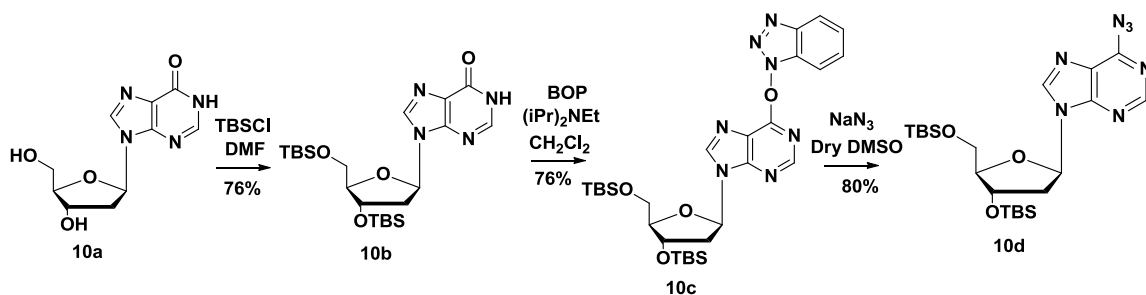


**Figure 34.** Synthesis of coumarin modified dA

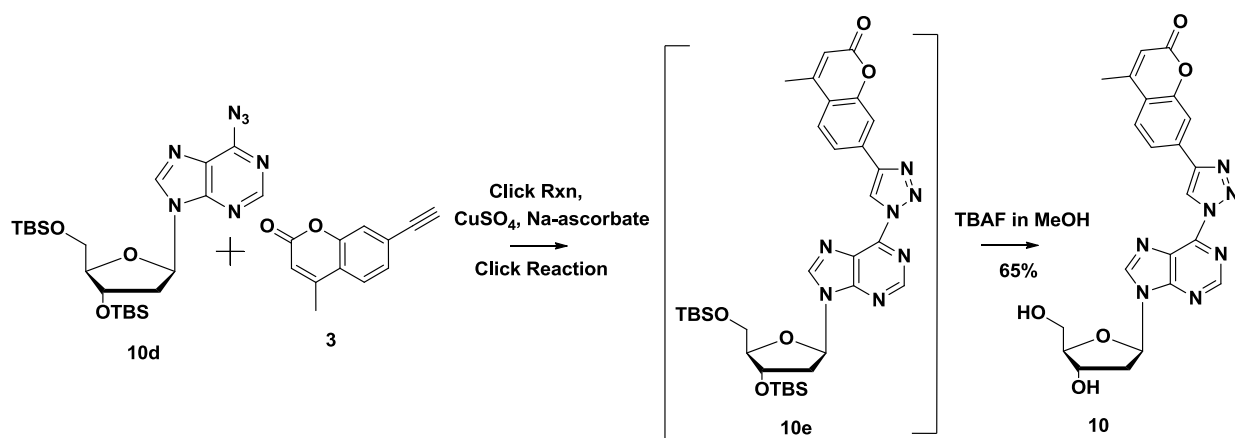
*Synthesis of 6-Azido-3',5'-Di-O-(tert-butyldimethylsilyl)-9-[2-deoxy-β-D-ribofuranosyl] adenosine (10d)* - Since basic condition for acetate deprotection was not compatible with coumarin-modified dA, we switched to the second route where dA was protected at the 3'- and 5'-OH functional group with silyl group. First, the silyl protection reaction was run with previously synthesized deaminated dA (**10a**) which reacted with tert-butyldimethylsilyl chloride (TBAF) in the presence of imidazole in dry DMF solution giving **10b** (Scheme 11) with 76% yield. Compound **10b** then reacted with BOP under the catalysis of (<sup>i</sup>Pr)<sub>2</sub>NEt in anhydrous CH<sub>2</sub>Cl<sub>2</sub> to form 76% of **10c**. Subsequent

reaction with sodium azide in anhydrous DMSO resulted in azide-modified adenosine with silyl-protected dA (**10d**) with 80% yield (Scheme 11).



**Scheme 11.** Synthesis of azide-modified dA

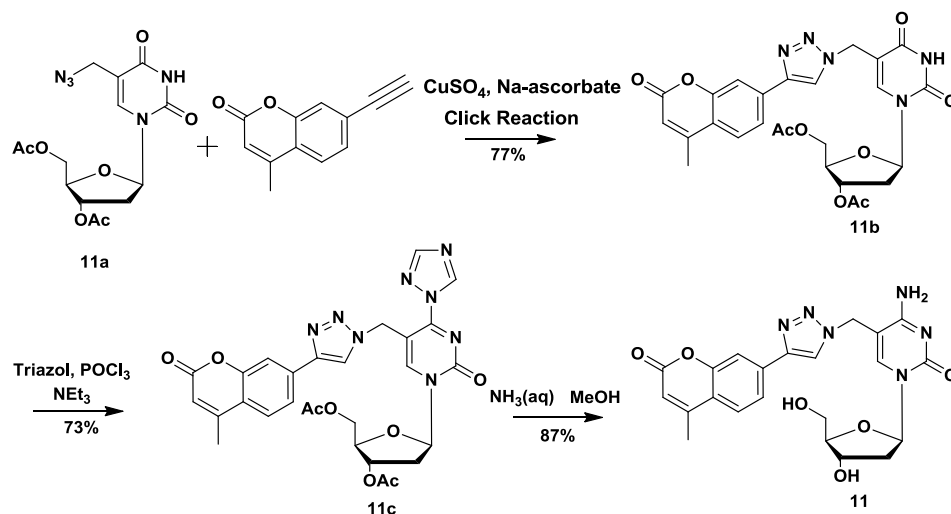
*Synthesis of 6-(4-methylchromen-2-one-1,2,3-triazol-1-yl)-9-[2-deoxy- $\beta$ -D-ribofuranosyl]purine (**10**)* - The next step involved the azide-alkyne “click” conjugation reaction using the optimized conditions (CuSO<sub>4</sub>/Na-ascorbate in CH<sub>2</sub>Cl<sub>2</sub>/H<sub>2</sub>O). Successful conjugation was taken place between presynthesized 7-ethynyl-4-methyl-chromen-2-one (**3**) and **10d** to form **10e**. Deprotection reaction of silyl group in compound **10e** was run without separation with TBAF in MeOH solution. The deprotection reaction went very well and the desired deprotected coumarin-conjugated dA, 6-(4-methylchromen-2-one-1,2,3-triazol-1-yl)-9-[2-deoxy- $\beta$ -D-ribofuranosyl]adenosine (**10**) was accomplished with 65% yield in two steps.



**Scheme 12.** Synthesis of coumarin-modified dA

#### 4.2.2 Synthesis of Coumarin-Containing dC (11)

To synthesize **11**, the optimized conditions of “click” reaction were used with sodium ascorbate and copper sulphate in water and dichloromethane solution. Successful coumarin ligation was performed via the reaction between previously synthesized precursor 7-ethynyl-4-methyl-chromen-2-one (**3**) and azide-modified dT (**11a**) to yield **11b** in a good yield (77%). Compound **11b** and 1,2,4-triazole were suspended in anhydrous  $\text{CH}_3\text{CN}$  and  $\text{Et}_3\text{N}$  and phosphorous oxytrichloride (2.2 mL, 24.0 mmol) was added. The reaction mixture was stirred at r.t. for one hour and compound **11c** was formed with 73% yield. Subsequently, deprotection reaction of **11c** was taken place with  $\text{NH}_3$  (Aq) in MeOH solution to produce coumarin-modified deprotected nucleoside 5-(4-methylchromen-2-one-1,2,3-triazol-1-yl)methyl-2'-deoxycytosine (**11**) with 65% yield (Scheme 13).



**Scheme 13.** Synthesis of coumarin-modified dC

### 4.3 Experimental parts.

**3',5'-Di-O-acetyl-O<sup>6</sup>-(benzotriazol-1-yl)-2'-deoxyinosine (10g).** In a clean, dry 100 mL round-bottom flask equipped with a stirring bar, placed 2'-deoxyinosine 3',5'-diacetate **10f** (300 mg, 0.893 mmol) and BOP (790 mg, 1.79 mmol) in anhydrous CH<sub>2</sub>Cl<sub>2</sub> (8.0 mL). To this stirred mixture, (i-Pr)<sub>2</sub>NEt<sub>3</sub> (0.31 mL, 1.79 mmol) was added, and the stirring was continued at room temperature for 22 h. The mixture was evaporated to dryness, and the residue was redissolved in EtOAc. The mixture was washed with water and then with brine. The organic layer was dried over Na<sub>2</sub>SO<sub>4</sub> and concentrated under reduced pressure. The crude product was purified by column chromatography on silica gel using EtOAc/hexanes (1:5-1:3) to provide **10g** as a white foamy solid (382 mg, 94% yield). <sup>1</sup>HNMR (300MHz, CDCl<sub>3</sub>) is similar to those described in ref [350]

**6-Azido-3'5'-Di-O-acetyl-O6-(benzotriazol-1-yl)-2'-deoxyinosine (10h).** In a clean, dry vial equipped with a stirring bar were placed **10g** (249mg, 0.550 mmol) and  $\text{NaN}_3$ (107 g, 1.65 mmol) in DMSO (2.5mL). The mixture was flushed with nitrogen gas and stirred at room temperature for 1 h at which time TLC indicated the reaction to be complete. The mixture was diluted with EtOAc and transferred to a separatory funnel. The mixture was extracted with 1:1 water-brine (3x), water (3x), and finally once with brine. The organic layer was dried over  $\text{Na}_2\text{SO}_4$  and evaporated under reduced pressure. Chromatography of the crude material on a silica gel column using EtOAc/hexanes (1:5-1:3) afforded a white foamy material **10h**(182 mg, 92% yield):  $^1\text{H}$ NMR(300MHz,  $\text{CDCl}_3$ ) is similar to those described in ref [350]

**6-Azido-(4-methylchromen-2-one-1,2,3-triazol-1-yl)-3'5'-Di-O-acetyl-O6-(benzotriazol-1-yl)-2'-deoxyinosine (10i).** To a solution of 6-Azido-3'5'-Di-O-acetyl-O6-(benzotriazol-1-yl)-2'-deoxyinosine **10h** (390 mg, 1.08 mmol) and compound **3** (175 mg, 0.954 mmol) in DCM (8 mL), a 0.296 M aqueous solution of Na-ascorbate (6 mL) was added followed by a 0.368 M aqueous solution of  $\text{Cu}_2\text{SO}_4$  (3.6 mL). After one hour, TLC confirmed completion of the reaction. The reaction mixture was evaporated to dryness and subjected to flash chromatography (DCM/MeOH, 20:1-7:1) yielding white foamy material **10i** (451 mg, 76% yield):  $^1\text{H}$  NMR (300 MHz,  $\text{CDCl}_3$ ):  $\delta$  9.36 (s, 1H), 9.17 (s, 1H), 8.57 (s, 1H), 8.17-8.11 (d,  $J=18$ , 1H), 8.87 (s, 1H), 8.77-8.73 (d,  $J=12$ , 1H), 7.37 (s, 1H), 6.61-6.59 (t,  $J=6.0$  Hz, 1H), 5.50-5.41 (m, 1H), 4.37-4.29 (m, 2H), 2.94-2.86 (m, 1H), 2.54-2.50 (s, 2H), 2.40 (s, 3H), 2.11 and 2.01 (2s, 6H).  $^{13}\text{C}$  NMR (300MHz,  $\text{CDCl}_3$ ):  $\delta$  170.1, 160.0, 253.1, 152.2, 151.9, 151.5, 148.0, 147.5, 147.3, 145.4, 133.8, 126.1, 125.6, 125.2,

124.1, 120.3, 121.2, 115.0, 116.1, 84.4, 83.1, 73.0, 63.4, 39.1, 19.8, 18.5. MALDI-ESI

[MH<sup>+</sup>] calcd. for C<sub>22</sub>H<sub>21</sub>N<sub>5</sub>O<sub>7</sub>, 446.17; found, 446.17.

**3',5'-O-Bis(tert-butyldimethylsilyl)-2'-deoxyinosine (10b).** Compound **10a** (252 mg, 1 mmol) was rendered by repeated co-evaporation with dry pyridine (3 times) and dry toluene (3 times) and dissolved in DMF (10 mL). To the solution were added imidazole (335 mg, 5 mmol) and tert-butyldimethylsilyl chloride (362 mg, 2.4 mmol). After being stirred at room temperature for 3 h, the solution was diluted with CHCl<sub>3</sub> (80 mL), and the mixture was washed three times with saturated NaHCO<sub>3</sub>. The organic layer was collected, dried over Na<sub>2</sub>SO<sub>4</sub>, filtered, and evaporated under reduced pressure. The crude product was purified by silica gel chromatography with 80% EtOAc in hexanes to give the product **10b** (363 mg, 76%): <sup>1</sup>HNMR(300MHz, CDCl<sub>3</sub>) is similar to those described in ref [350]

**3',5'-O-Bis(tert-butyldimethylsilyl)-O6-(benzotriazol-1-yl)-2'-deoxyinosine (10c).** In a clean, dry vial equipped with a stirring bar were placed **10b** (300 g, 0.625 mmol), BOP (673 mg, 1.52 mmol), anhydrous CH<sub>2</sub>Cl<sub>2</sub> (8.0mL), and (i-Pr)<sub>2</sub>NEt (0.26 mL, 1.52 mmol). The crude product was purified by column chromatography on silica gel using 40% EtOAc in hexane to provide **10c** as a white foamy solid (283 mg, 76% yield). <sup>1</sup>HNMR(300MHz, CDCl<sub>3</sub>) is similar to those described in ref [350]

**6-Azido-9-[2-deoxy-3,5-di-O-(tert-butyldimethylsilyl)-β-D-ribofuranosyl]purine (10d).** In a clean, dry 50 mL round-bottomed flask equipped with a stirring bar were placed O6-(benzotriazol-1-yl)-2',3'-di-O-(tert-butyldimethylsilyl)-2'-deoxyinosine (**10c**) (1.036 g, 1.73 mmol) and NaN<sub>3</sub> (326 mg, 5.0 mmol) in anhydrous DMSO (8.6 mL). The

reaction mixture was transferred to a separatory funnel and partitioned between EtOAc and a 1:1 mixture of water-brine. The organic layer was washed with 1:1 water-brine mixture, then with water, and finally with brine. The organic layer was dried over  $\text{Na}_2\text{SO}_4$  and evaporated under reduced pressure. Filtration of the crude material through a silica gel plug using 20% EtOAc in hexanes solution afforded **10d** as a clear gum (700 mg, 80%).  $^1\text{H}$ NMR (300MHz,  $\text{CDCl}_3$ ) is similar to those described in ref [350]

**Synthesis of 6-(4-methylchromen-2-one-1,2,3-triazol-1-yl]-9-(2'-deoxy- $\beta$ -D-ribofuranosyl)purine (10).** To a solution of 7-ethynyl-4-methyl-chromen-2-one (**3**, 200 mg, 1.08 mmol) and **10d** (270 mg, 0.534 mmol) in MeOH (8 mL), a 0.296 M aqueous solution of Na-ascorbate (6 mL) was added followed by a 0.368 M aqueous solution of  $\text{Cu}_2\text{SO}_4$  (3.6 mL). After one hour, TLC confirmed completion of the reaction. The reaction mixture of nucleoside derivative **10e** was evaporated to dryness and dissolved in methanol (25 mL) and tetrabutylammomium fluoride (4 mL 1.0 M solution in THF, 4.0mmol) was added to the solution. The reaction mixture was stirred at 60°C for 3 hours for complete deprotection reaction of silyl group. After cooling to room temperature, the crude product was evaporated and purified on silica gel (DCM:MeOH=5:1) to obtain **10** as a white solid (0.35 mmol, 65 % yield in two steps).  $^1\text{H}$  NMR (300 MHz,  $\text{DMSO}-d_6$ ):  $\delta$  9.36 (s, 1H), 9.17 (s, 1H), 8.57 (s, 1H), 8.17-8.11 (d,  $J=18$ , 1H), 8.87 (s, 1H), 8.77-8.73 (d,  $J=12$ , 1H), 7.37 (s, 1H), 6.61-6.59 (t,  $J=6.0$  Hz, 1H), 5.50-5.41 (m, 1H), 4.37-4.29 (m, 2H), 2.94-2.86 (m, 1H), 2.54-2.50 (s, 2H), 2.40 (s, 3H), 2.11 and 2.01 (2s, 6H).  $^{13}\text{C}$  NMR (300MHz,  $\text{CDCl}_3$ ): $\delta$  170.1, 160.0, 253.1, 152.2, 151.9, 151.5,

148.0, 147.5, 147.3, 145.4, 133.8, 126.1, 125.6, 124.1, 120.3, 121.2, 115.0, 116.1, 84.4, 83.1, 73.0, 63.4, 39.1, 20.91, 19.8, 18.5.

**5-(4-methylchromen-2-one-1,2,3-triazol-1-yl)methyl-2'-deoxyuridine (11b).** To a solution of 7-ethynyl-4-methyl-chromen-2-one (**3**, 200 mg, 1.08 mmol) and 5-azido-methyl-2'-deoxyuridine (**11a**) (350 mg, 0.954 mmol) in MeOH (8 mL), a 0.296 M aqueous solution of Na-ascorbate (6 mL) was added followed by a 0.368 M aqueous solution of Cu<sub>2</sub>SO<sub>4</sub> (3.6 mL). After one hour, TLC confirmed completion of the reaction. The reaction mixture was evaporated to dryness and subjected to flash chromatography (DCM/MeOH, 20:1-7:1) yielding compound **11b** (405 mg, 77%) as a white foam. <sup>1</sup>H NMR (CDCl<sub>3</sub>, 300 MHz): δ 8.29 (s, 1H), 7.95 (s, 1H), 7.85-7.80 (d, *J* = 3 Hz, 1 H), 7.76 (s, 1H), 7.58-7.57 (d, *J* = 3 Hz, 1H), 7.56 (s, 1H), 7.54 (s, 1H), 6.39 (s, 1H), 6.19-6.15 (t, *J* = 12 Hz, 1H), 5.29-5.27 (m, 1H), 5.26 (s, 2H), 5.06-5.03 (t, *J* = 9 Hz, 1H), 4.28-4.25 (m, 1H), 3.81-3.80 (d, *J* = 3Hz, 1H), 3.62-3.56 (d, *J* = 18, 2H), 3.33 (s, 3H), 2.19-2.15 (t, *J* = 12Hz, 2H), 2.11 and 2.01 (2s, 6H).

**3',5'-bis-O-Acetyl-5-(4-methylchromen-2-one-1,2,3-triazol-1-yl)methyl-N4-triazoyl-2'-deoxyuridine (11c).** Compound **11b** (2.80g, 5.2 mmol) and 1,2,4-triazole (7.25 g, 0.105 mol) were suspended in anhydrous CH<sub>3</sub>CN (50 mL). Et<sub>3</sub>N (16 mL) and phosphorous oxytrichloride (2.2 mL, 24.0 mmol) were added. The reaction mixture was stirred at r.t. for one hour, diluted with ethyl acetate (100 mL) and washed with saturated NaHCO<sub>3</sub> and brine. The organic solution was dried over anhydrous Na<sub>2</sub>SO<sub>4</sub>, concentrated and the residue was submitted to flash chromatography (column 6 × 12 cm, EtOAc/Hexanes, 1:1 →4:1) yielding a colorless foam **11c** (2.3 g, 73 %). <sup>1</sup>H NMR



(CDCl<sub>3</sub>, 300 MHz):  $\delta$  8.21 (s, 1H), 8.19 (s, 1H), 7.85-7.80 (d,  $J = 3$  Hz, 1 H), 8.79 (s, 1H), 7.58-7.57 (d,  $J = 3$  Hz, 1H), 7.56 (s, 1H), 7.82 (s, 1H), 6.39 (s, 1H), 6.19-6.15 (t,  $J = 12$  Hz, 1H), 5.29-5.27 (m, 1H), 5.26 (s, 2H), 5.06-5.03 (t,  $J = 9$  Hz, 1H), 4.28-4.25 (m, 1H), 3.81-3.80 (d,  $J = 3$ Hz, 1H), 3.62-3.56 (d,  $J = 18$ , 2H), 3.33 (s, 3H), 2.19-2.15 (t,  $J = 12$ Hz, 2H), 2.11 and 2.01 (2s, 6H): <sup>13</sup>C NMR (DMSO-*d*<sub>6</sub>, 300 MHz): $\delta$  170.6, 170.1, 163.05, 160.23, 153.98, 155.0, 154.1, 153.50, 152.74, 145.07, 141.89, 134.77, 126.59, 123.17, 121.43, 119.45, 114.51, 112.75, 99.52, 88.04, 85.02, 70.62, 61.64, 47.03, 36.98, 21.3, 21.4, 18.52

**5-(4-methylchromen-2-one-1,2,3-triazol-1-yl)methyl-2'-deoxycytidine (11)**. Compound **11c** (2.2 g, 3.65 mmol) was dissolved in dioxane (45 mL). Aqueous NH<sub>3</sub> (28%, 45 mL) was added and the reaction mixture was stirred at r.t. overnight. After evaporation, the residue was subjected to flash chromatography (column 6 × 12 cm, CH<sub>2</sub>Cl<sub>2</sub>/MeOH, 9:1 → 4:1). The fractions containing the desired material were collected and evaporated to dryness to give **11** as colorless solid (1.12 g, 87%). <sup>1</sup>H NMR (DMSO-*d*<sub>6</sub>, 300 MHz):  $\delta$  8.70 (s, NH<sub>2</sub>), 8.11 (s, 1H), 7.90 (s, 1H), 7.85-7.80 (d,  $J = 3$  Hz, 1 H), 7.88-7.87 (d,  $J = 3$  Hz, 1H), 7.82 (s, 1H), 6.39 (s, 1H), 6.19-6.15 (t,  $J = 12$  Hz, 1H), 5.29-5.27 (m, 1H), 5.26 (s, 2H), 5.06-5.03 (t,  $J = 9$  Hz, 1H), 4.28-4.25 (m, 1H), 3.81-3.80 (d,  $J = 3$ Hz, 1H), 3.62-3.56 (d,  $J = 18$ , 2H), 3.33 (s, 3H), 2.19-2.15 (t,  $J = 12$ Hz, 2H): <sup>13</sup>C NMR (DMSO-*d*<sub>6</sub>, 300 MHz): $\delta$  163.05, 160.23, 153.98, 153.50, 152.74, 145.07, 141.89, 134.77, 126.59, 123.17, 121.43, 119.45, 114.51, 112.75, 99.52, 88.04, 85.02, 70.62, 61.64, 47.03, 22.98, 18.52; MALDI-MS [MH<sup>+</sup>] calcd. for C<sub>22</sub>H<sub>22</sub>N<sub>6</sub>O<sub>6</sub>, 467.1667; found, 467.1667.

## Chapter 5

### Modified 2'-Deoxythymidine (dT) and Oligodeoxynucleotide (ODN) Containing Triazole and Phenyl Triazole: Synthesis and Properties

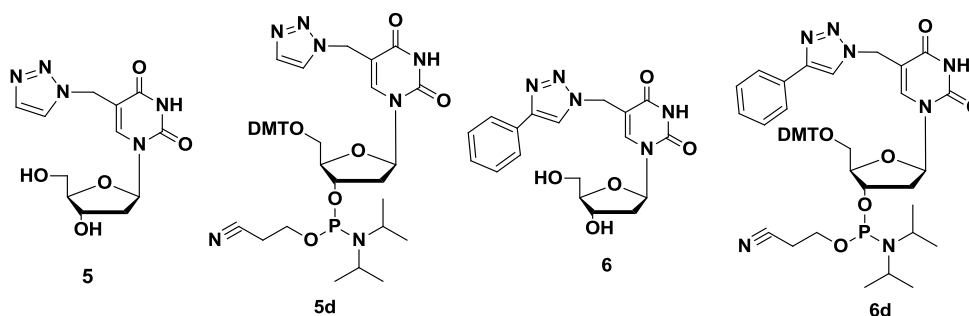
#### 5.1 Background

Among the broad range of heterocyclic molecule, triazole is an ideal molecule and great attraction for researchers. Significant amount of research have shown that the triazole and its derivatives have strong effect on anti-antiviral anti-HIV, antibacterial [143], antitubercular [174], anti-allergenic, antimicrobial, cytostatic, virostatic, anti-inflammatory, anti-bacterial activities, antifungal [175-177], and antitumor [178] activities. Moreover they have been used as herbicides, light stabilizers, fluorescent whiteners, optical brightening agents, pigments, and corrosion retardants. However, there is currently no significant research involving the photo-physical activities of triazole heterocycles with pyrimidine in nucleic acids. Considering the broad spectrum of activities that triazole exhibit; 1,2,3-triazole and phenyl substituted 1,2,3-triazole was conjugated with dT and their photophysical property in DNA was investigated as they might change the microenvironment of the DNA duplex and significantly alter the biological properties relative to a bare DNA.

In this research, 1,2,3-triazole- and 4-phenyl-1,2,3-triazole-conjugated dT (**5** and **6**) were respectively obtained by using the CuAAC (Cu-catalyzed alkyn-azide cycloaddition) "click" reaction and were introduced into the ODN after making the

appropriate phosphoramidite building blocks (**5d** and **6d**) in only a few synthetic steps.

Stability and photophysical characteristics were analyzed.

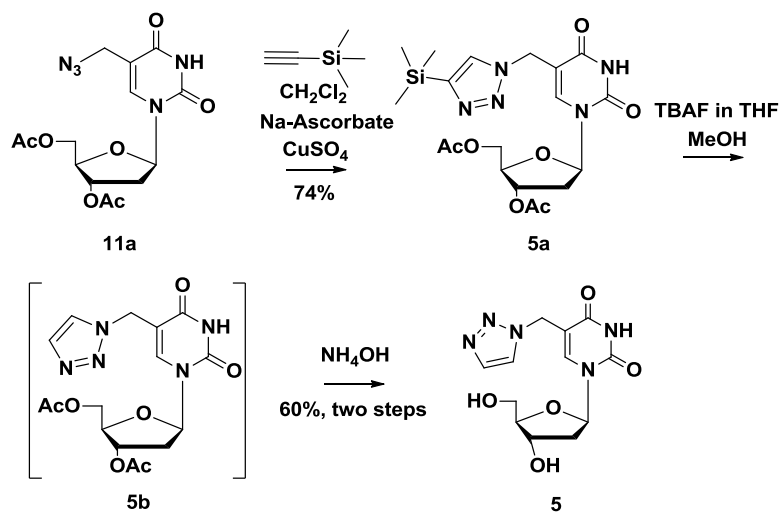


**Scheme 15.** Structures of modified dT (**5-6**).

## 5.2 Results and Discussion

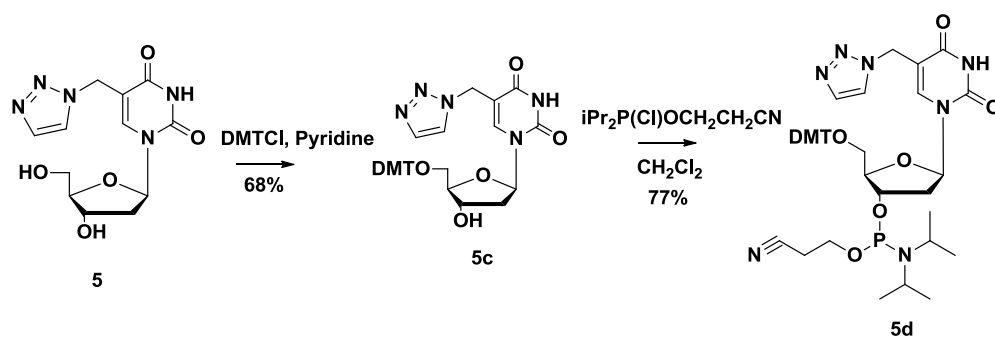
### 5.2.1 Synthesis of Triazole-Conjugated dT (**5**)

In order to investigate the photophysical properties of triazole-conjugated pyrimidine nucleosides in DNA, 1,2,3-triazole conjugated dT (**5**) was designed and synthesized. To accomplish compound **5**, “click” reaction was performed between trimethylsilylacetylene and 3',5'-bis-*O*-acetyl-5-azedomethyl-2'-deoxyuridine (**11a**) under the catalysis of sodium ascorbate and copper sulphate in water solution, the reaction took place successfully to produce compound **5a** with a 74% yield. Then two consecutive deprotection reactions were performed with TBAF in MeOH solution and 25% of NH<sub>3</sub>(aq) in MeOH solution without separation in between, yielding triazole conjugated compound 5-(1,2,3-triazol-1-yl)methyl-2'-deoxyuridine (**5**) with a 60% yield in two steps (Scheme 16).



**Scheme 16.** Synthesis of 1,2,3-triazole-modified dT

*Synthesis of phosphoramidite derived from 5* – Phosphoramidite **5d** was synthesized to accomplish the incorporation of compound **5** in ODN by automated DNA solid phase synthesis. At first, the DMT residue was introduced in 5'-OH functional group of compound **5** with 68% yield by reacting with DMTCl in anhydrous pyridine solution. The DMT-derivative **5c** was converted into the phosphoramidite building block **5d** with 77% yield by phosphorylation under the Ar atmosphere reacting with diisopropylethylamine and 2-cyanoethyl-*N,N*-diisopropylchlorophosphoramidite (Scheme 17).



**Scheme 17.** Synthesis of phosphoramidite derived from **5**

## 5.2.2 Modified ODN Containing 5: Synthesis and Properties

### 5.2.2.1 Synthesis of Modified ODN Containing 5

The purpose of this project was to study the photophysical properties of triazole in ODN. Therefore, triazole-modified dT **5** was incorporated in ODN **107** by solid phase synthesis using the phosphoramidite chemistry protocol (Table 5). The ODN was purified by 20% PAGE analysis and confirmed by MALDI mass analysis. After quantification of synthesized ODN, radiolabeling was carried out according to the standard protocols with  $[\gamma\text{-}^{32}\text{P}]$  ATP. Modified  $[\gamma\text{-}^{32}\text{P}]$ ATP-labelled ODN**107** was hybridized to form duplex **20** with presynthesized complementary ODN **6b** by mixing 1.5 equiv from 65<sup>0</sup>C to room temperature in a buffer of potassium phosphate, pH 7.0, and 1M NaCl, followed by slow-cooling to room temperature overnight.

**Table 5.** Synthesized ODNs and duplexes

ID	Sequence
ODN-107	5'-dAGATGGAT <b>5</b> TAGGTAC
ODN-6b	3'-dTCTACCTAAATCCATG
Duplex-6	5'-dAGATGGAT <b>T</b> TAGGTAC 3'-dTCTACCTAAATCCATG
Duplex-20	5'-dAGATGGAT <b>5</b> TAGGTAC 3'-dTCTACCTAAATCCATG

#### 5.2.2.2 ICL Study with Triazole-modified dT

The modified ODN duplex **20** and previously synthesized non-modified ODN duplex **6** were photo-irradiated at 350 nm for 2 hours using a Rayonet Photochemical Chamber Reactor (Model RPR-100) as the wavelength of 350 nm is compatible with biological molecules. The UV-irradiation of duplex **20** resulted in a new band. The new band showed that the modified nucleoside **5** was covalently bound with the complementary strand strand leading the formation of ICL (Figure 35). Further reaction analysis in different pH showed that the highest ICL yield was observed under the acidic conditions at pH-5 (Table 6).

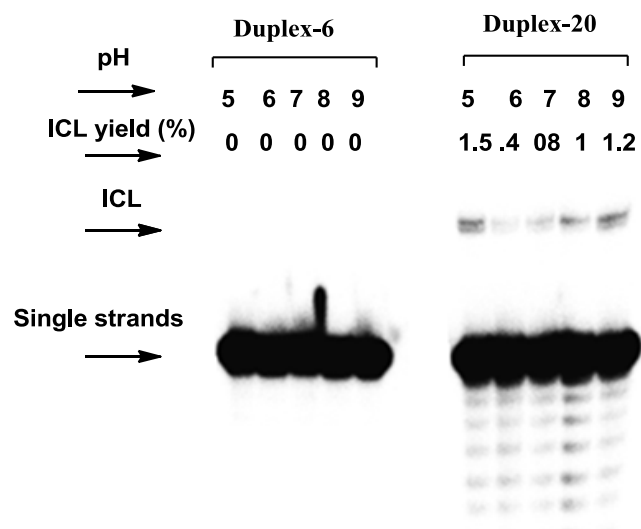


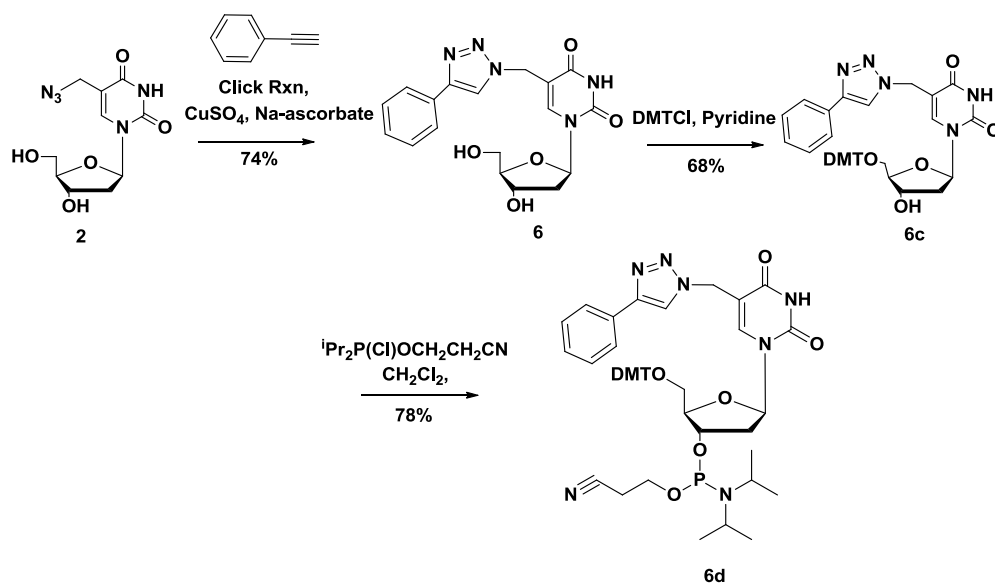
**Figure 35.** PAGE analysis of ICL formation for duplex **6** and duplex **20**

**Table 6.** Percentage of ICL formation under variable pH for duplex **20**

pH	5	6	7	8	9
ODN Duplex	% of ICL	% of ICL	% of ICL	% of ICL	% of ICL
Duplex-6	0	0	0	0	0
Duplex-20	1.5	0.4	0.8	1.1	1.2

### 5.2.3 Synthesis of Phenyl-triazole-Conjugated dT (6)

To accomplish phenyl-substituted triazole modified dT (**6**), we first performed a “click” reaction between phenylalkyne- group and 5-azidomethyl-2'-deoxyuridine (**2**) with the catalysis of sodium ascorbate and copper sulphate in water and methanol solution, the reaction took place successfully to produce compound **6** with 74% yield. For solid phase synthesis of ODN containing compound **6**, the corresponding phosphoramidite **6d** was prepared. The DMT residue was introduced at the 5'-OH functional group of compound **6**. The reaction went well in pyridine solution with 68% yield of **6c**. The DMT derivative **6c** was converted into the phosphoramidite **6d** in 78% yield by phosphitylation under Ar atmosphere reacting with diisopropylethylamine and 2-cyanoethyl-*N,N*-diisopropylchlorophosphoramidite (Scheme 18).



**Scheme 18.** Synthesis of the phosphoramidite **6d** derived from **6**.



## 5.2.4 Modified-ODN Containing **6**: Synthesis and Properties

### 5.2.4.1 Synthesis of Modified-ODN Containing **6**

The purpose of this project was to study the photophysical properties of phenyl-triazole in DNA. Therefore, phenyl-triazole-modified dT (**6**) was incorporated in ODN **15** by solid phase synthesis using the phosphoramidite chemistry protocol (Table 7). The ODN was purified by 20% PAGE analysis and confirmed by MALDI mass analysis. After quantification of synthesized ODN, radiolabeling was carried out according to the standard protocols with [ $\gamma$ - $^{32}$ P]ATP. Modified [ $\gamma$ - $^{32}$ P]ATP-labelled ODN **15** was hybridized to form duplex **21** with presynthesized complement ODN **6b** by mixing 1.5 equiv. from 65°C to room temperature in a buffer of potassium phosphate, pH 7.0, and 1M NaCl, followed by slow-cooling to room temperature overnight.

**Table 7.** Synthesized ODNs and duplexes

ID	Sequence
ODN- <b>15</b>	5'-dAGATGGAT <b>6</b> TAGGTAC
ODN- <b>6b</b>	3'-dTCTACCTAAATCCATG
Duplex- <b>6</b>	5'-dAGATGGAT <b>T</b> TAGGTAC 3'-dTCTACCTAAATCCATG
Duplex- <b>21</b>	5'-dAGATGGAT <b>6</b> TAGGTAC 3'-dTCTACCTAAATCCATG

### 5.2.4.2 ICL Study with Phenyl-triazole Modified dT

The modified ODN **duplex 21** and previously synthesized non-modified ODN **duplex 6** were **photo-irradiated** at 350 nm. The UV-irradiation of duplex **21** resulted in a new band. The new band showed that the modified nucleoside **6** was covalently binded with the complementary strand leading to the formation of the ICLs (Figure 36). Further reaction analysis in different pH showed that the highest ICL yield was observed under the acidic conditions at pH-5 (Table 8).

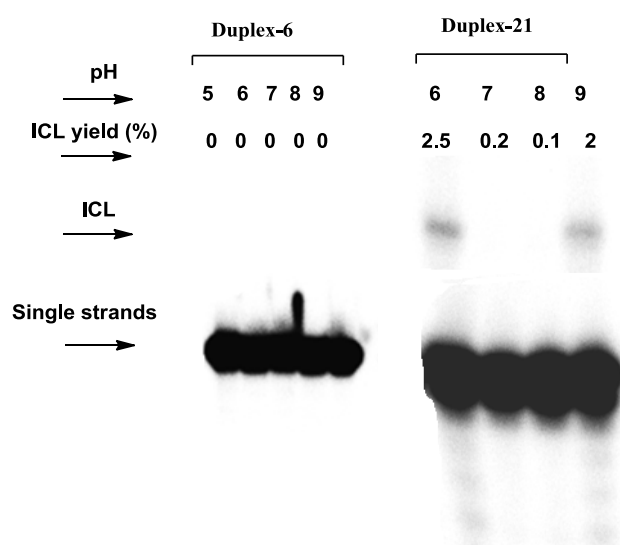


**Figure 36.** PAGE analysis of the ICL formation with duplex **6** and duplex **21**.

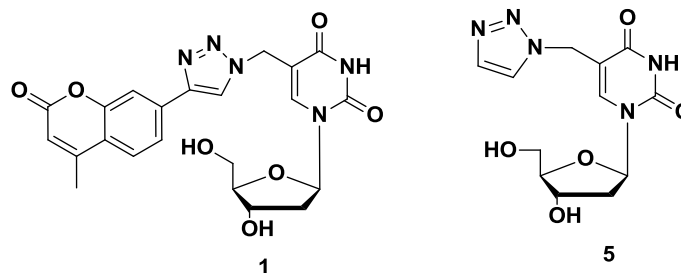
**Table 8.** Percentage of ICL formation under variable pH with duplex **21**

pH	6	7	8	8
ODN Duplex	% of ICL	% of ICL	% of ICL	% of ICL
Duplex-6	0	0	0	0
Duplex-21	2.5	0.2	10.1	2.0

### 5.2.5 Melting Temperature (MT) Study of the Modified ODNs

Duplex-7 5' -A GAT GGA T 1 T AGG TAC -3'  
3'-T CTA CCT A A A TCC ATG -5'

Duplex-20 5' -A GAT GGA T 5 T AGG TAC-3'  
3'-T CTA CCT A A A TCC ATG -5'



**Scheme 19**

To explore whether the modified ODN duplex can be utilized for ODN hybridization, the thermal denaturation experiments were conducted. It is important to note that the basic condition has a relatively higher constructive effect on duplex stability as determined by thermal denaturation measurements. The highest melting point ( $T_m$ ) was observed at pH 8 while the lowest  $T_m$  was found at pH 5. This result indicated that the most stable duplex DNA was formed at a higher pH while the least stable one is formed at a lower pH.

**Table 9.** Melting temperature ( $T_m$ ) study of the modified ODN duplexes

pH values	pH=5	pH=6	pH=7	pH=8
Melting Temperature ( $T_m$ )	$^{\circ}\text{C}$	$^{\circ}\text{C}$	$^{\circ}\text{C}$	$^{\circ}\text{C}$
<b>Duplex-7</b>	48.05	52.30	53.92	57.26
<b>Duplex-20</b>	47.24	50.87	51.40	56.70

### 5.3 Experimental Part

**5-(1,2,3-Triazol-1-yl)methyl-2'-deoxyuridine (5a).** To a solution of **11a** (395 mg, 1.08 mmol) and Trimethylsilylacetylene (118 mg, 1.20 mmol) in DCM (8 mL), a 0.296 M aqueous solution of Na-ascorbate (6 mL) was added, followed by a 0.368 M aqueous solution of  $\text{Cu}_2\text{SO}_4$  (3.6 mL). After one hour, TLC confirmed completion of the reaction. The reaction mixture was evaporated to dryness and subjected to flash chromatography (DCM/MeOH, 10:1-7:1) yielding compound **5a** (365 mg, 74%) as a white foam.  $^1\text{H}$  NMR ( $\text{CDCl}_3$ , 300 MHz):  $\delta$ 9.5 (s, 1H), 7.89 (s, 1H), 7.79 (s, 1H), 6.20 (t, 1H,  $J=6.4$  Hz), 5.25 (d, 1H,  $J=4.4$  Hz), 5.20 (s, 1H), 5.19 (t, 1H,  $J=4.8$  Hz), 3.83 (q, 1H,  $J=3.6$  Hz), 3.72-3.58 (m, 2H), 2.23 (m, 1H), 2.20 (m, 1H), 2.10 (s, s, 6H), 0.51 (s, s, s, 9H):  $^{13}\text{C}$  NMR ( $\text{CDCl}_3$ , 300 MHz):  $\delta$ 171.2, 163.05, 150.23, 148.98, 140.50, 130.74, 110.07, 85.89, 82.77, 77.9, 77.5, 76.1, 73.59, 45.17, 38.43, 20.1, 5.2, 1.1, 0.8.

**5-(1,2,3-Triazol-1-yl)methyl-2'-deoxyuridine (5).** Compound **5a** (300 mg, 0.645 mmol) was dissolved in methanol (25 mL) and tetrabutylammomium fluoride (4.5 mL 1.0 M solution in THF, 4.0 mmol) was added in the solution. The reaction mixture was

stirred at 60°C for 3 hours for complete deprotection of the silyl group. After cooling to room temperature, the crude product was evaporated and aqueous NH<sub>3</sub> (28%, 50 mL) was added without further separation and the reaction mixture was stirred at r.t. overnight. After evaporation, the residue was subjected to flash chromatography (DCM/MeOH, 20:1-7:1) yielding compound **5** (120 mg, 60%) as a white foam. <sup>1</sup>H NMR (DMSO-*d*<sub>6</sub>, 300 MHz): δ 11.5 (s, 1H), 8.49 (s, 1H), 8.29 (s, 1H), 7.82 (s, 1H), 6.20 (t, 1H, *J* = 6.4 Hz), 5.25 (d, 1H, *J* = 4.4 Hz), 5.20 (s, 1H, *J* = 4.8 Hz), 4.27 (m, 1H), 3.83 (q, 1H, *J* = 3.6 Hz), 3.72-3.58 (m, 2H), 2.23 (m, 1H), 2.12 (m, 1H); MALDI-MS [MH<sup>+</sup>] calcd. for C<sub>12</sub>H<sub>15</sub>N<sub>5</sub>O<sub>5</sub>, 332.0971; found, 332.0965.

**5'-O-(4,4'-Dimethoxytriphenylmethyl)-5-(4-methylchromen-2-one-1,2,3-triazol-1-yl)methyl-2'-deoxyuridine (5c).** Compound **5** (0.198 g, 0.64 mmol) was co-evaporated with anhydrous pyridine (3×5 mL) and then dissolved in pyridine (5 mL). To the solution, DMTCl (0.304 g, 0.90 mmol) was added in two portions and the reaction mixture was stirred at r.t. for 5 h. The reaction was quenched by addition of MeOH and was concentrated *in vacuum*. The crude product was purified by flash chromatography (CH<sub>2</sub>Cl<sub>2</sub>/MeOH/Et<sub>3</sub>N = 96/3/1) to give **5c** (0.267 g, 68%) as off-white solid. <sup>1</sup>H NMR (CDCl<sub>3</sub>, 300 MHz): δ 11.5 (s, 1H), 8.19 (s, 1H), 7.89 (s, 1H), 7.82 (s, 1H), 7.67-7.31 (m, 14H), 6.20 (t, 1H, *J* = 6.4 Hz), 5.19 (t, 1H, *J* = 4.8 Hz), 4.27 (m, 1H), 3.83 (q, 1H, *J* = 3.6 Hz), 3.72-3.58 (m, 2H), 3.5 (s,s, 6H), 2.23 (m, 1H), 2.12 (m, 1H); <sup>13</sup>C NMR (300 MHz, CDCl<sub>3</sub>): δ 162.4, 158.3, 150.8, 148, 146.6, 141.4, 135.2, 131.4, 130.4, 130.14, 130.12, 130.04, 129.9, 129.8, 129.19, 129.09, 129.01, 125.4, 121.4, 112, 108.4, 87.3, 86, 85.4, 78.3, 72.7, 65,

62.5, 55.8, 45.2, 44.1, 41, 35.2, 31.1, 29.3, 26, 22.1, 19.6, 13.4. MALDI-MS [MNa<sup>+</sup>] calcd. for C<sub>33</sub>H<sub>33</sub>N<sub>5</sub>O<sub>7</sub>, 634.2278; found, 634.2278.

**5'-O-(4,4'-Dimethoxytriphenylmethyl)-5-(4-methylchromen-2-one-1,2,3-triazol-1-yl)methyl-2'-deoxyuridine-3'-(2-cyanoethyl)-N,N-diisopropylphosphoramidite (5d).**

Compound **5c** (0.153 g, 0.25 mmol) was dissolved in anhydrous CH<sub>2</sub>Cl<sub>2</sub> (5 mL) under Ar atmosphere. Diisopropylethylamine (96 μL, 0.55 mmol) and 2-cyanoethyl-*N,N*-diisopropylchlorophosphoramidite (96 μL, 0.43 mmol) were added. The reaction mixture was stirred at r.t. for 30 min, diluted with CH<sub>2</sub>Cl<sub>2</sub> (30 mL), washed with 5% aqueous NaHCO<sub>3</sub> solution, followed by brine. The organic solution was dried over anhydrous Na<sub>2</sub>SO<sub>4</sub>, filtered, and concentrated. The residue was submitted to flash chromatography (EtOAc/CH<sub>2</sub>Cl<sub>2</sub>/Et<sub>3</sub>N = 66/33/1) to yield product **5d** (0.157 g, 77%) as a white foam. <sup>31</sup>P NMR (CDCl<sub>3</sub>, 300 MHz): δ 150.0, 150.2.

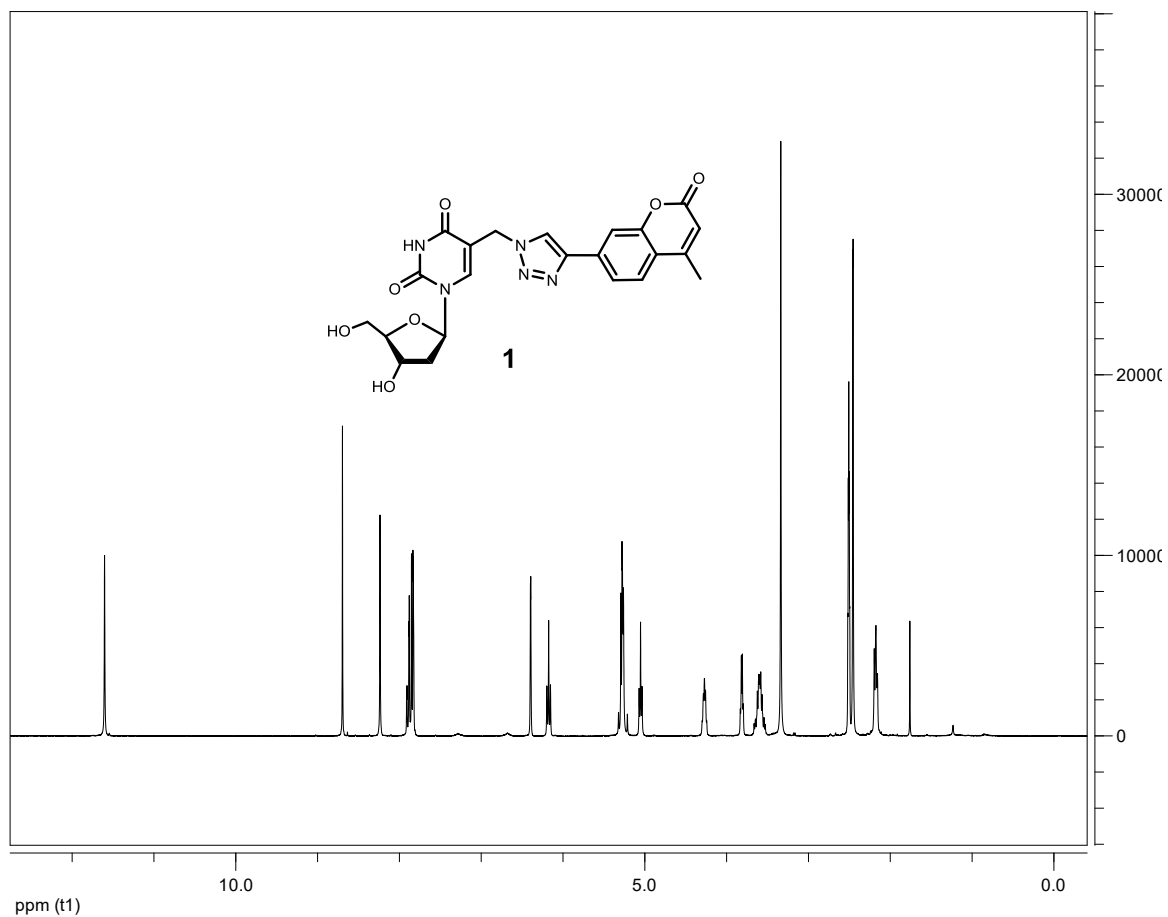
**5-(4-Phenyl-1,2,3-triazol-1-yl)methyl-2'-deoxyuridine (6).** To a solution of phenylacetylene (110 mg, 1.08 mmol) and 5-azido-methyl-2'-deoxyuridine (**2**) (270 mg, 0.954 mmol) in MeOH (8 mL), a 0.296 M aqueous solution of Na-ascorbate (6 mL) was added, followed by a 0.368 M aqueous solution of Cu<sub>2</sub>SO<sub>4</sub> (3.6 mL). After one hour, TLC confirmed completion of the reaction. The reaction mixture was evaporated to dryness and subjected to flash chromatography (DCM/MeOH, 20:1-7:1) yielding compound **6** (273 mg, 74%) as a white foam. <sup>1</sup>H NMR (DMSO-*d*<sub>6</sub>, 300 MHz): δ 11.5 (s, 1H), 8.49 (s, 1H), 8.29 (s, 1H), 7.82 (s, 1H), 7.47-7.31 (m, 5H), 6.20 (t, 1H, *J* = 6.4 Hz), 5.25 (d, 1H, *J* = 4.4 Hz), 5.19 (t, 1H, *J* = 4.8 Hz), 4.27 (m, 1H), 3.83 (q, 1H, *J* = 3.6 Hz), 3.72-3.58 (m, 2H), 2.23 (m, 1H), 2.12 (m, 1H). <sup>13</sup>C NMR (300 MHz, DMSO-*d*<sub>6</sub>): δ 162.4, 152.8, 146.6, 141.4, 132.4,

129.9, 129.1, 125.4, 121.4, 109, 88.4, 87.3, 85.4, 71.7, 60.8, 49.2, 47.1; MALDI-MS [MH<sup>+</sup>] calcd. for C<sub>22</sub>H<sub>21</sub>N<sub>5</sub>O<sub>7</sub>, 386.1519; found, 386.1515.

**5'-O-(4,4'-Dimethoxytriphenylmethyl)-5-(4-Phenyl-1,2,3-triazol-1-yl)methyl-2'-deoxyuridine (6c).** Compound **6** (0.246 g, 0.64 mmol) was co-evaporated with anhydrous pyridine (3×5 mL) and then dissolved in pyridine (5 mL). To the solution, DMTCl (0.304 g, 0.90 mmol) was added in two portions and the reaction mixture was stirred at r.t. for 5 h. The reaction was quenched by addition of MeOH and was concentrated *in vacuo*. The crude product was purified by flash chromatography (CH<sub>2</sub>Cl<sub>2</sub>/MeOH/Et<sub>3</sub>N = 10/5/1) to give **6c** (0.3 g, 68%) as an off-white solid. <sup>1</sup>H NMR (CDCl<sub>3</sub>, 300 MHz): δ 11.5 (s, 1H), 8.19 (s, 1H), 7.89 (s, 1H), 7.82 (s, 1H), 7.67-7.31 (m, 18H), 6.20 (t, 1H, *J* = 6.4 Hz), 5.19 (t, 1H, *J* = 4.8 Hz), 4.27 (m, 1H), 3.83 (q, 1H, *J* = 3.6 Hz), 3.72-3.58 (m, 2H), 3.5 (s,s, 6H), 2.23 (m, 1H), 2.12 (m, 1H); <sup>13</sup>C NMR (300 MHz, CDCl<sub>3</sub>): δ 162.4, 158.3, 150.8, 148, 146.6, 141.4, 135.2, 131.4, 130.4, 130.14, 130.12, 130.04, 129.9, 129.8, 129.19, 129.09, 129.01, 125.4, 121.4, 112, 108.4, 87.3, 86, 85.4, 78.3, 72.7, 65, 62.5, 55.8, 45.2, 44.1, 41, 35.2, 31.1, 29.3, 26, 22.1, 19.6, 13.4.

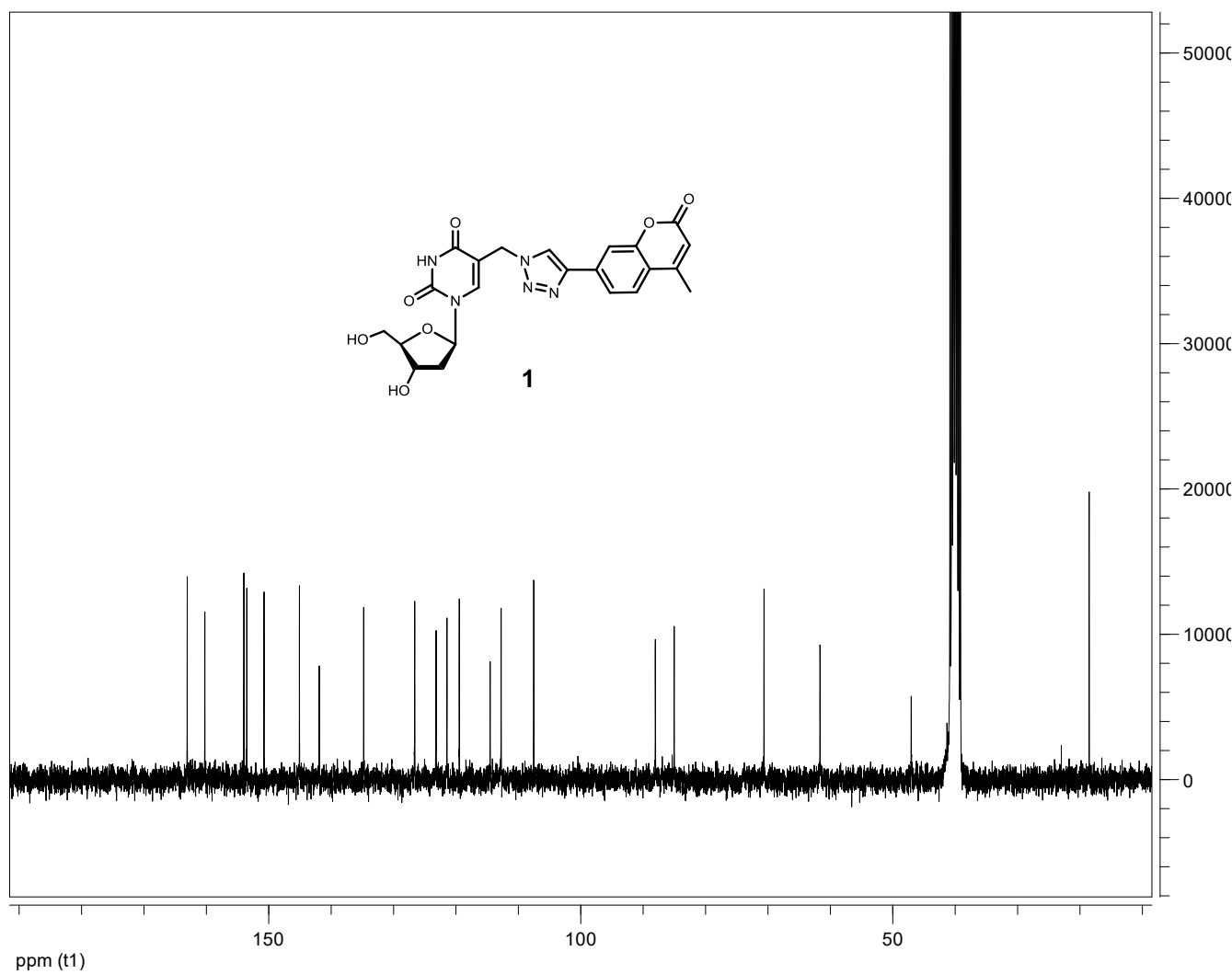
**5'-O-(4,4'-Dimethoxytriphenylmethyl)-5-(4-Phenyl-1,2,3-triazol-1-yl)methyl-2'-deoxyuridine-3'-(2-cyanoethyl)-*N,N*-diisopropylphosphoramidite (6d).** Compound **6c** (0.172 g, 0.25 mmol) was dissolved in anhydrous CH<sub>2</sub>Cl<sub>2</sub> (5 mL) under Ar atmosphere. Diisopropylethylamine (96 μL, 0.55 mmol) and 2-cyanoethyl-*N,N*-diisopropylchlorophosphoramidite (96 μL, 0.43 mmol) were added. The reaction mixture was stirred at r.t. for 30 min, diluted with CH<sub>2</sub>Cl<sub>2</sub> (30 mL), washed with 5% aqueous NaHCO<sub>3</sub> solution, followed by brine. The organic solution was dried over anhydrous

Na<sub>2</sub>SO<sub>4</sub>, filtered, and concentrated. The residue was submitted to flash chromatography (EtOAc/CH<sub>2</sub>Cl<sub>2</sub>/Et<sub>3</sub>N = 66/33/1) to yield product **6d** (0.170 g, 78%) as a white foam. <sup>31</sup>P NMR (CDCl<sub>3</sub>, 300 MHz): δ 150.0, 150.2.

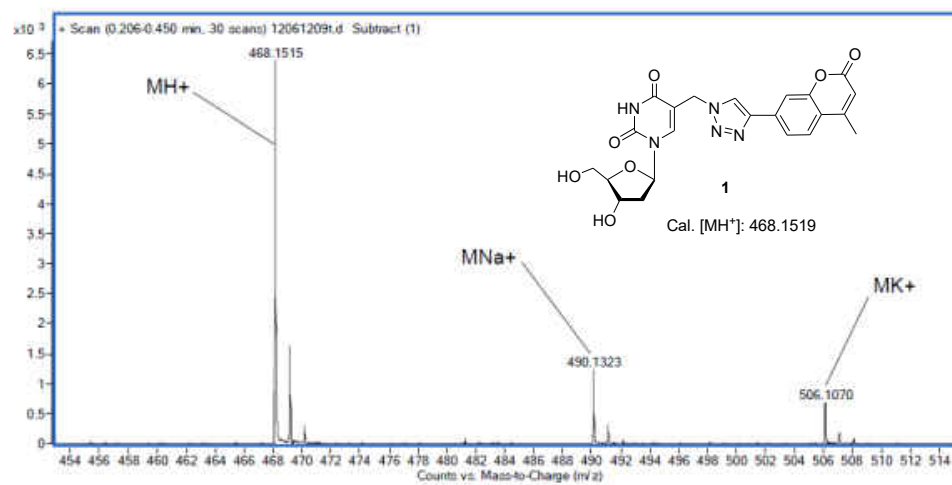


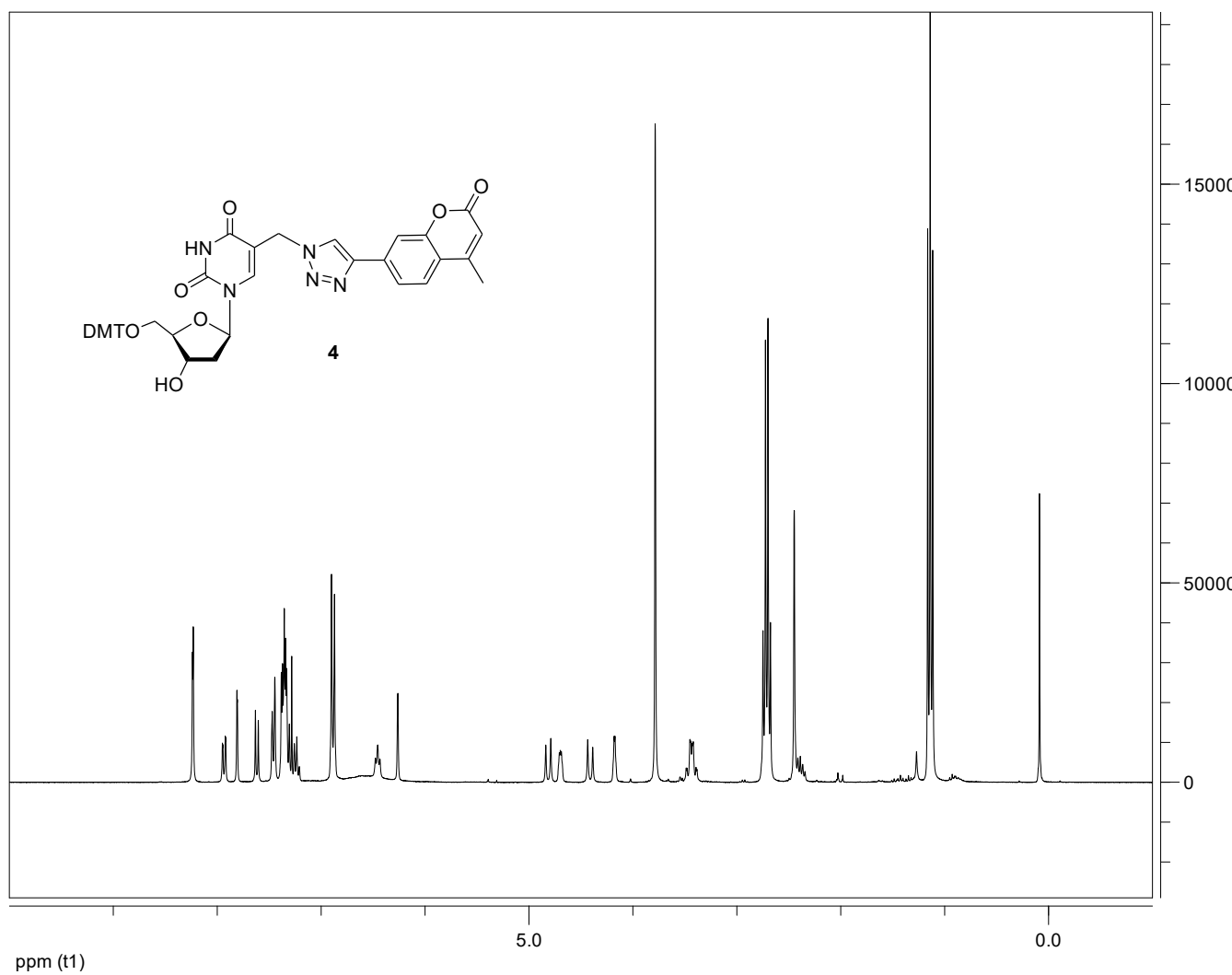
<sup>1</sup>H NMR (DMSO-*d*<sub>6</sub>, 300 MHz) of nucleoside **1**



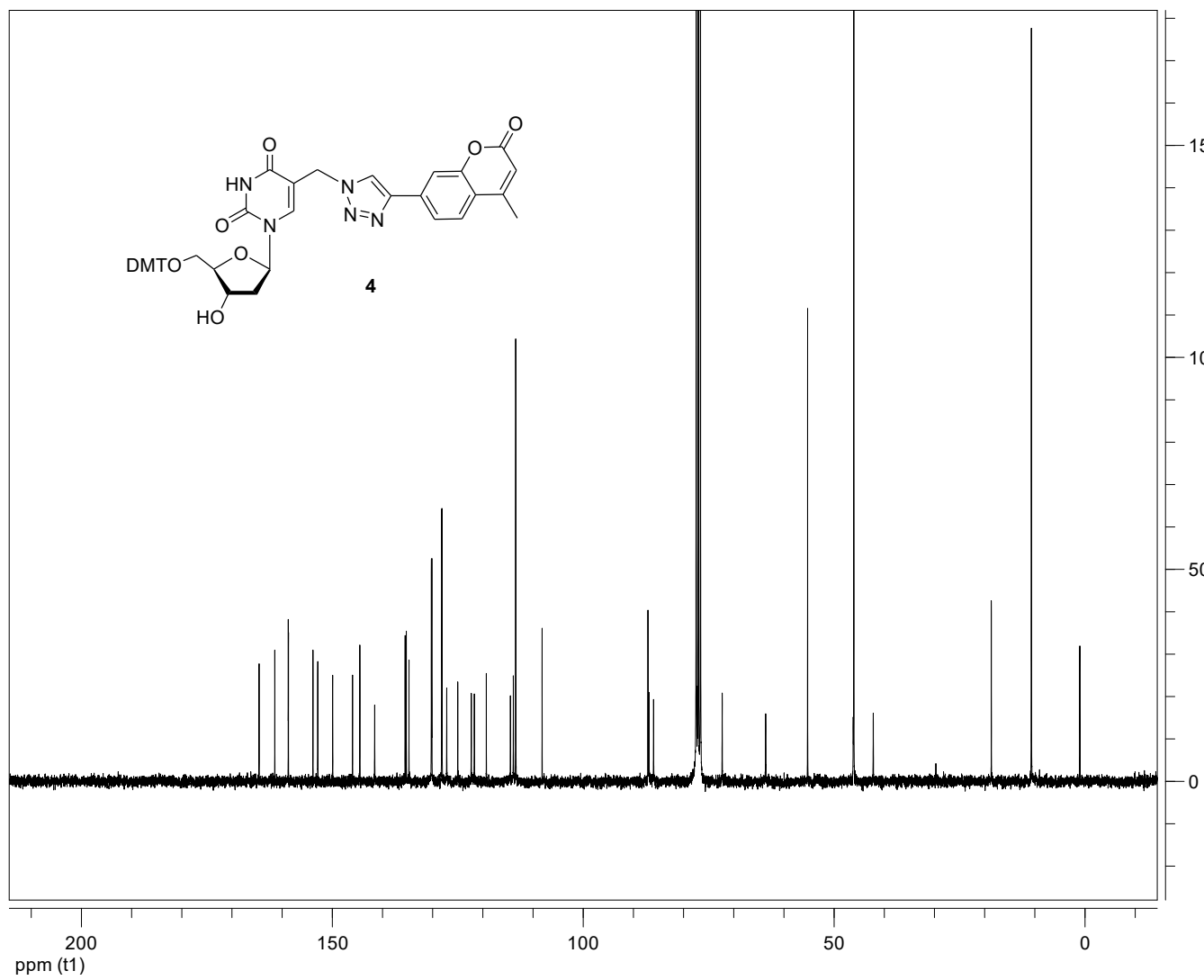


$^{13}\text{C}$  NMR ( $\text{DMSO-}d_6$ , 300 MHz) of nucleoside **1**

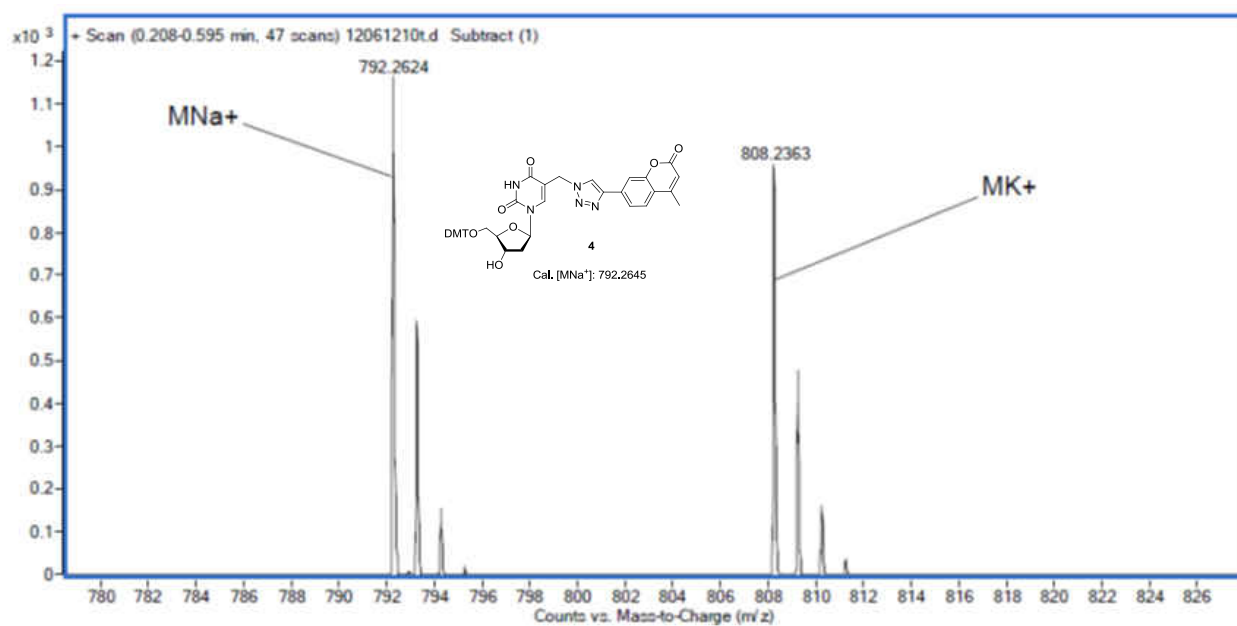
MS spectrum of nucleoside **1**



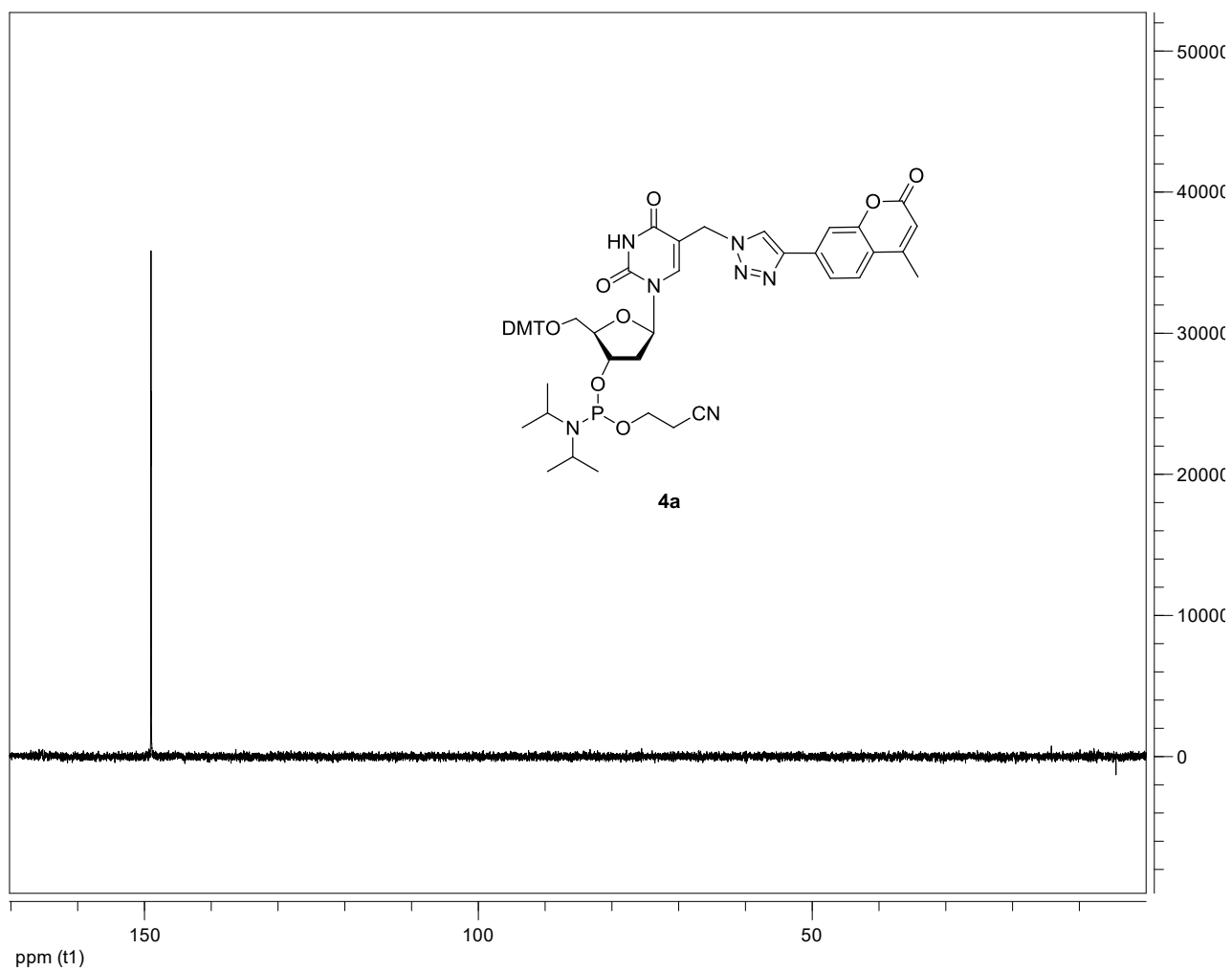
$^1\text{H-NMR}$  ( $\text{CDCl}_3$ , 300 MHz) of the DMT-protected nucleoside **4**.



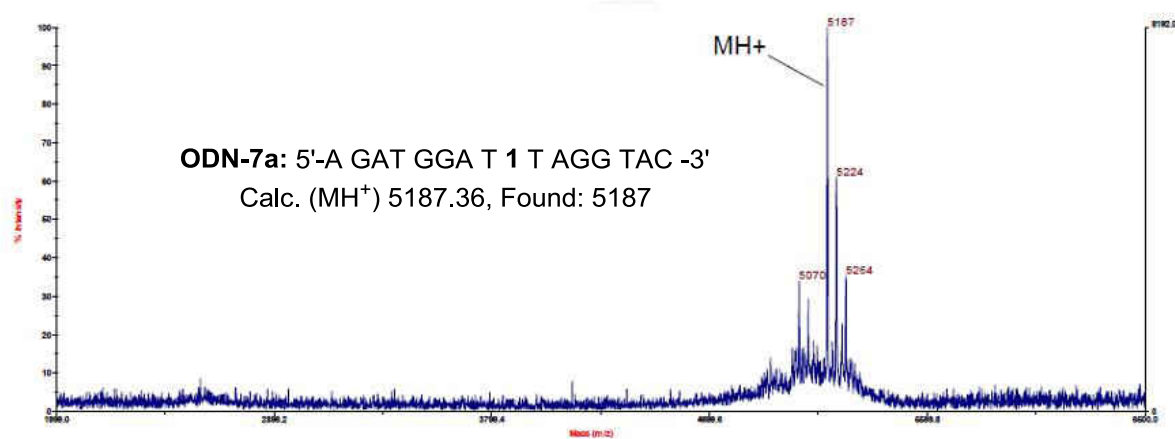
$^{13}\text{C}$ -NMR ( $\text{CDCl}_3$ , 300 MHz) of the DMT-protected nucleoside **4**



MS spectrum of compound 4



$^{31}\text{P}$ -NMR ( $\text{CDCl}_3$  300 MHz) of nucleoside **4a**

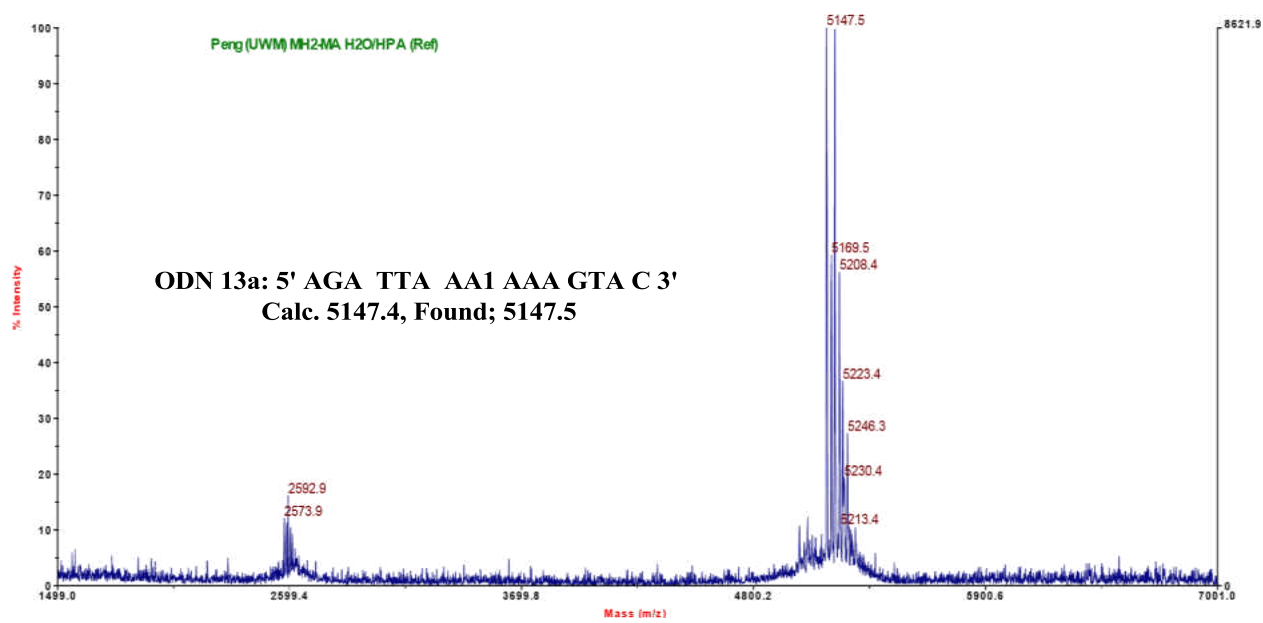


MS spectrum of ODN-7a

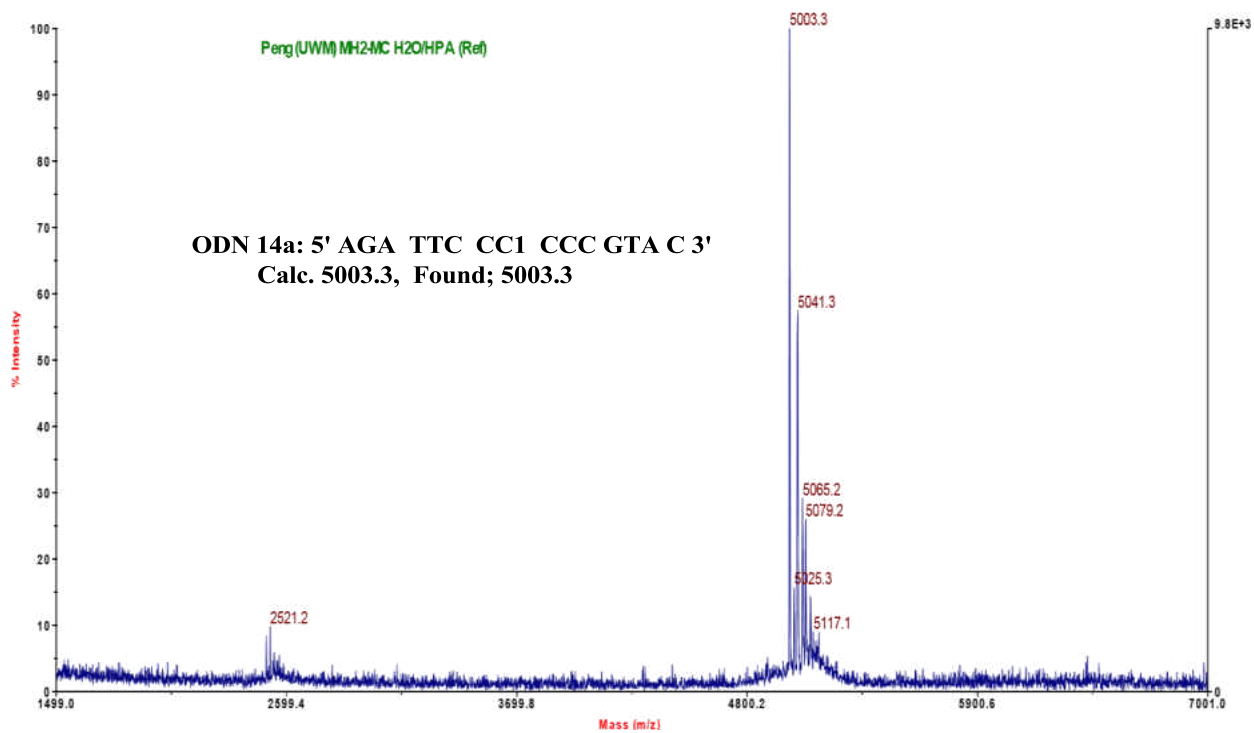


MS spectrum of ODN-12a

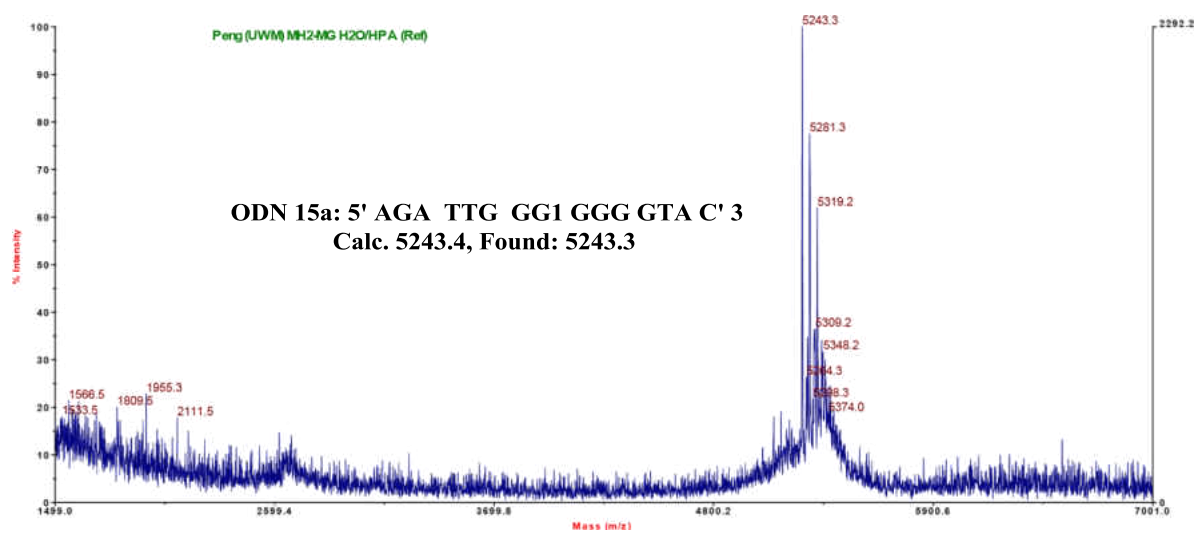




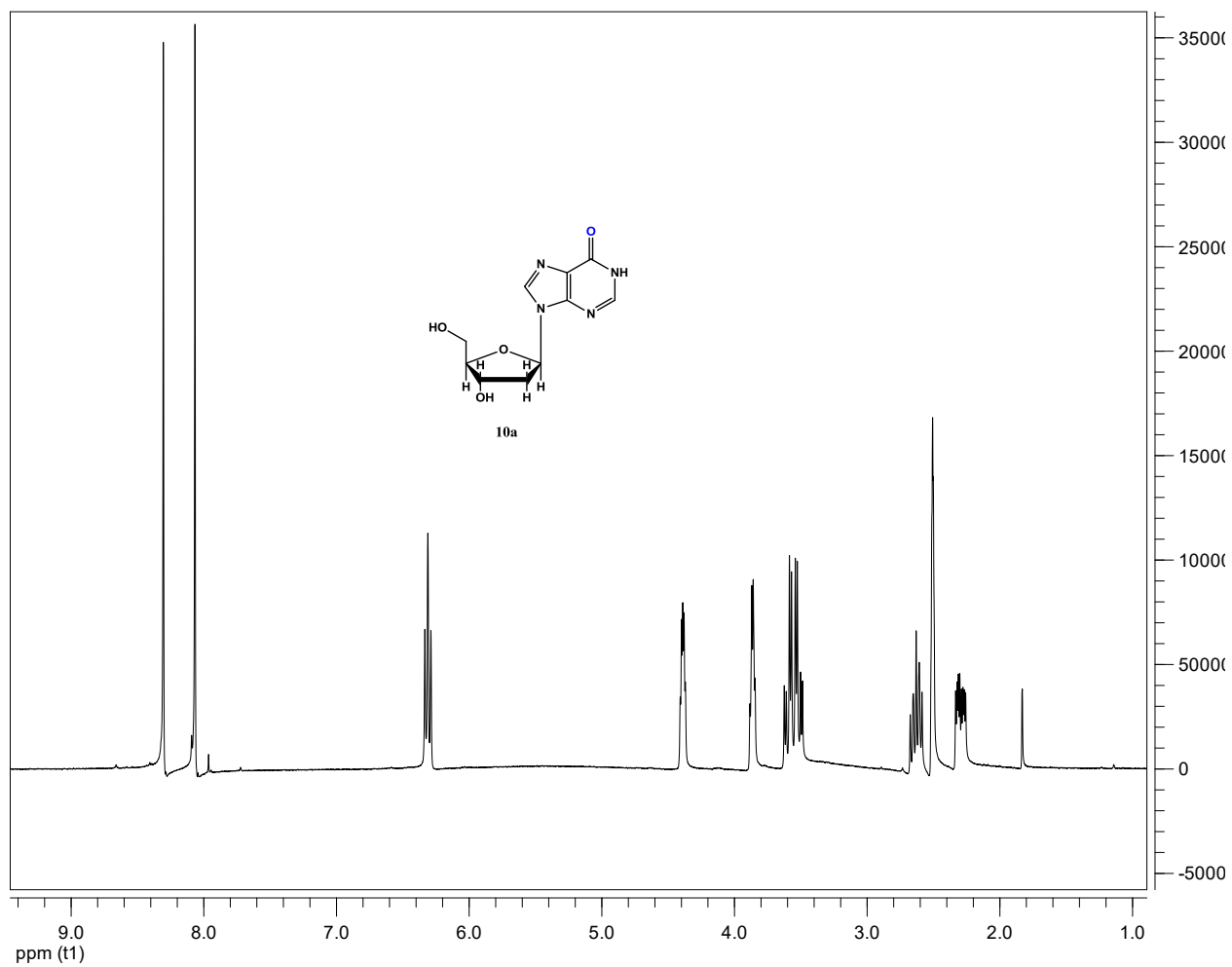
MS spectrum of ODN-13a



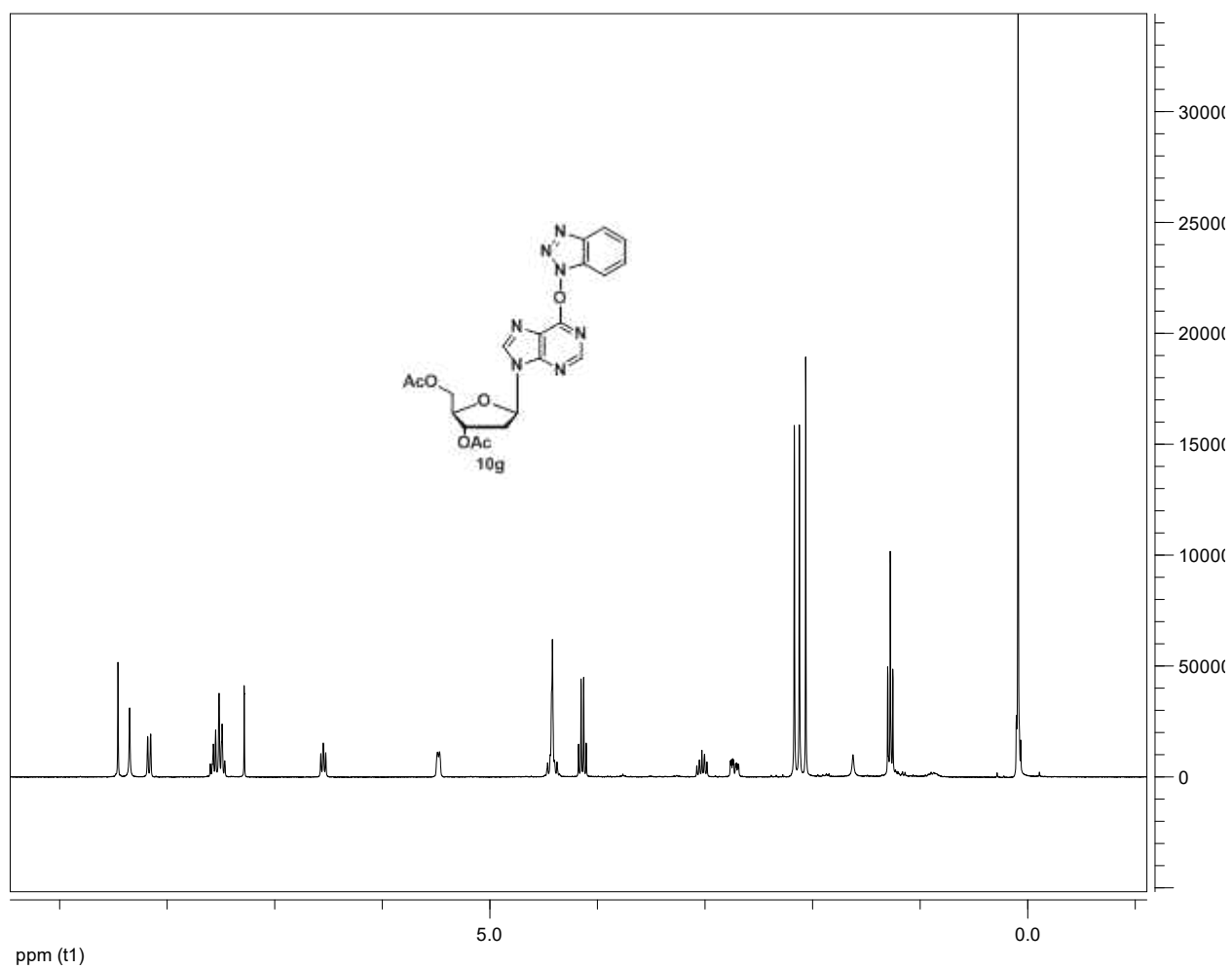
MS spectrum of ODN-14a



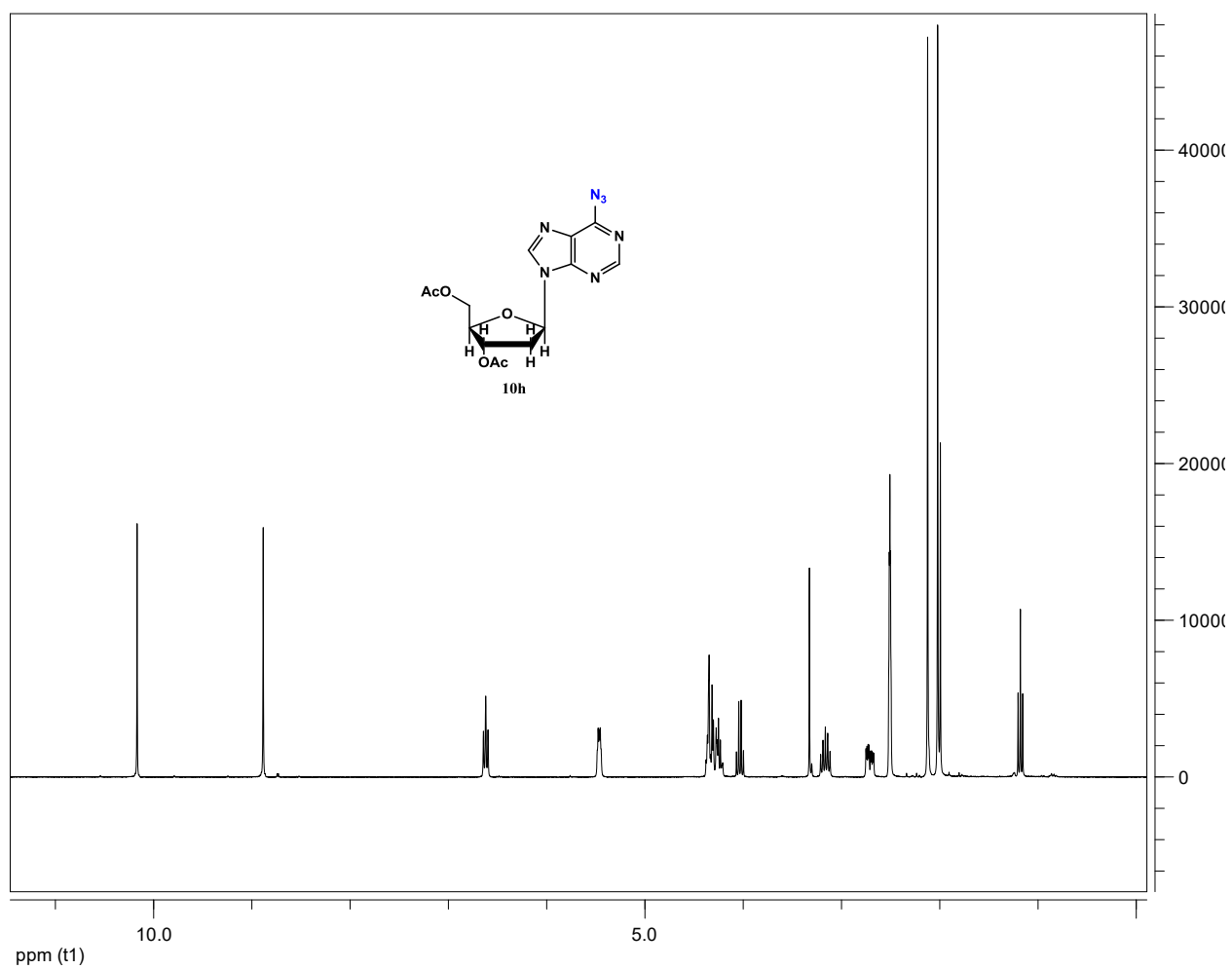
MS spectrum of ODN-15a



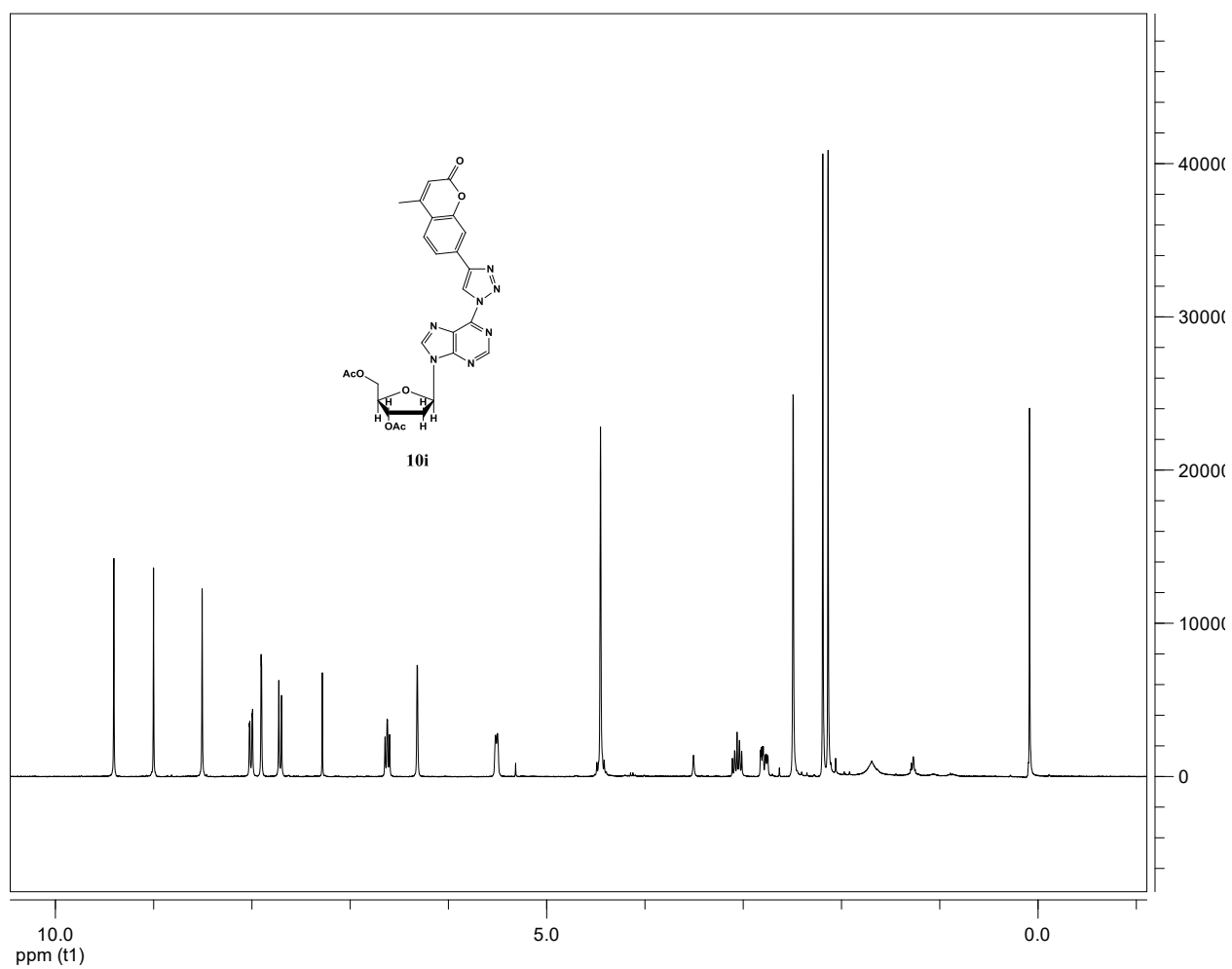
$^1\text{H-NMR}$  (DMSO, 300 MHz) of the nucleoside **10a**



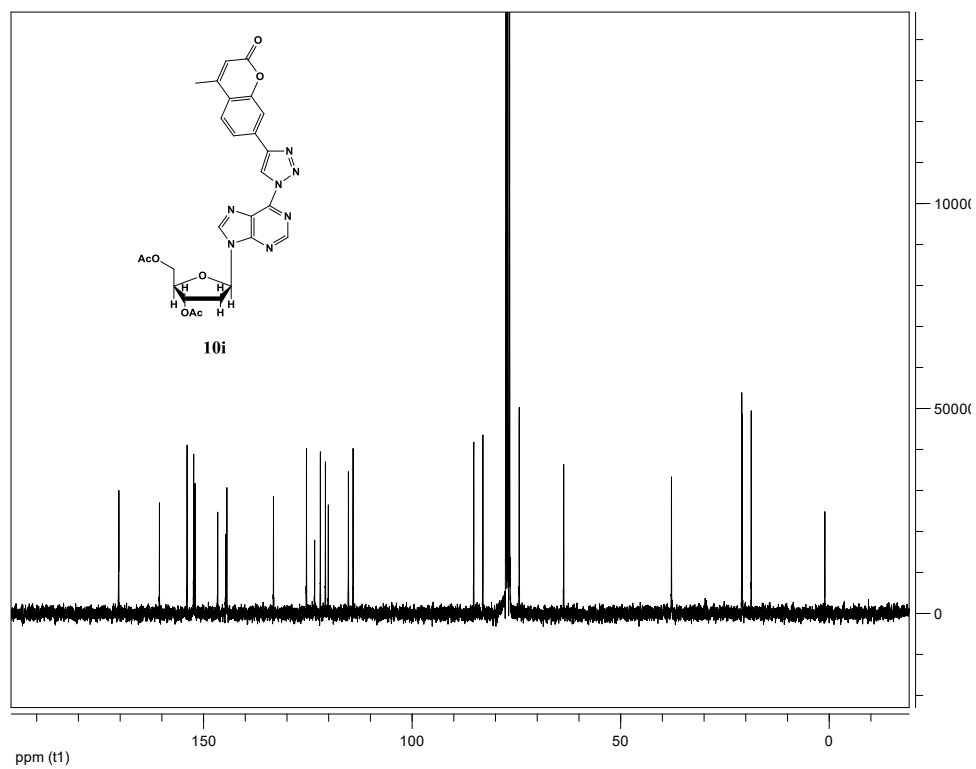
<sup>1</sup>H-NMR (CDCl<sub>3</sub>, 300 MHz) of the nucleoside **10g**



$^1\text{H-NMR}$  (CDCl<sub>3</sub>, 300 MHz) of the nucleoside **10h**



<sup>1</sup>H-NMR (CDCl<sub>3</sub>, 300 MHz) of the nucleoside **10i**

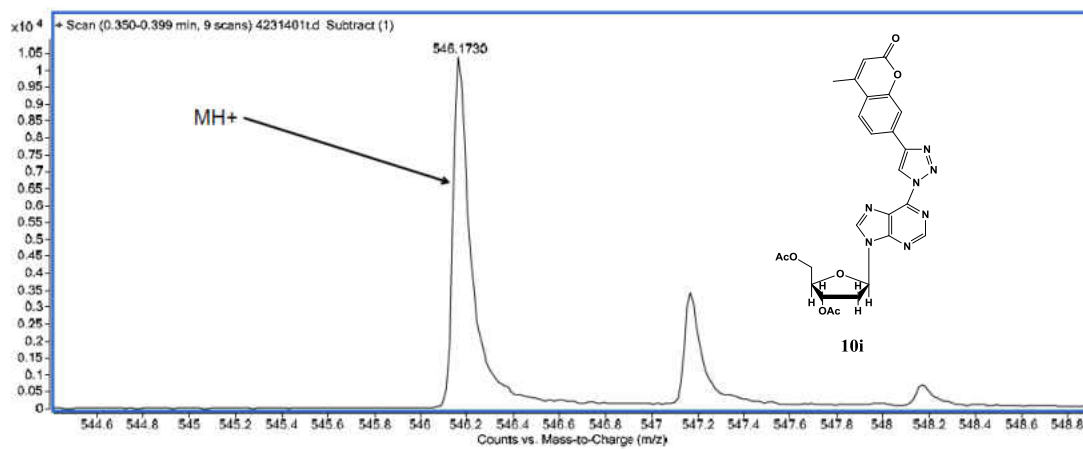


$^{13}\text{C}$ -NMR ( $\text{CDCl}_3$ , 300 MHz) of the nucleoside **10i**

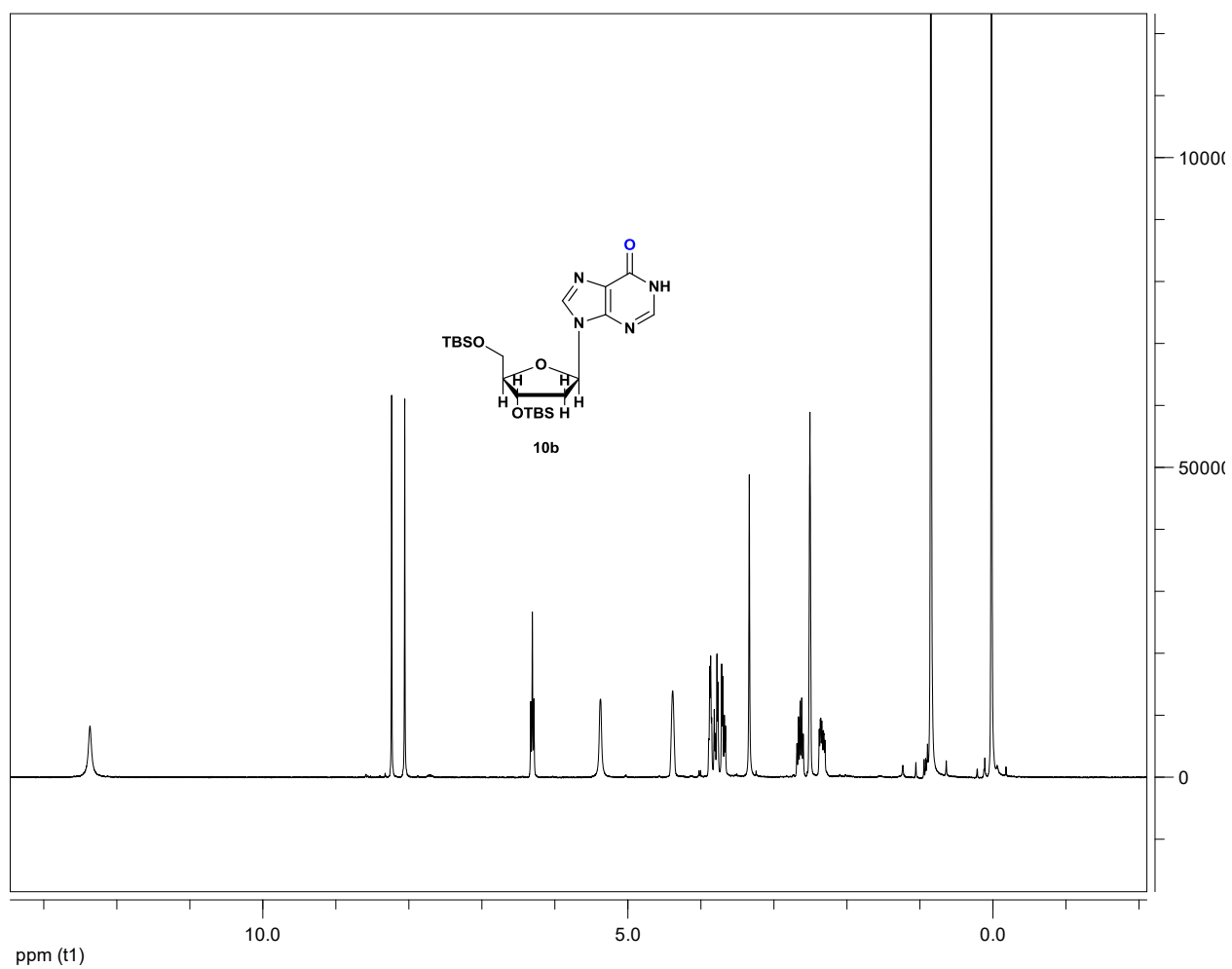


Mass Analysis;

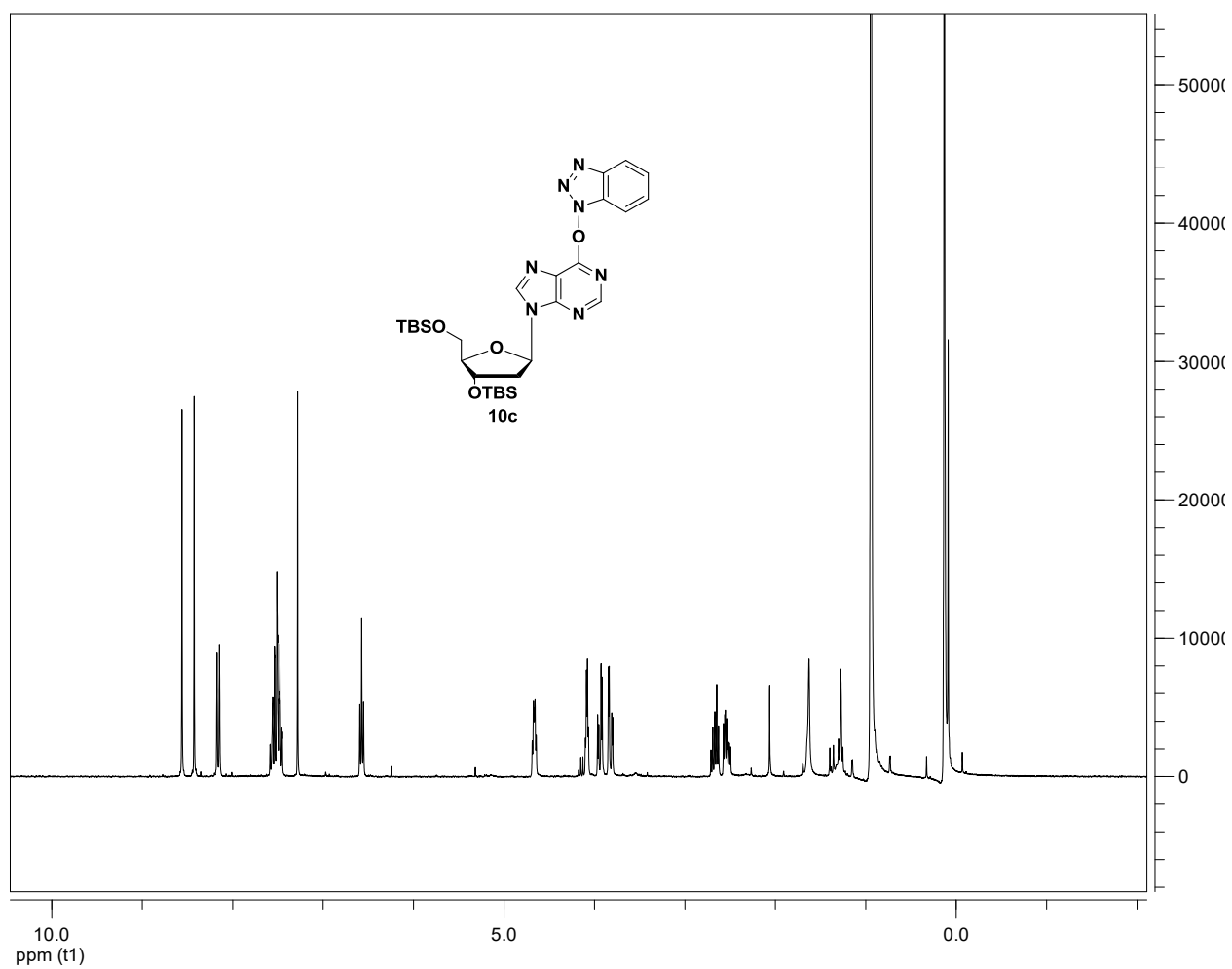
ESI/APCI



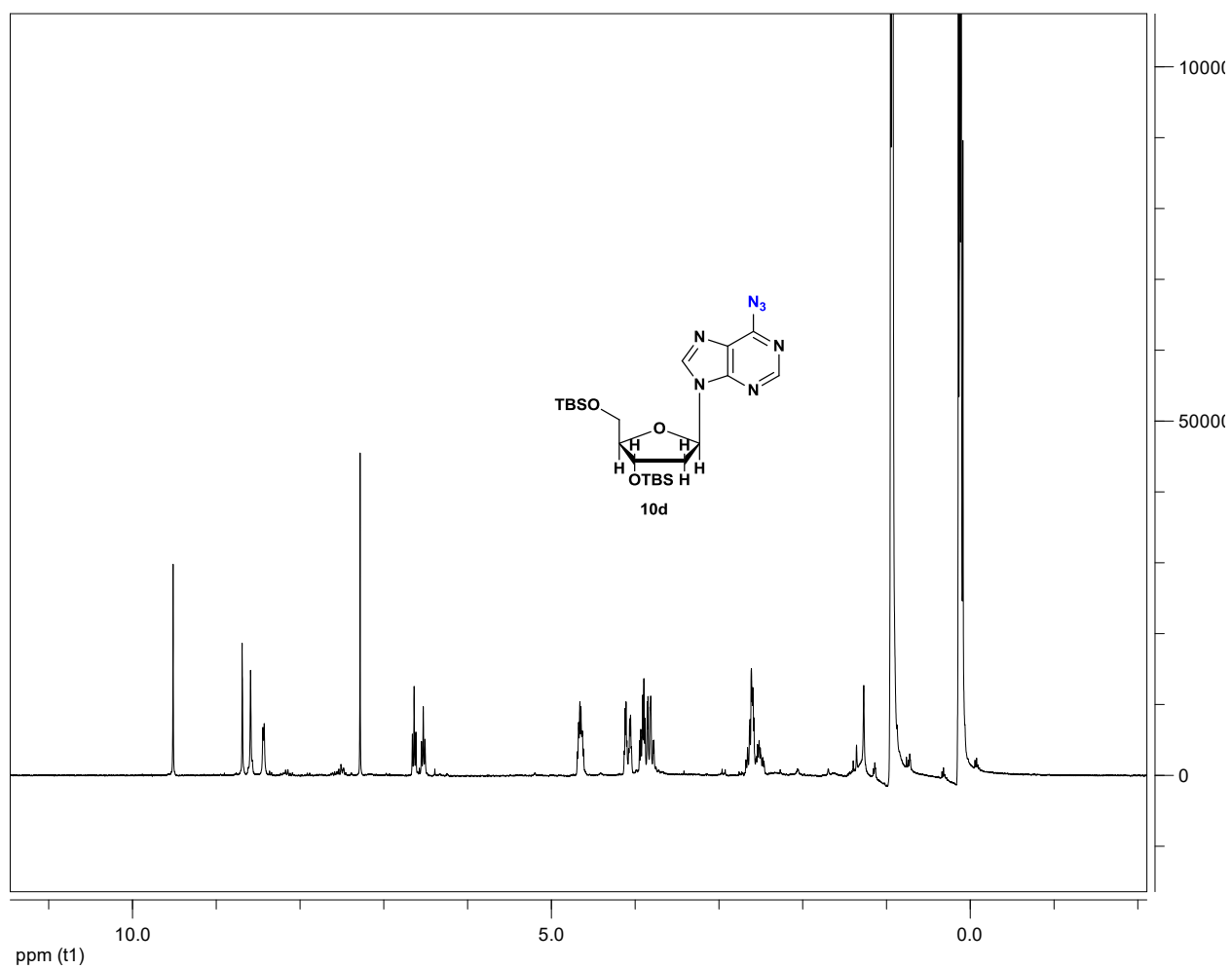
MS spectrum of compound **10i**: Cal; 446.17, Found; 446.17



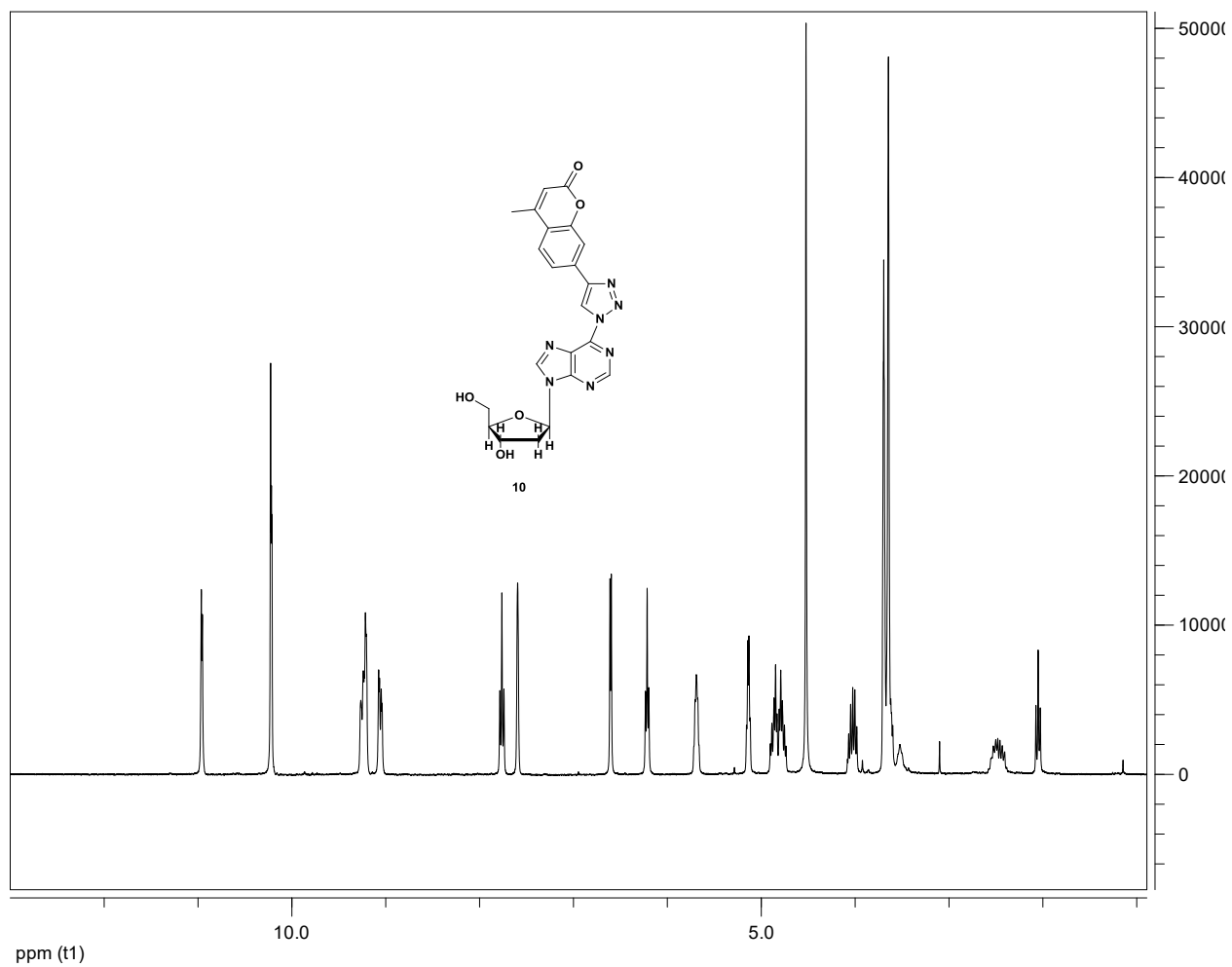
$^1\text{H-NMR}$  (CDCl<sub>3</sub>, 300 MHz) of the nucleoside **10b**



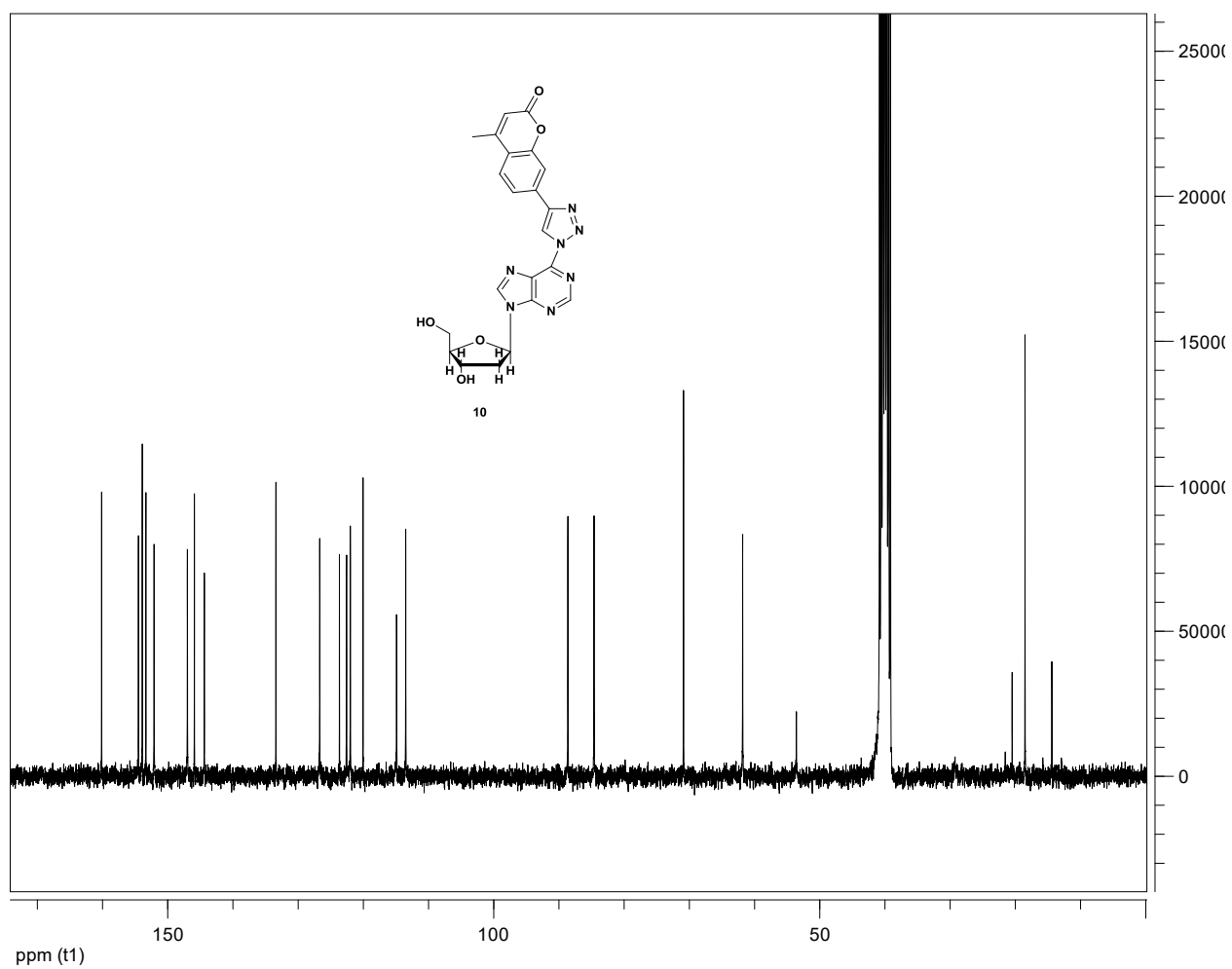
$^1\text{H-NMR}$  ( $\text{CDCl}_3$ , 300 MHz) of the nucleoside **10c**



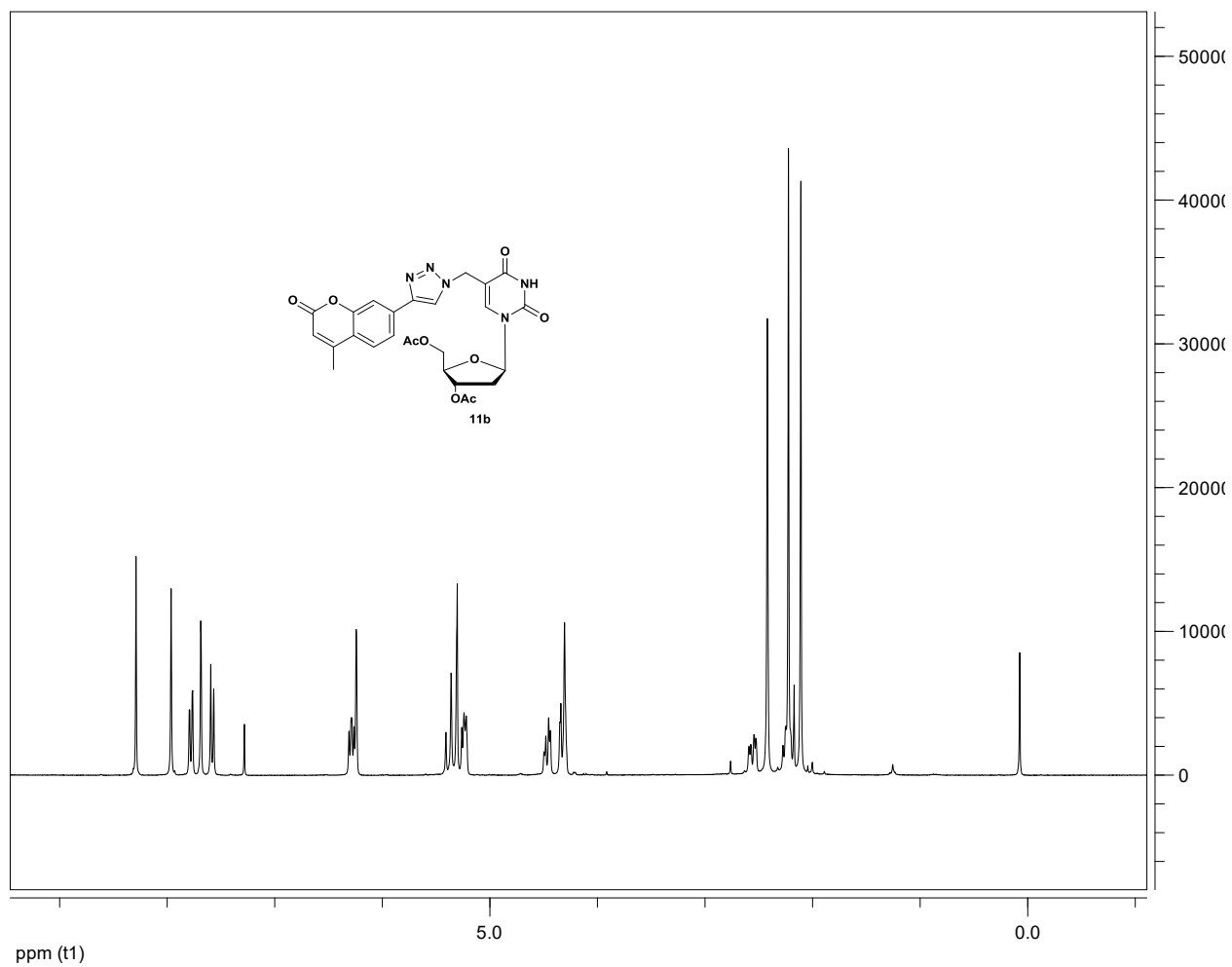
<sup>1</sup>H-NMR (CDCl<sub>3</sub>, 300 MHz) of the nucleoside **10d**



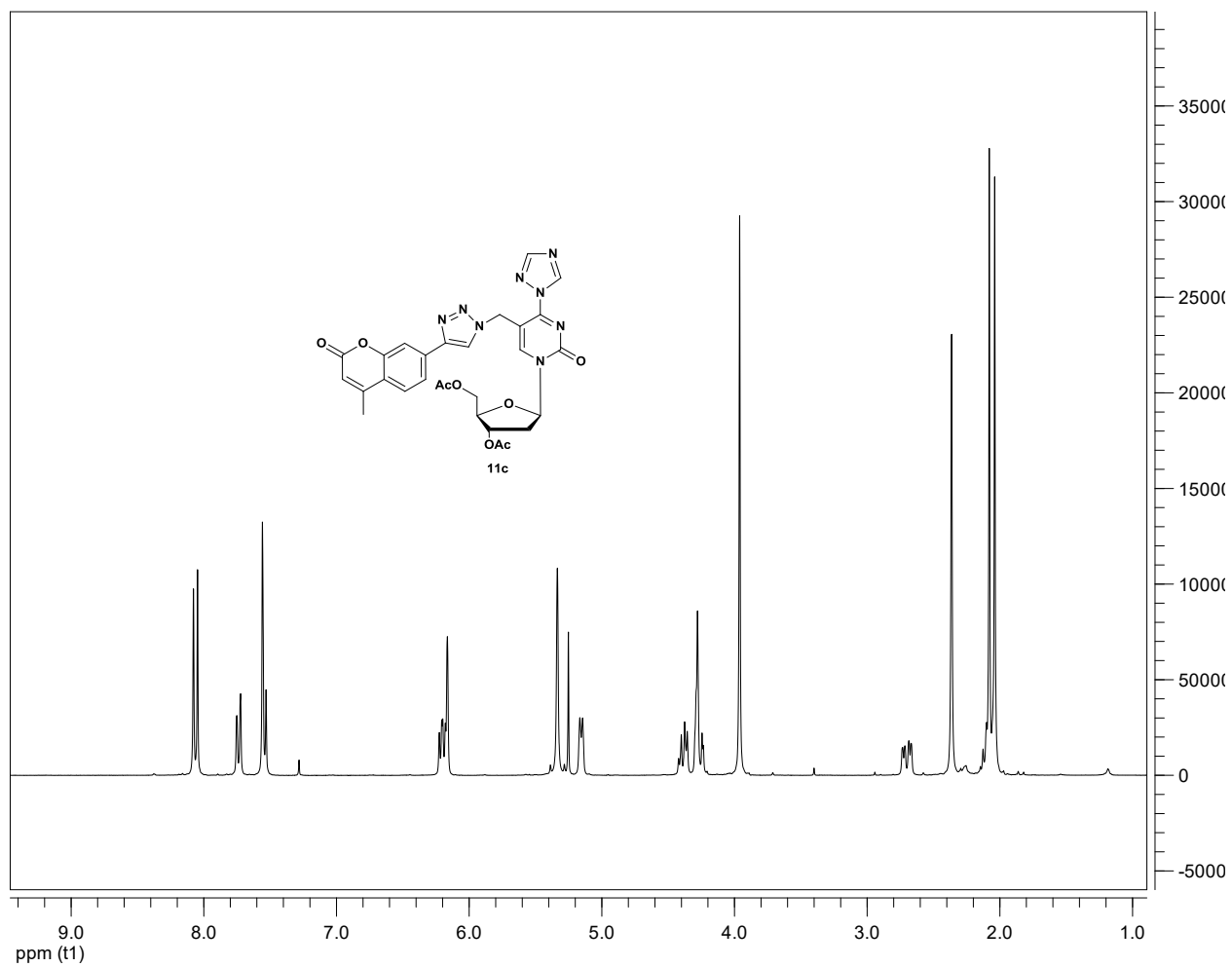
$^1\text{H-NMR}$  (DMSO, 300 MHz) of the nucleoside **10**



$^{13}\text{C}$ -NMR ( $\text{CDCl}_3$ , 300 MHz) of the nucleoside **10**

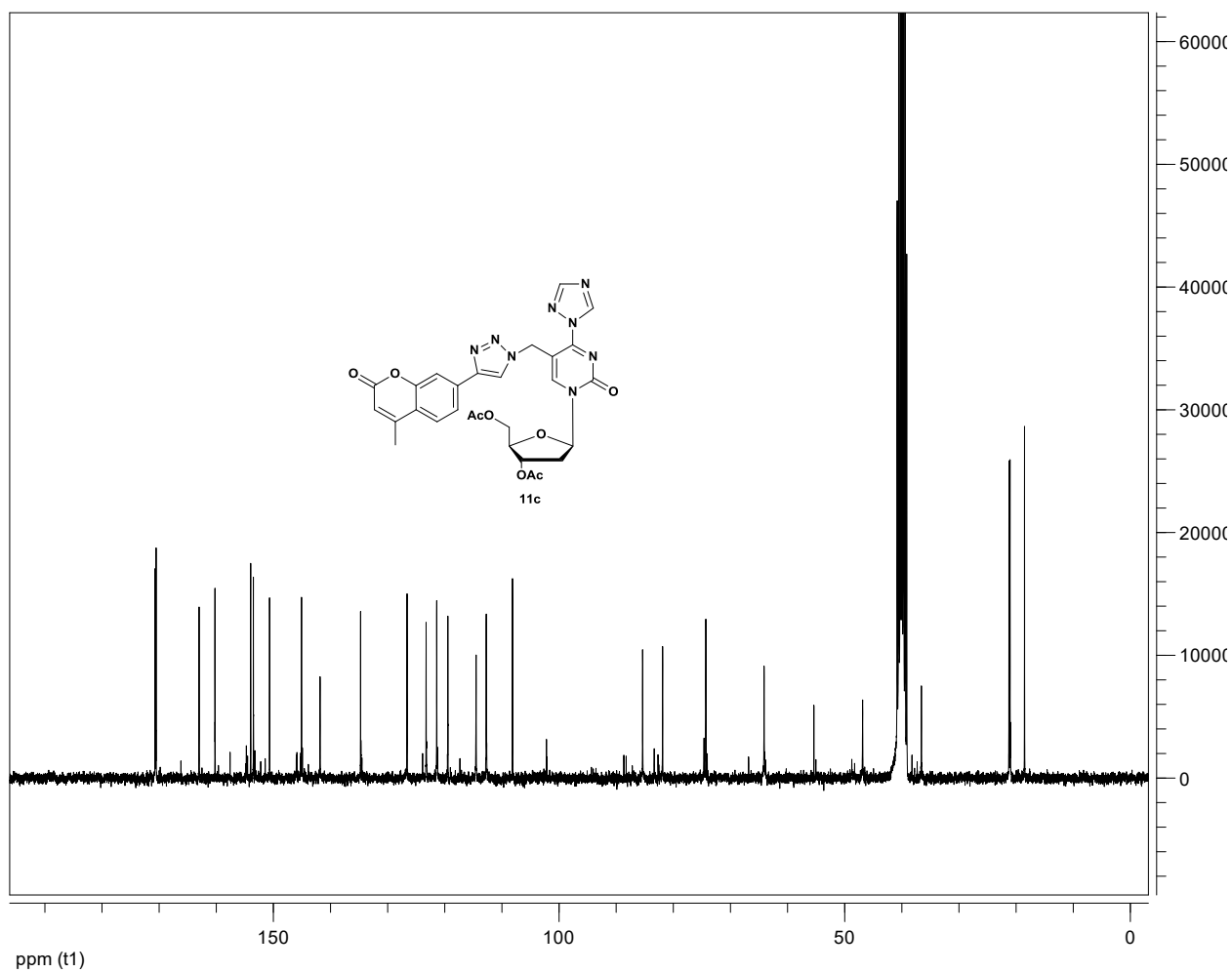


$^1\text{H-NMR}$  (CDCl<sub>3</sub>, 300 MHz) of the nucleoside **11b**

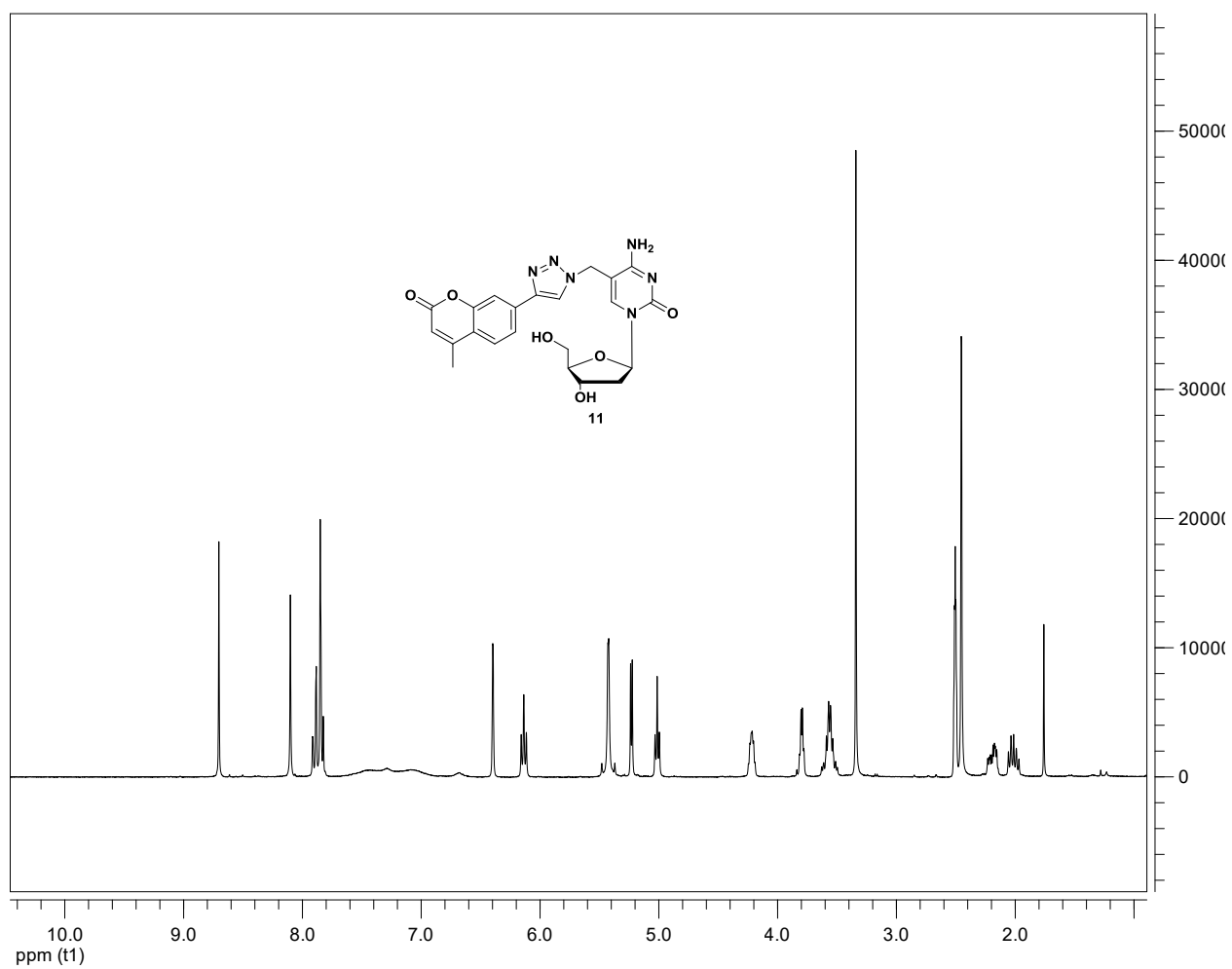


$^1\text{H-NMR}$  ( $\text{CDCl}_3$ , 300 MHz) of the nucleoside **11c**

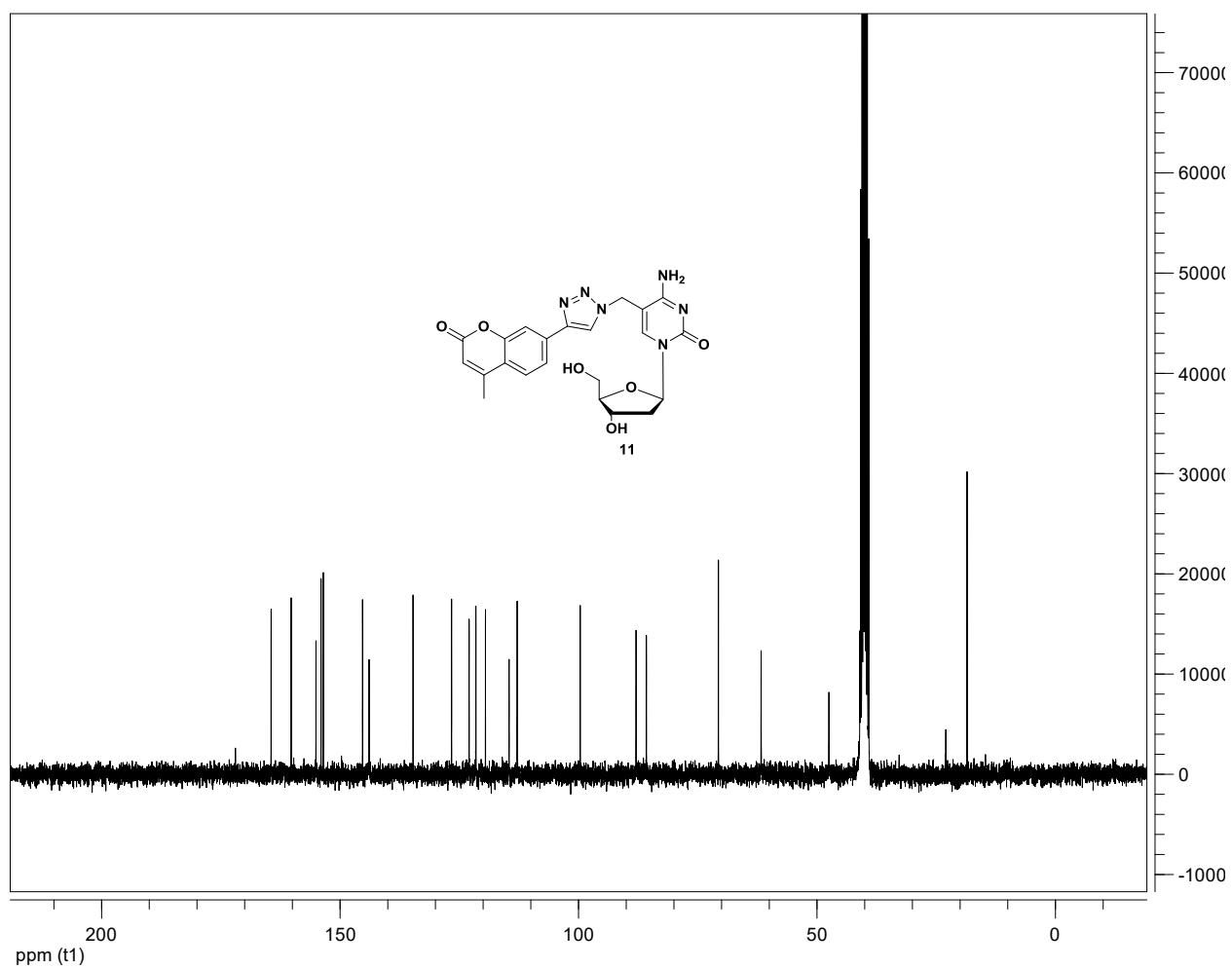




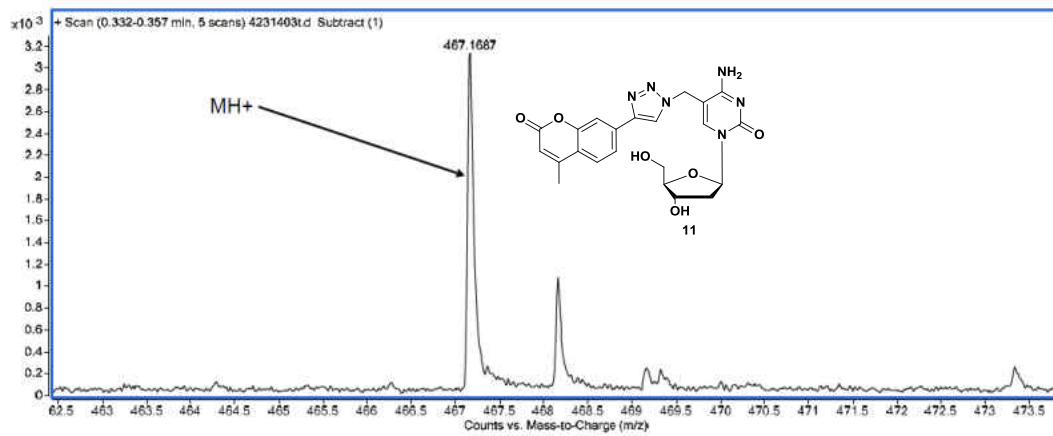
$^{13}\text{C}$ -NMR ( $\text{CDCl}_3$ , 300 MHz) of the nucleoside **11c**



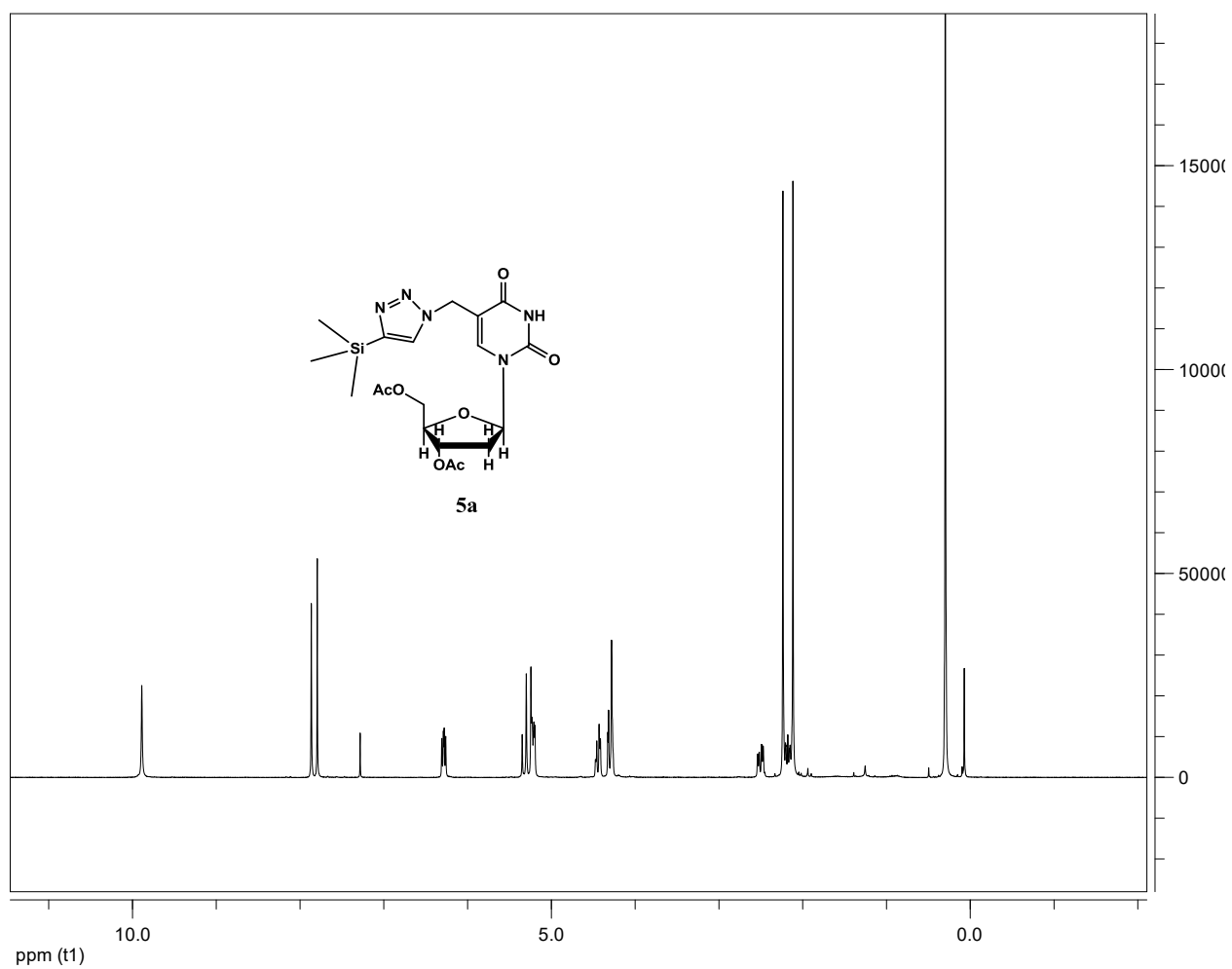
$^1\text{H-NMR}$  ( $\text{DMSO}$ , 300 MHz) of the nucleoside **11**



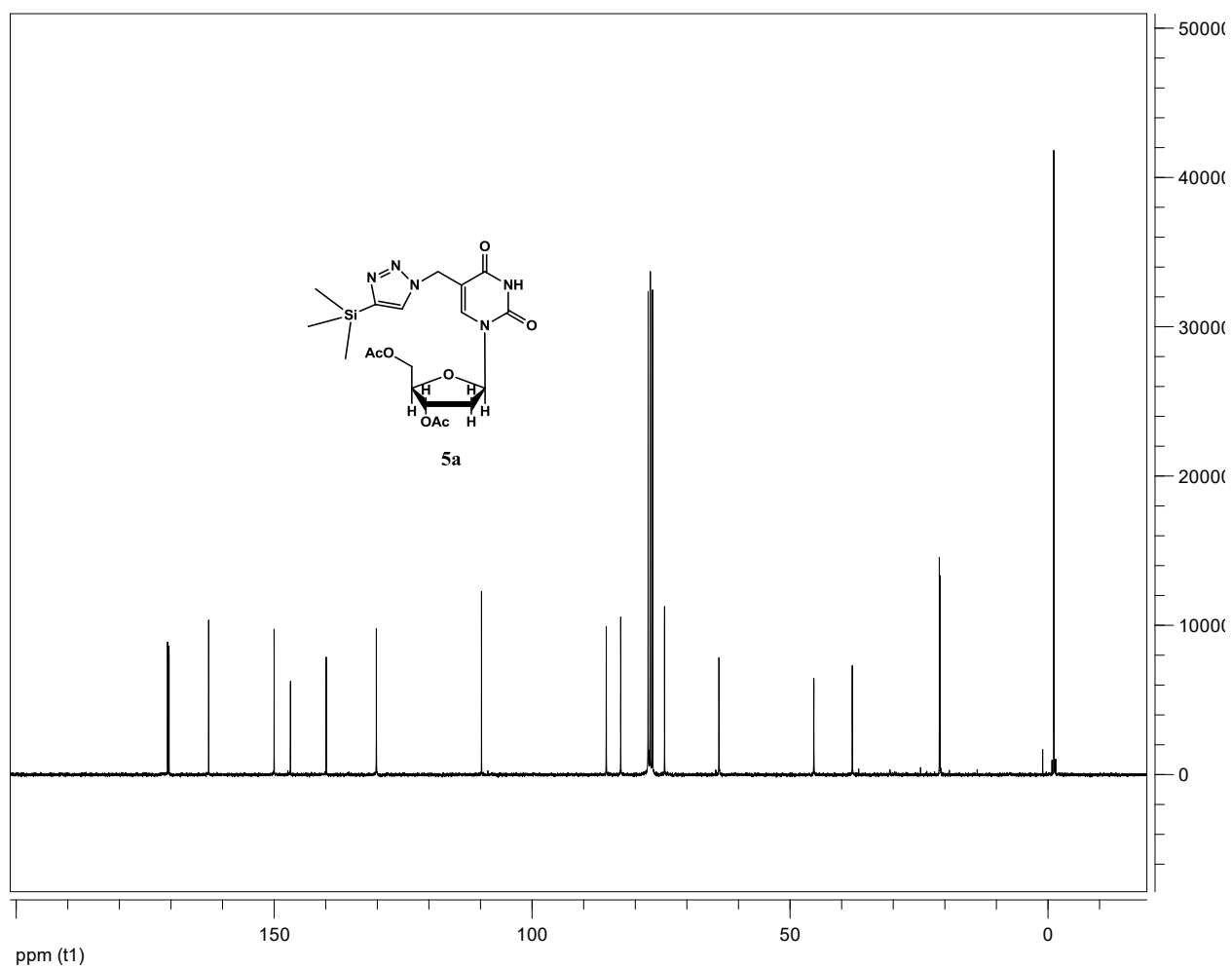
$^{13}\text{C}$ -NMR (DMSO, 300 MHz) of the nucleoside **11**



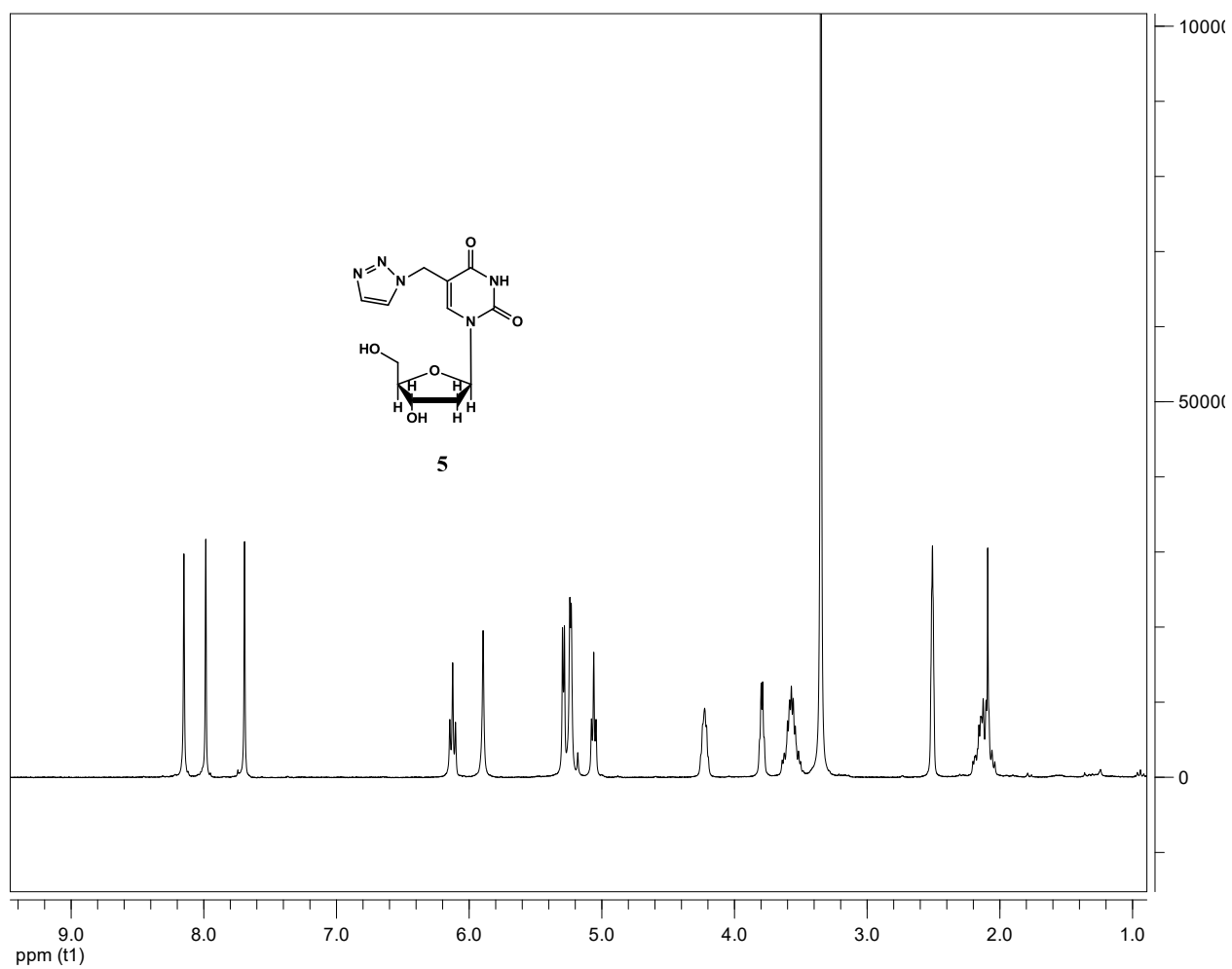
MS spectrum of compound **11**: Cal; 467.16, Found; 467.16



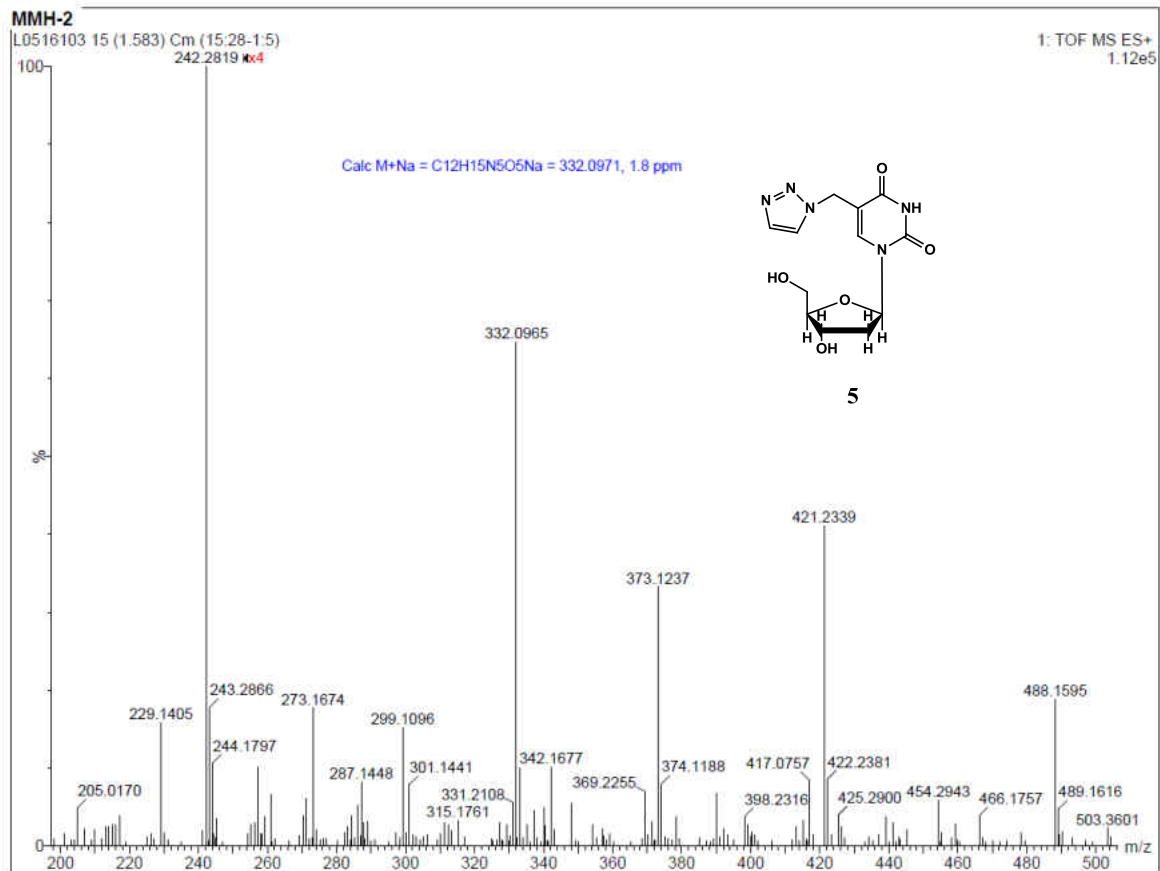
$^1\text{H-NMR}$  (CDCl<sub>3</sub>, 300 MHz) of the nucleoside **5a**



$^{13}\text{C}$ -NMR ( $\text{CDCl}_3$ , 300 MHz) of the nucleoside **5a**

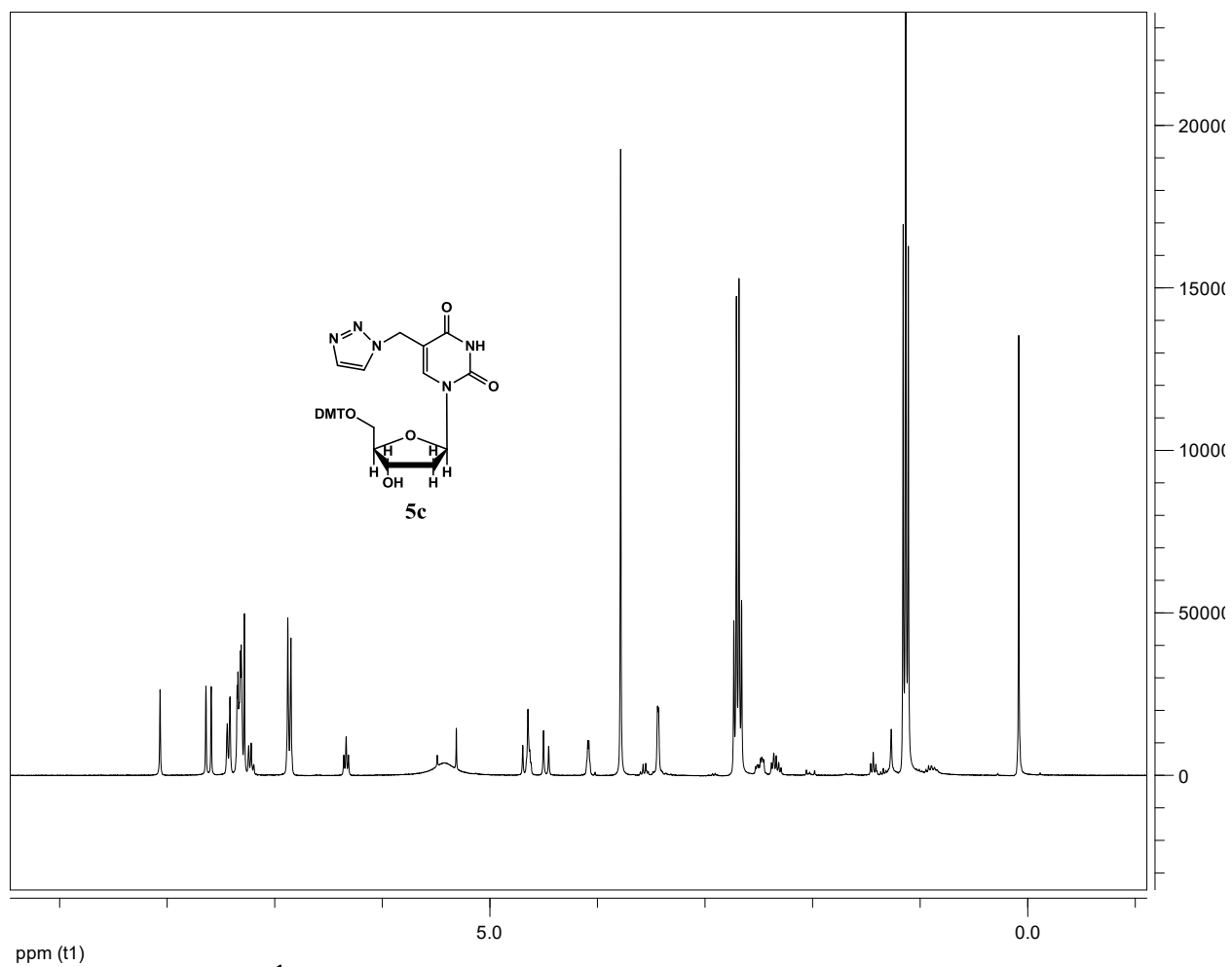


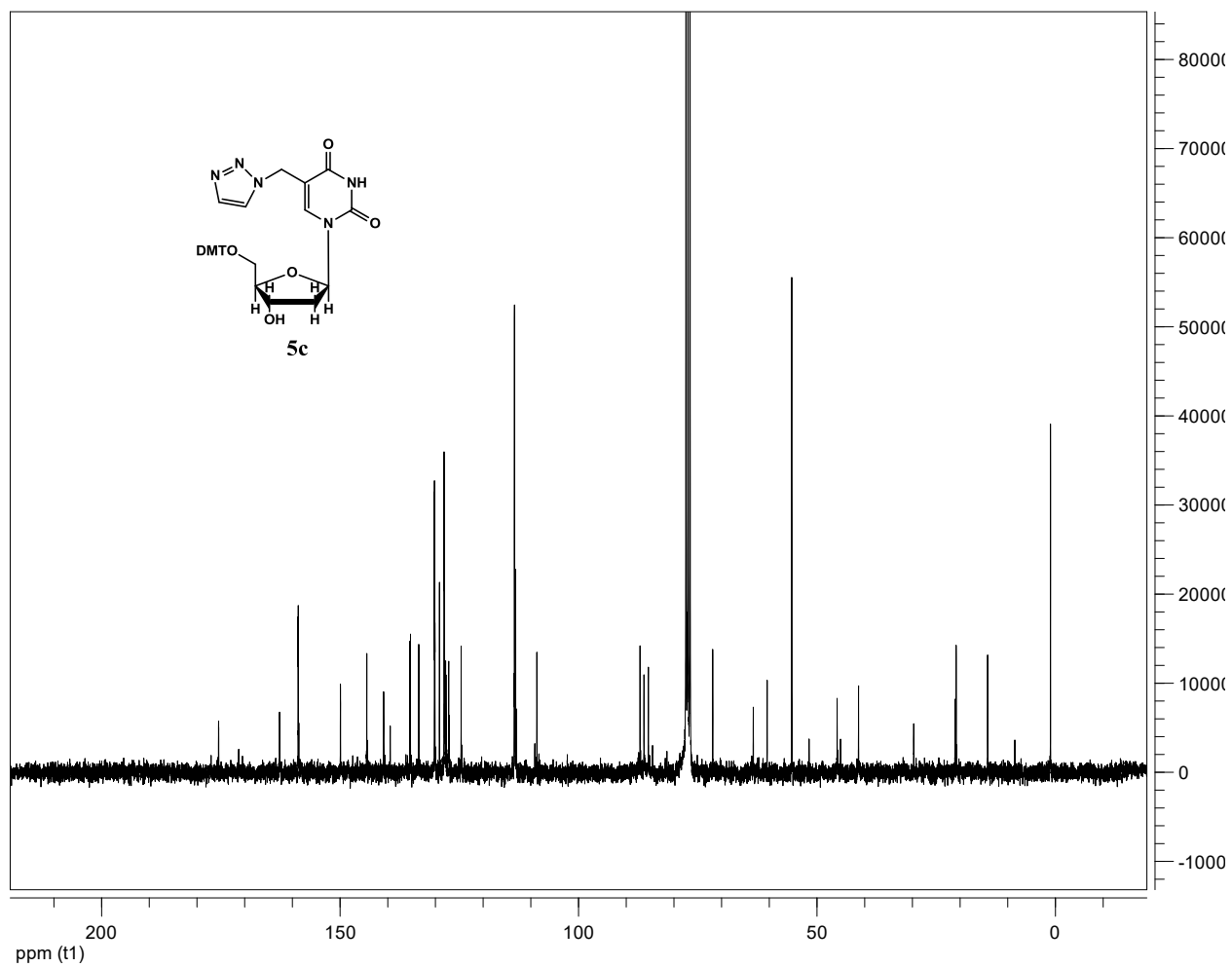
$^1\text{H-NMR}$  (DMSO, 300 MHz) of the nucleoside **5**



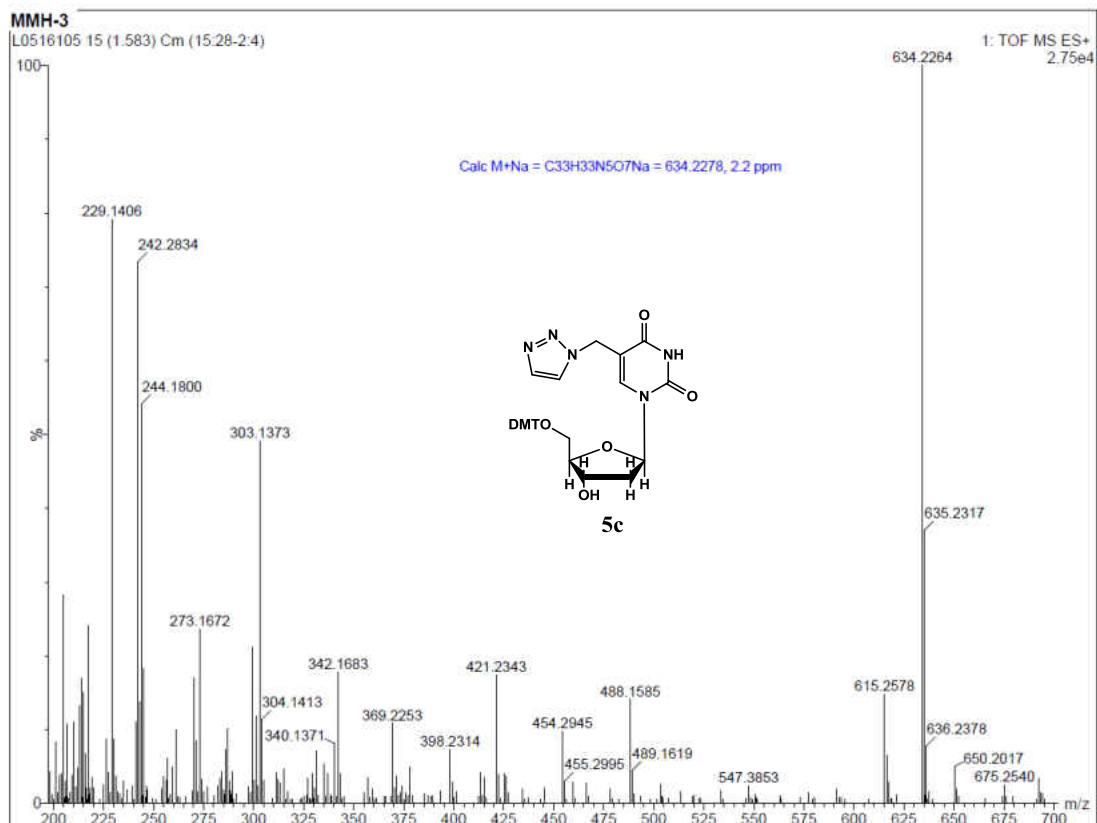
MS spectrum of 5

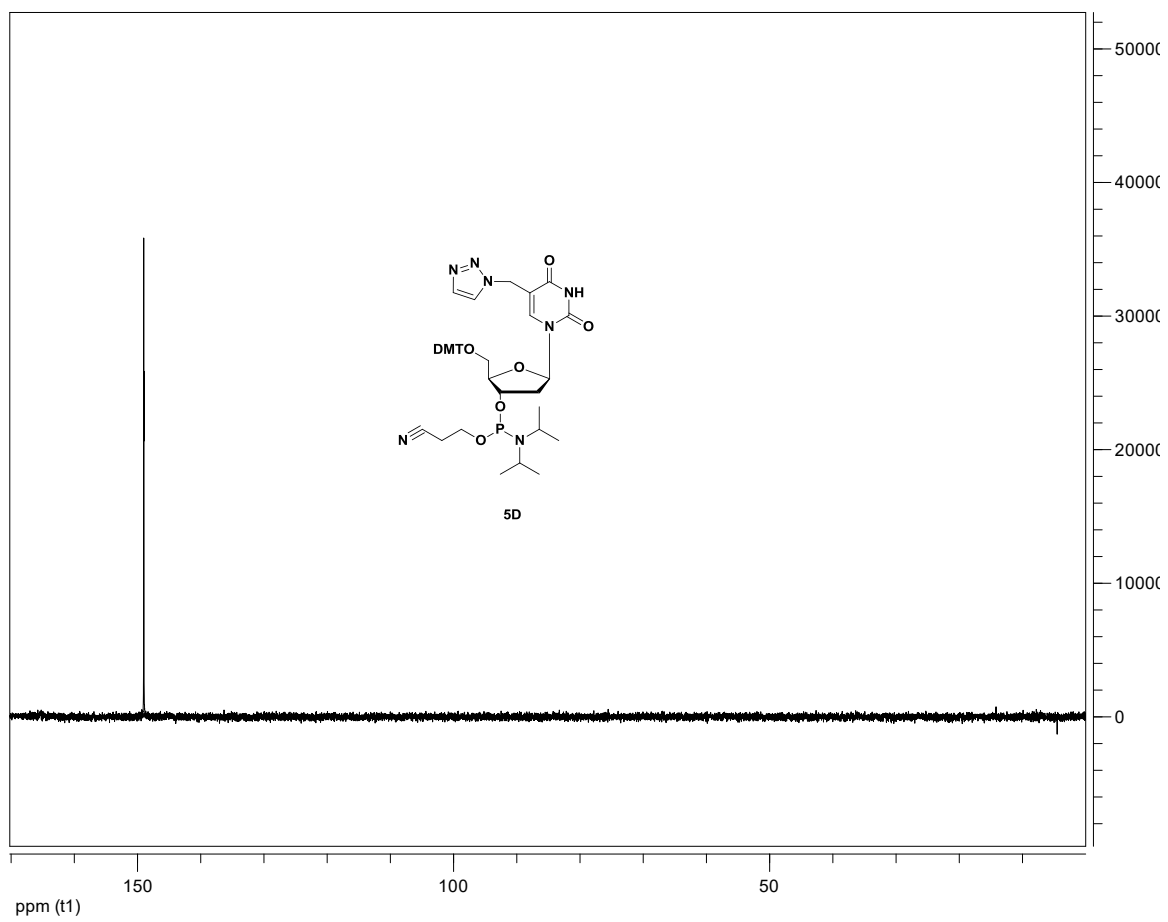




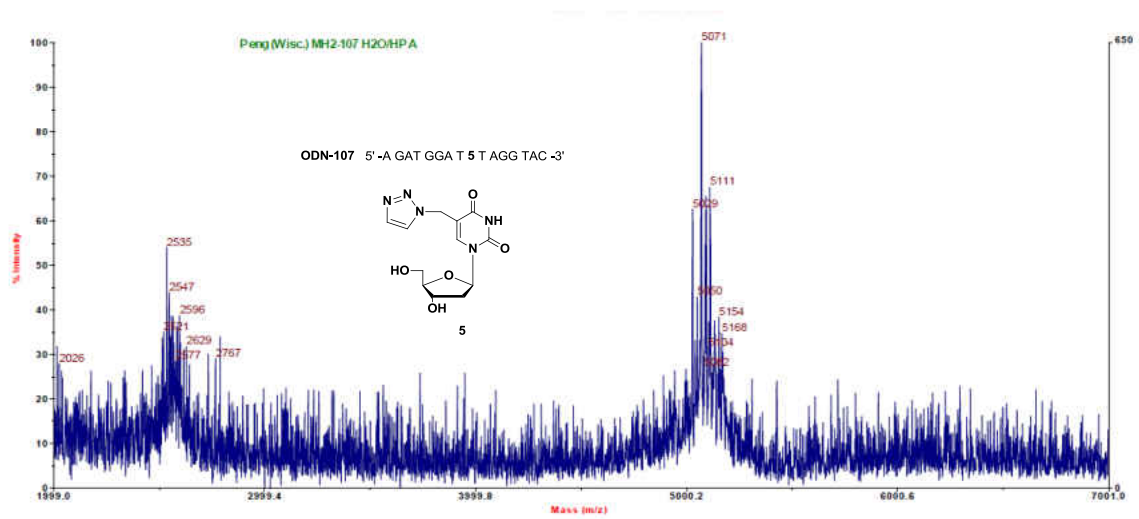


$^{13}\text{C}$ -NMR ( $\text{CDCl}_3$ , 300 MHz) of the nucleoside **5c**

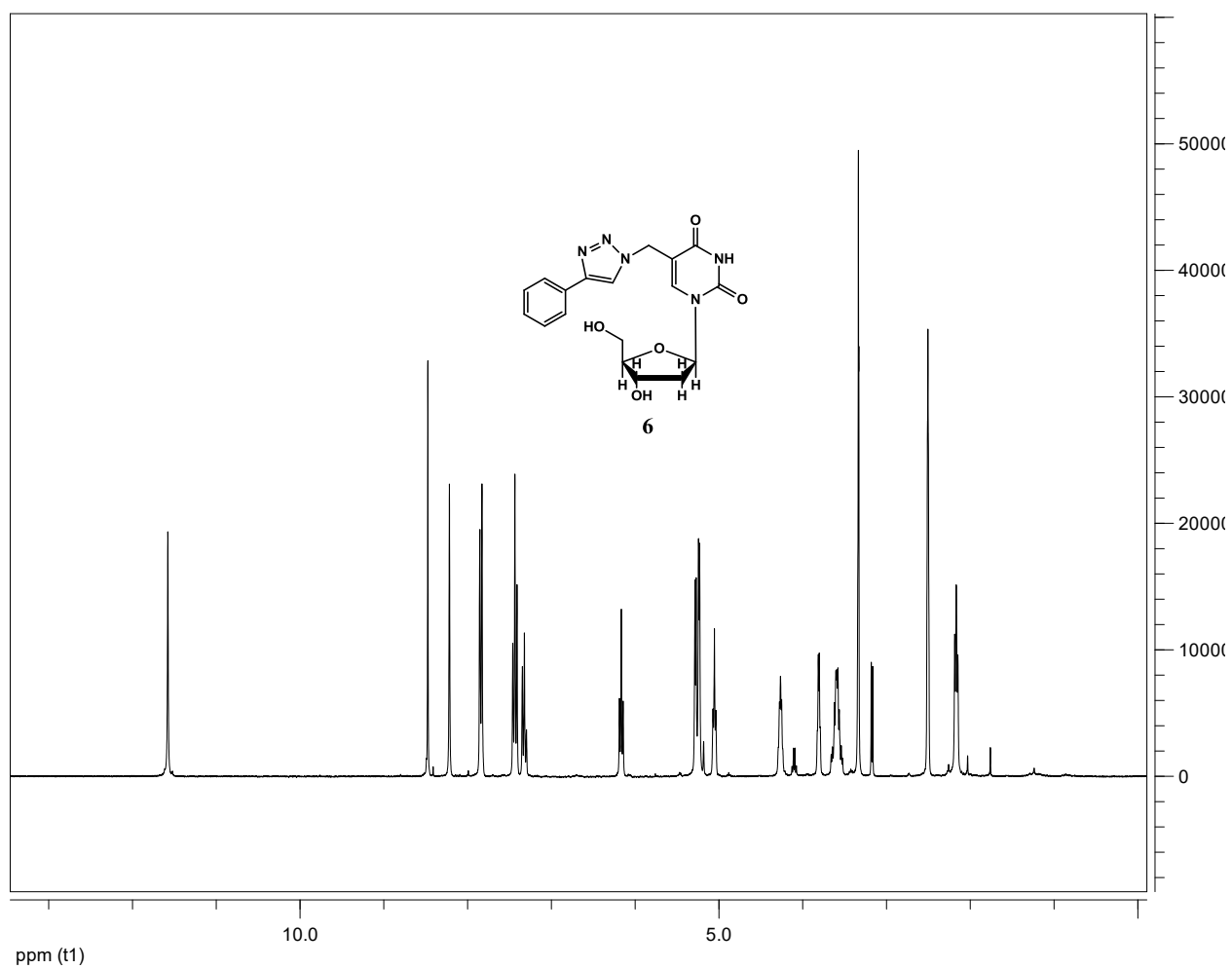
MS spectrum of **5c**



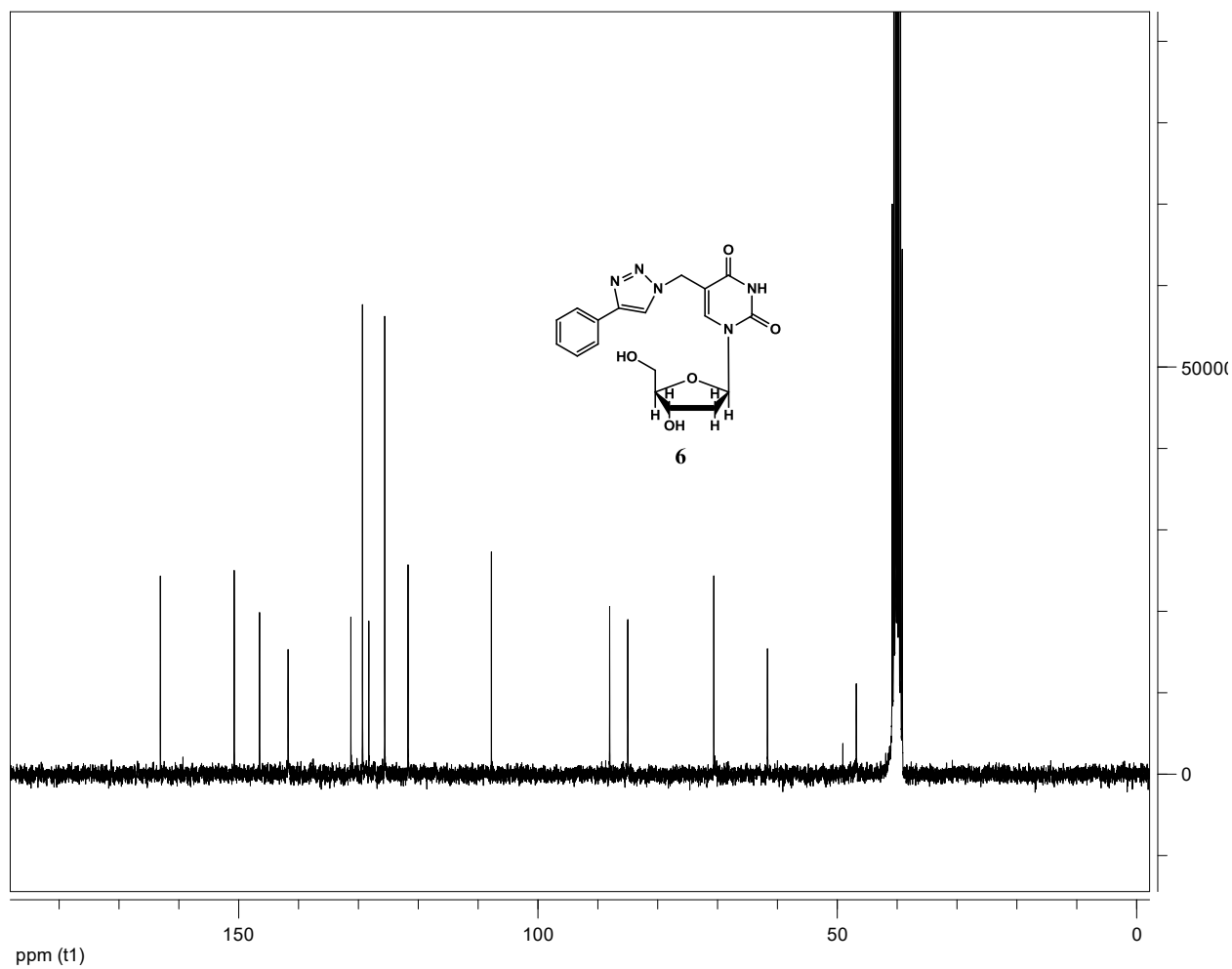
$^{31}\text{P}$ -NMR ( $\text{CDCl}_3$  300 MHz) of nucleoside **5d**



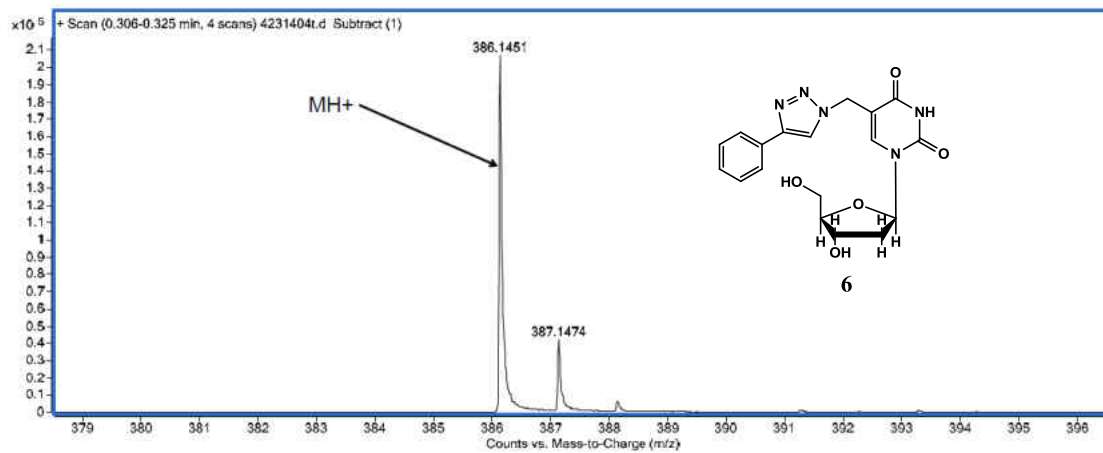
MS spectrum of ODN-107: Calculated; 5071, Found; 5071



$^1\text{H-NMR}$  (DMSO, 300 MHz) of the nucleoside **6**

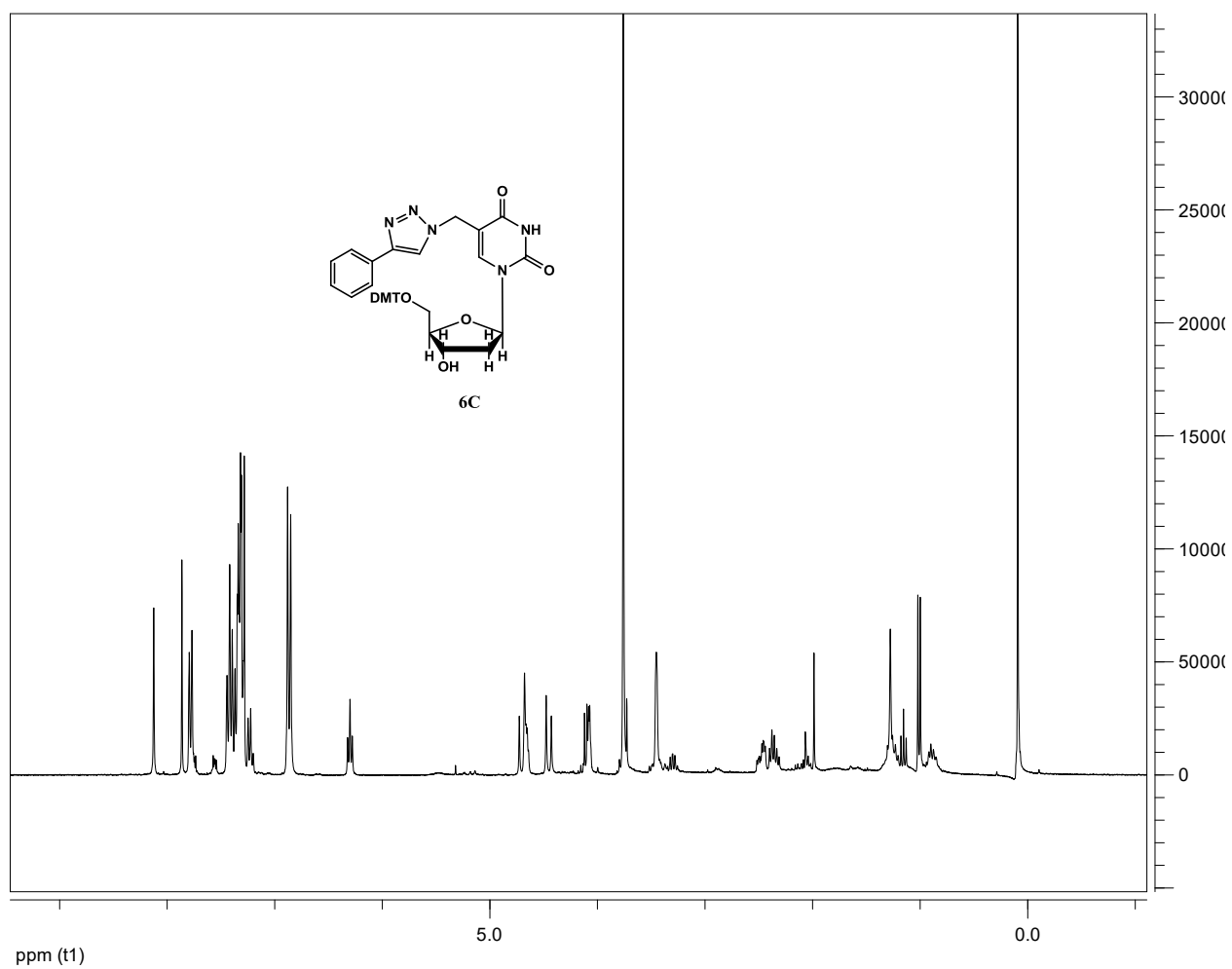


$^{13}\text{C}$ -NMR (DMSO, 300 MHz) of the nucleoside **6**

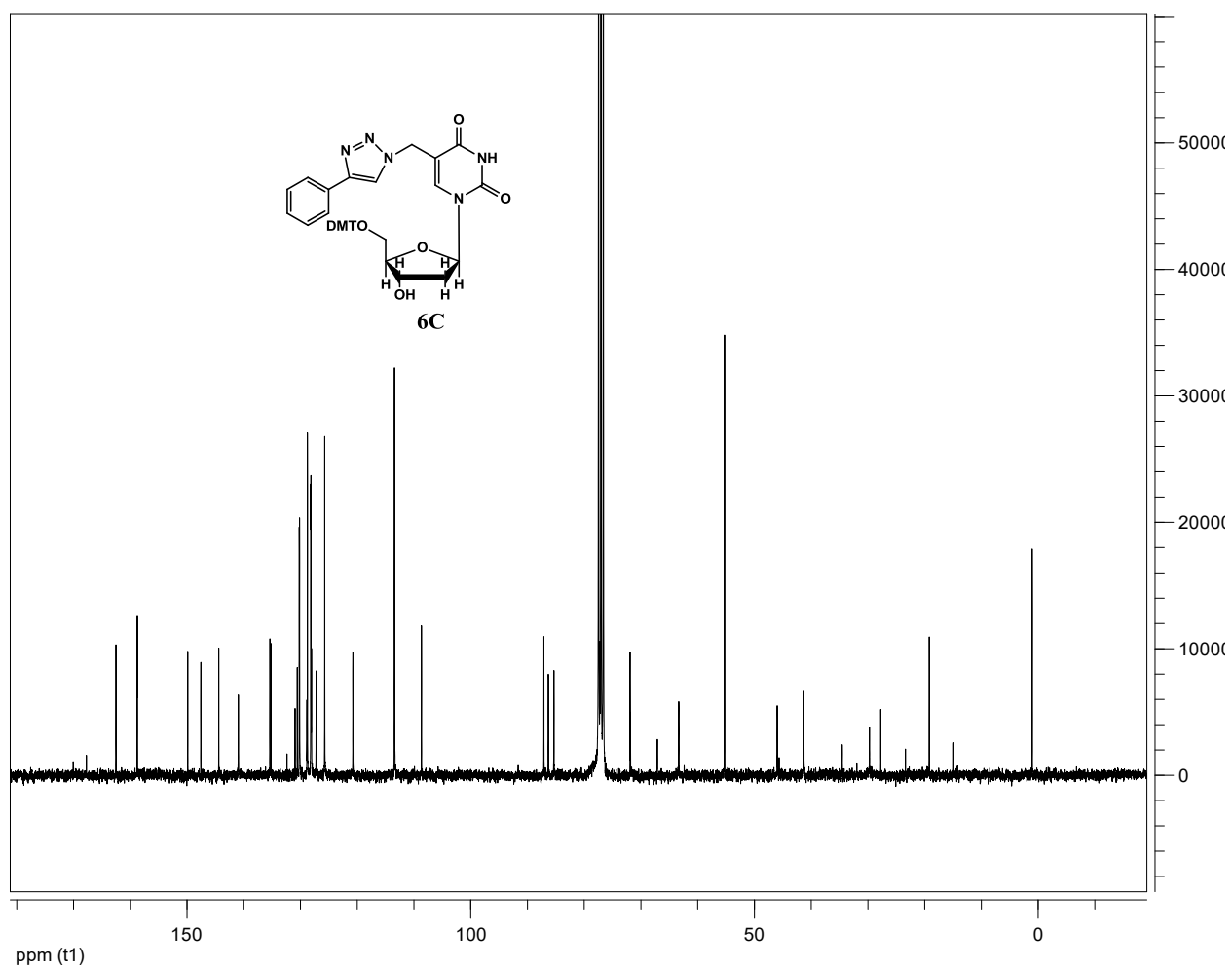


MS spectrum of compound **6**: Calculated; 386.15, Found; 386.15

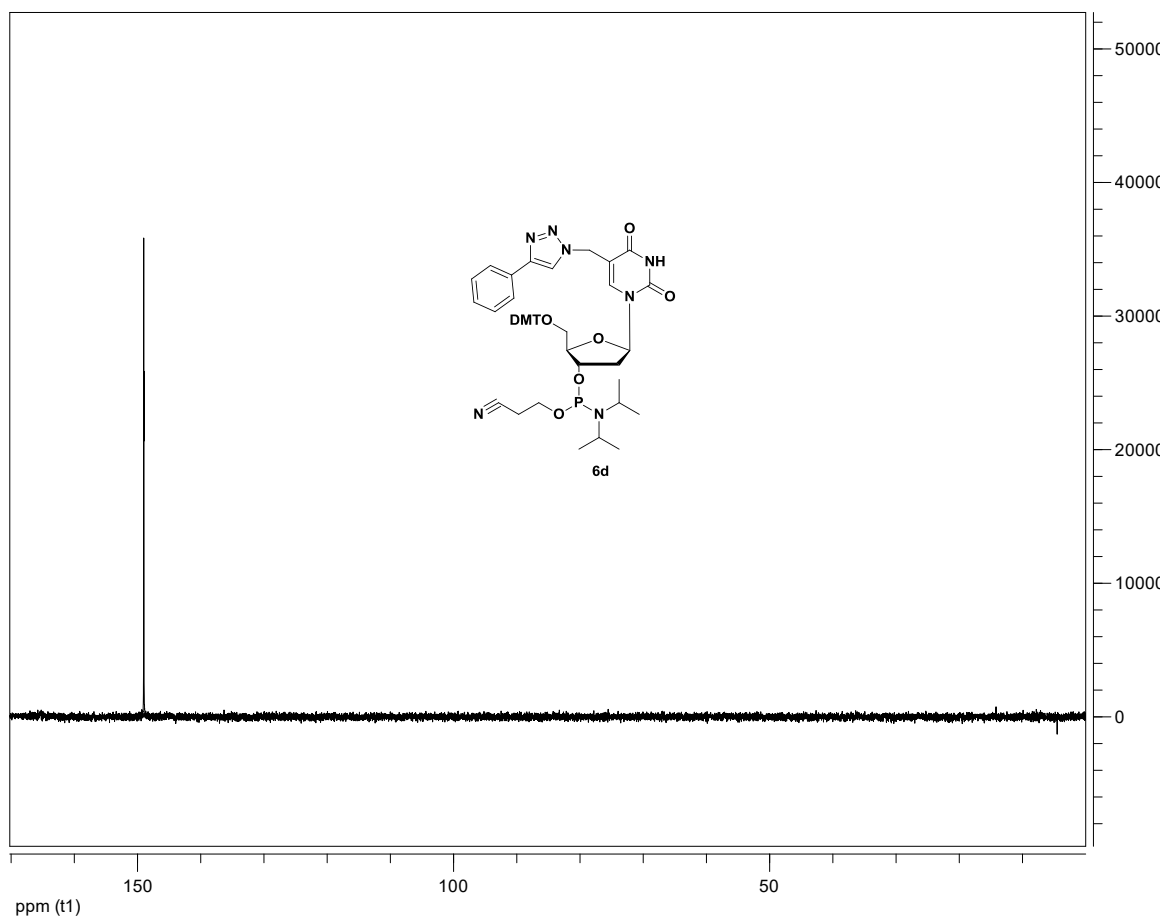




$^1\text{H-NMR}$  ( $\text{CDCl}_3$ , 300 MHz) of the nucleoside **6c**



$^{13}\text{C}$ -NMR ( $\text{CDCl}_3$ , 300 MHz) of the nucleoside **6c**



$^{31}\text{P}$ -NMR ( $\text{CDCl}_3$  300 MHz) of nucleoside **6d**

## 6. REFERENCES

- [1] Gottesfeld, J. M.; Neely, L.; Trauger, J. W. *Nature* **1997**, *387*, 202-205.
- [2] van der Marel, G. A.; Roelen, H. L.; van Boom, J. H.; Wang, A. H. *Embo. Journal* **1992**, *11*, 225-232.
- [3] Andersen, N. K.; Dossing, N.; Jensen, F.; Vester, B.; Nielsen, P. J. *Org. Chem.* **2011**, *76*, 6177-6187.
- [4] Levene, P. A. *J. Bio. Chem.* **1919**, *40*, 415-424.
- [5] Amblard, F.; Cho, J. H.; Schinazi, R. F. *Chem. Rev.* **2009**, *109*, 4207-4220.
- [6] Senoh, S.; Daly, J.; Axelrod, J.; Witkop, B. *J. Am. Chem. Soc.* **1959**, *81*, 6240-6245.
- [7] Martienssen, R. A.; Colot, V. *Science* **2001**, *293*, 1070-1074.
- [8] Henderson, I. R.; Jacobsen, S. E. *Nature* **2007**, *447*, 418-424.
- [9] Ahlert, D.; Stegemann, S.; Kahlau, S.; Ruf, S.; Bock, R. *Mol. Genet. Genomics* **2009**, *282*, 17-24.
- [10] Wang, X.; Song, Y.; Song, M.; Wang, Z.; Wang, T. H. *Anal. Chem.* **2009**, *81*, 7885-7891.
- [11] Peng, X.; Greenberg, M. *J. Am. Chem. Soc.* **2008**, *130*, 10299-10306.
- [12] Egan, D.; O'Kennedy, R.; Moran, E.; Cox, D.; Prosser, E.; Thornes, R. D. A. *Drug Metab. Rev.* **1990**, *22*, 503-529.
- [13] Egan, D.; O'Kennedy, R. *J. Chromatogr.* **1992**, *582*, 137-143.
- [14] Finn, G.; Kenealy, E.; Creaven, B. S.; Egan, D. A. *Cancer Lett.* **2002**, *183*, 61-68.
- [15] Long, L.; Zhou, L.; Wang, L.; Meng, S.; Gong, A.; Dub, F.; Zhang, C. *Org. Biomol. Chem.* **2013**, *11*, 8214-8220
- [16] Jone, G.; Rahman, M. A. *J. Phys. Chem.* **1994**, *98*, 13028-13037.

- [17] Jones, G.; Jackson, W. R.; Choi, C. Y.; Bergmark, W. R. *J. Phys. Chem.* **1985**, *89*, 294-300.
- [18] Stathatos, E.; Lianos, P.; Stangar, U. L.; Orel, B. *Chem. Phys. Letters* **2001**, *345*, 381-385.
- [19] Cohen, B.; Huppert, D. *J. Phys. Chem.* **2001**, *105*, 7157-7164.
- [20] Huang, Y.; Lu, Z.; Peng, Q.; Xie, R.; Xie, M.; Peng, J.; Cao, Y. *Journal of Materials Science* **2005**, *40*, 601-604.
- [21] Singh, S.; Kanetkar, V. R.; Sridhar, G.; Muthuswamy, V.; Raja, K. *J. Lumin.* **2003**, *101*, 285-291.
- [22] Wheelock, C. *J. Am. Chem. Soc.* **1959**, *81*, 1348-1352.
- [23] Mantulin, W.; Song, P. *J. Am. Chem. Soc.* **1973**, *95*, 5122-5129.
- [24] Singh, T. S.; Rao, B. S.M.; Mohan, H.; Mittal, J. P. *Journal of Photochemistry and Photobiology a-Chemistry* **2002**, *153*, 163-171.
- [25] Oh, J. K.; Wu, J.; Winnik, M. A.; Craun, G. P.; Rademacher, J. *Polym. Sci., Part A: Polym. Chem.* **2002**, *40*, 1594-1607.
- [26] Ammar, H.; Fery-Forgues, S.; El Gharbi, R. *Dyes and Pigments*, **2003**, *57*, 259-269.
- [27] Aihara, S.; Hirano, Y.; Tajima, T.; Tanioka, K.; Abe, M.; Saito, N.; Kamata, N.; Terunuma, D. *Appl. Phys. Lett.* **2003**, *82*, 511-515.
- [28] Murase, S.; Teramoto, M.; Furukawa, H.; Miyashita, Y.; Horie, K. *Macromolecules* **2003**, *36*, 964-966.
- [29] Voet, D.; Gratzer, W. B.; Cox, R. A.; Dotty, P. *Biopolymers* **1963**, *1*, 193-208.
- [30] Seela, F.; Sirivolu, V. R.; Chittepu, P. *Bioconjugate Chem.* **2008**, *19*, 211-224.
- [31] Guo, P.; Yan, S.; Hu, j.; Xing, X.; Wang, C.; Xu, X.; Qiu, X.; Ma, W.; Lu, C.; Weng, X. Zhou, X. *Org. Lett.* **2013**, *15*, 3266-3269.
- [32] Franzini, R. M.; Kool, E. T. *ChemBioChem.* **2008**, *9*, 2981 - 2988.
- [33] Seela, F.; Sirivolu, V. R.; Chittepu, P. *Bioconjugate Chem.* **2008**, *19*, 211-224.

- [34] Seela, F.; Pujari, S. S. *Bioconjugate Chem.* **2010**, *21*, 1629–1641.
- [35] Willner, I.; Rubin S. *Angew. Chem. Int. Ed. Engl.* **1996**, *35*, 367–385.
- [36] Asanuma, H.; Liang, X.; Yoshida, T.; Yamazawa, A.; Komiyama, M. *Angew. Chem. Int. Ed. Engl.* **2000**, *39*, 1316–1318.
- [37] Yamazawa, A.; Liang, X.; Asanuma, H.; Komiyama, M. *Angew. Chem. Int. Ed. Engl.* **2000**, *39*, 2356–2357.
- [38] Borisenko, V.; Burns, D. C.; Zhang, Z. H.; Woolley, G. A. *J. Am. Chem. Soc.* **2000**, *122*, 6364–6370.
- [39] Osman, P.; Martin, S.; Milojevic, D.; Tansey, C.; Separovic, F. *Langmuir* **1998**, *14*, 4238–4242.
- [40] Haiqian, Z.; Hiroaki, S.; Ning, G.; Hiroshi, S.; Masahiko, S. *J. Southeast Univ.* **2011**, *17*, 22–26.
- [41] Behrendt, R.; Renner, C.; Schenk, M.; Wang, F. Q.; Wachtveitl, J.; Oesterhelt, D.; Moroder, L. *Angew. Chem. Int. Ed.* **1999**, *38*, 2771–2774.
- [42] Behrendt, R.; Schenk, M.; Musiol, H. J.; Moroder, L. *J. Pept. Sci.* **1999**, *5*, 519–529.
- [43] Renner, C.; Behrendt, R.; Heim, N.; Moroder, L. *Biopolymers* **2002**, *63*, 382–393.
- [44] Renner, C.; Cramer, J.; Behrendt, R.; Moroder, L. *Biopolymers* **2000**, *54*, 501–514.
- [45] Ciamician, G.; Silber, P. *Berichte der Deutschen Chemischen Gesellschaft, zu Berlin* **1902**, *35*, 4128.
- [46] Kaval, N.; Drmolatev, D.; Appukkuttan, P.; Dehaen, W.; Kappe, C. O. *J. Comb. Chem.* **2005**, *7*, 490–502.
- [47] Rudolph, A. et al. *J. Org. Chem.* **2001**, *66*, 1242–1251.
- [48] Menapace, J. A.; Marlin, J. E.; Bruss, D. R.; Dascher, R. V. *J. Phys. Chem.* **1991**, *95*, 5509–5517.
- [49] Swamy, S. N.; Basappa, B. S.; Prabhuswamy, B.; Doreswamy, B. H. *Eur. J. Med. Chem.* **2006**, *41*, 531–538.

- [50] Kolb, H. C.; Finn, M. G.; Sharpless, K. B. *Angew. Chem. Int. Ed. Engl.* **2001**, *40*, 2004-2021.
- [51] Breinbauer, R.; Kohn, M. et al. *ChemBioChem.* **2003**, *4*, 1147-1149.
- [52] Tornøe, C. W.; Christensen, C.; Meldal, M. *J. Org. Chem.* **2002**, *67*, 3057-3064.
- [53] Sonogashira, K.; Tohda, Y.; Hagihara, N. *Tett. Lett.* **1975**, *16*, 4467-4470.
- [54] Zhang, L.; Chen, X.; Xue, P.; Sun, H. H. Y.; Williams, I. D.; Sharpless, K. B.; Fokin, V. V.; Jia, G. *J. Am. Chem. Soc. Comm.* **2005**, *127*, 15998-15999.
- [55] Rostovtsev, V. V.; Green, L. G.; Fokin, V. V.; Sharpless, K. B. *Angew. Chem. Int. Ed. Engl.* **2002**, *41*, 2596-2599.
- [56] Tornøe, C. W.; Christensen, C.; Meldal, M. *J. Org. Chem.* **2002**, *67*, 3057-3064.
- [57] El-Sagheer, A. H.; Brown, T. *Chem. Soc. Rev.* **2010**, *39*, 1388-1405.
- [58] Seela, F.; Ingale, S. A. *J. Org. Chem.* **2010**, *75*, 284-295.
- [59] Seo, T. S.; Li, Z.; Ruparel, H.; Ju, J. *J. Org. Chem.* **2003**, *68*, 609-612.
- [60] Nakane, M.; Ichikawa, S.; Matsuda, A. *J. Org. Chem.* **2008**, *73*, 1842-1851.
- [61] Ichikawa, S.; Ueno, H.; Sunadome, T.; Sato, K.; Matsuda, A. *Org. Lett.* **2013**, *15*, 694-697.
- [62] Mirkin, E. C.; Nguyen, S. T.; Eryazic, I. *Nanoscape* **2010**, *7*, 6-10.
- [63] Weller, R. L.; Rajsiki, S. R. *Org. Lett.* **2005**, *7*, 2141-2144.
- [64] Wang, Q.; Chan, T. R.; Hilgraf, R.; Fokin, V. V.; Sharpless, K. B.; Finn, M. G. *J. Am. Chem. Soc.* **2003**, *125*, 3192-3193.
- [65] Breinbauer, R.; Kohn, M. *ChemBioChem.* **2003**, *4*, 1147-1149.
- [66] Best, M. D. *Biochemistry* **2009**, *48*, 6571-6584.
- [67] Varizhuk, A. M.; Kaluzhny, D. N.; Novikov, R. A.; Chizhov, A. O.; Smirnov, I. P.; Chuvilin, A. N.; Tatarinova, O. N.; Fisunov, G. Y.; Pozmogova, G. E.; Florentiev, V. L. *J. Org. Chem.* **2013**, *78*, 5964-5969.

- [68] Kumar, R.; Ei-Saheer, A.; Tumpene, J.; Lincoln, P.; Wilhelmsson, L. M.; Brown, T. J. *Am. Chem. Soc.* **2007**, *129*, 6859-6864.
- [69] Peng, X.; Li, H.; Seidman, M. *Eur. J. Org. Chem.* **2010**, 4194–4197.
- [70] Sun, H.; Peng, X. *Bioconjugate Chem.* **2013**, *24*, 1226–1234.
- [71] Pujari, S. S.; Xiong, H.; Seela, F. *J. Org. Chem.* **2010**, *75*, 8693–8696.
- [72] Holden, M. J. *J. Agric. Food Chem.* **2003**, *51*, 2468–2474.
- [73] Li, H. Broughton-Head, V. J.; Peng, G. *Bioconjugate Chem.* **2006**, *17*, 1561–1567.
- [74] Puri, N. Majumdar, A.; Cuenoud, B. *Biochemistry* **2002**, *41*, 7716–7726.
- [75] Puri, N.; Majumdar, A.; Cuenoud, B.; Miller, P.; Seidman, M. *Biochemistry* **2004**, *43*, 1343–1351.
- [76] Nagatsugi, F. et al. *Nucleic Acids Res.* **2003**, *31*, e31.
- [77] Nguyen, H. T. et al. *J. Nat. Prod.* **2009**, *72*, 527–539.
- [78] Rossi, M. et al. *J. Nat. Prod.* **2001**, *64*, 26–31.
- [79] Noll, D. M.; Mason, T. M.; Miller, P. S. *Chem. Rev.* **2006**, *106*, 277-301.
- [80] Dronkert, M. L. G.; Kanaar, R. *Mutat. Res.* **2001**, *486*, 217-247.
- [81] Peng, X.; Ghosh, A.; Houten, B. V.; Greenberg, M. M. *Biochem.* **2010**, *49*, 304-311.
- [82] Peng, X.; Pigli, Y.; Rice, P. A.; Greenberg, M. M. *J. Am. Chem. Soc.* **2008**, *130*, 12890-12891.
- [83] Weng, M.; Zheng, Y.; Jasti, V.; Champeil, E.; Tomasz, M.; Wang, Y.; Basu, A.; Tang, M. *Nucleic Acids Res.* **2010**, *38*, 6976-6984.
- [84] Peng, X.; Greenberg, M. M. *Nucleic Acids Res.* **2008**, *36*, e31.
- [85] Sun, H.; Peng, X. *Bioconjugate Chem.* **2013**, *24*, 1226-1234.



- [86] Doria, F.; Nadai, M.; Folini, M.; Scalabrin, M.; Germani, L.; Sattin, G.; Mella, M.; Palumbo, M.; Zaffaroni, N.; Fabris, D.; Freccero, M.; Richter, S. N. *Chem. Eur. J.* **2013**, *19*, 1457–1465.
- [87] Doria, F.; Nadai, M.; Folini, M.; Di Antonio, M.; Germani, L.; Percivalle, C.; Sissi, C.; Zaffaroni, N.; Alcaro, S.; Artese, A.; Richter, S. N.; Freccero, M. *Org. Biomol. Chem.* **2012**, *10*, 2798–2806.
- [88] Rusling, D. A.; Nandhakumar, I. S.; Brown, T.; Fox, K. R. *Chem. Commun.* **2012**, *48*, 9592–9594.
- [89] Seeman, N. C. *Nature* **2003**, *421*, 427–431.
- [90] Turberfield, J. *Phys. World* **2005**, *16*, 43–46.
- [91] He, Y.; Liu, H.; Chen, Y.; Tian, Y.; Deng, Z.; Ko, S. H.; Ye, T.; Mao, C. *Microsc. Res. Tech.* **2007**, *70*, 522–529.
- [92] Yan, H. *Science*, **2004**, *306*, 2048–2049.
- [93] Steinhauer, C.; Jungmann, R.; Sobey, T. L.; Simmel F. C.; Tinnefeld, P. *Angew. Chem. Int. Ed. Engl.* **2009**, *121*, 9030–9034.
- [94] Aldaye, F. A.; Palmer, A. L.; Sleiman, H. F. *Science* **2008**, *321*, 1795–1799.
- [95] Genereux, J. C.; Barton, J. K. *Chem. Rev.* **2010**, *110*, 1642–1662.
- [96] Matsuura, H.; Hirai, A.; Yamada, F.; Matsumoto, T.; Kawai, T. *J. Am. Chem. Soc.* **2008**, *130*, 5002–5003
- [97] Gao, L. et al. *ACS Nano*, **2012**, *6*, 689–695
- [98] Niemeyer, C. M.; Ceyhan, B.; Noyong, M.; Simon, U. *Biochem. Biophys. Res. Comm.* **2003**, *311*, 995–999.
- [99] Storhoff, J. J.; Lazarides, A. A.; Mucic, R. C.; Mirkin, C. A.; Letsinger, R. L.; Schatz, G. C. *J. Am. Chem. Soc.* **2000**, *122*, 4640–4650.
- [100] Storhoff, J. J.; Mirkin, C. A. *ChemRev.* **1999**, *99*, 1849–1862.
- [101] Cao, S.; Peng, X. *Curr. Org. Chem.* **2014**, *18*, 1–15.
- [102] Haque, M. M.; Sun, H.; Peng, X. *Angew. Chem. Int. Ed. Engl.* **2014**, *53*, 5001–7005.

- [103] Trenor, S. R. et al. *Chem. Rev.* **2004**, *104*, 3059–3078.
- [104] Killard, A. J.; O'Kennedy, R.; Bogan, D. P. *J. Pharm. Biomed. Anal.* **1996**, *14*, 1585–1590.
- [105] Appendino, G. J. et al. *Nat. Prod.* **2004**, *67*, 532–536.
- [106] Semple, S. J.; Nobbs, S. F.; Pyke, S. M.; Reynolds, G. D.; Flower, R. J. *Ethnopharmacol* **1999**, *68*, 283–288.
- [107] Reed, M. W. et al. *J. Org. Chem.* **1988**, *53*, 4166–4171.
- [108] Mal, N. K. et al. *Chem. Mater.* **2003**, *15*, 3385–3394.
- [109] Liu, X. et al. *J. Phys. Chem.* **2012**, *116*, 727–737.
- [110] Madari, H. et al. *J. Nat. Prod.* **2004**, *67*, 1204–1210.
- [111] Egan, D.; O'Kennedy, R.; Moran, E.; Cox, D.; Prosser, E.; Thornes, R. D. *Drug Metabolism Reviews* **1990**, *22*, 503–529.
- [112] Luo, K. W.; Sun, J. G.; Chan, J. Y. et al. *Chemotherapy* **2011**, *57*, 449–459.
- [113] Choi, J.; Lee, K. T.; Ka, H.; Jung, W. T.; Jung, H. J.; Park, H. J. *Arch. Pharmacol Res.* **2001**, *24*, 418–423.
- [114] Ren, R.; Chaudhuri, N. C.; Paris, P.L.; Rumney, S.; Kool, E. T. *J. Am. Chem. Soc.* **1996**, *118*, 7671–7678.
- [115] Strassler, C.; Davis, N. E.; Kool, E. T. *Helv. Chim. Acta.* **1999**, *82*, 2160–2171.
- [116] Antonio, M. D.; Doria, F.; Mella, M.; Merli, D.; Profumo, A.; Freccero, M. *J. Org. Chem.* **2007**, *72*, 8354–8360.
- [117] Verga, D.; Nadai, M.; Doria, F.; Percivalle, C.; Antonio, M. D.; Palumbo, M.; Richter, S. N.; Freccero, M. *J. Am. Chem. Soc.* **2010**, *132*, 14625–14637.
- [118] Wang, P.; Liu, R.; Wu, X.; Ma, H.; Cao, X.; Zhou, P.; Zhang, J.; Weng, X.; Zhang, X.; Qi, J.; Zhou, X.; Weng, L. *J. Am. Chem. Soc.* **2003**, *125*, 1116–1117.
- [119] Doria, F.; Percivalle, C.; Freccero, M. *J. Org. Chem.* **2012**, *77*, 3615–3619.

- [120] Shahid, K. A.; Majumdar, A.; Alam, R.; Liu, S. T.; Kuan, J. Y.; Sui, X. F.; Cuenoud, B.; Glazer, P. M.; Miller, P. S.; Seidman, M. M. *Biochemistry* **2006**, *45*, 1970-1978.
- [121] Majumdar, A.; Muniandy, P. A.; Liu, J.; Liu, J. L.; Liu, S. T.; Cuenoud, B.; Seidman, M. M. *J. Biol. Chem.* **2008**, *283*, 11244-11252.
- [122] Thazhathveetil, A. K.; Liu, S. T.; Indig, F. E.; Seidman, M. M. *Bioconjug. Chem.* **2007**, *18*, 431-437.
- [123] Takasugi, M.; Guendouz, A.; Chassignol, M.; Decout, J. L.; Lhomme, J.; Thuong, N. T.; *Natl. Acad. Sci. U.S.A.* **1991**, *88*, 5602-5606.
- [124] Wagner, B. D. *Molecules* **2009**, *14*, 210-237.
- [125] Michalski, R.; Zielonka, j.; Gapys, E.; Marcinek, A.; Joseph, J.; Kalyanaraman, B. *J. Biol. Chem.* **2014**, *289*, 22536-22553.
- [126] Cao, H.; Hearst, J. E.; Corash, L.; Wang, Y. *Anal. Chem.* **2008**, *80*, 2932-2938.
- [127] Hong, I. S.; Greenberg, M. M. *J. Am. Chem. Soc.* **2005**, *127*, 3692-3693.
- [128] Hong, I. S.; Ding, H.; Greenberg, M. M. *J. Am. Chem. Soc.* **2006**, *128*, 485-491.
- [129] Hong, I. S.; Greenberg, M. M. *J. Am. Chem. Soc.* **2005**, *127*, 10510-10511.
- [130] Hong, I. S.; Ding, H.; Greenberg, M. M. *J. Am. Chem. Soc.* **2006**, *128*, 2230-2231.
- [131] Ding, H.; Greenberg, M. M. *J. Org. Chem.* **2010**, *75*, 535-544.
- [132] Kuang, Y.; Sun, H.; Blain, J. C.; Peng, X. *Chem. Eur. J.* **2012**, *18*, 12609-12613.
- [133] Rostovtsev, V. V.; Green, L. G.; Fokin, V. V.; Sharpless, K. B. *Angew. Chem. Int. Ed. Engl.* **2002**, *41*, 2596-2599.
- [134] Sun, H.; Peng, X. *Bioconjugate Chem.* **2013**, *24*, 1226-1234.
- [135] Herdewijn, P.; Ruf, K.; Pfeleiderer, W. *Helvetica Chimica Acta* (Impact Factor: 1.38). **2004**, *74*, 7 - 23.
- [136] Mentel, R.; Kurek, S.; Wegner, U.; Janta-Lipinski, M.; Gurtler, L.; Matthes, E. *Med Microbiol Immunol.* **2000**, *89*, 91-5
- [137] Bergstrom, D. E. et al. *J. Med. Chem.* **1984**, *27*, 285-292.

- [138] Simons, C.; Langhorne, P. A. *Gordon and Breach Science Publishers* **2001**, *43*, 83–102.
- [139] De Clercq, E. *Nat. Rev. Drug Discovery* **2002**, *1*, 13–25.
- [140] Weber, U. S.; Steffen, B.; Siegers, C. P. *Res. Commun. Mol. Pathol. Pharmacol.* **1998**, *99*, 193-206.
- [141] Egan, D.; James, P.; Cooke, D.; O'Kennedy, R. *Cancer Lett.* **1997**, *118*, 201-211.
- [142] Cooke, D. et al. *Eur. J. Med. Chem.* **2003**, *38*, 597-603.
- [143] Budzisz, E.; Brzezinska, E.; Krajewska, U.; Rozalski, M. *Eur. J. Med. Chem.* **2003**; *38*: 597-603.
- [144] Robertson, E.; Deussen, W.; Minsk, L. *J. Appl. Polym. Sci.* **1959**, *2*, 308-311.
- [145] Minsk, L. M.; Van Deussen, W. P.; Wright J. F. *J. App. Poly. Science* **1959**, *2*, 302-311.
- [146] Decker, C.; Bianchi, C. *Polym. Int.* **2003**, *52*, 722-732.
- [147] Schonberg, A.; Latif, N.; Moubasher, R.; Awad, W. *J. Chem. Soc.* **1950**, 374-379.
- [148] Trenor, S. R.; Long, T. E.; Love, B. *J. Macromolecular Chemistry and Physics* **2004**, *205*, 715-723.
- [149] Yatsushashi, T.; Nakashima, N. *J. Phys. Chem.* **2000**, *104*, 1095–1099.
- [150] Anet, R. et al. *Can. J. Chem.* **1962**, *40*, 1249-1256.
- [151] Dawn, S. et al. *J. Am. Chem. Soc.* **2011**, *133*, 7025–7032.
- [152] Straub, K. et al. *J. Am. Chem. Soc.* **1981**, *103*, 2347-2355.
- [153] Cimino, G. D. et al. *Ann. Rev. Biochem.* **1985**, *54*, 1151-1153.
- [154] Chen, Y.; Geh, J. L. *Polymer* **1996**, *37*, 4473-4477.
- [155] Chen, Y.; Geh, J. L. *Polymer* **1996**, *37*, 177-181.
- [156] Chen, Y.; Hong, R. T. *J. Polym. Sci., Part A: Polym. Chem.* **1997**, *35*, 2999-3008.

- [157] Chen, Y.; Jean, C. S. *J. Appl. Polym. Sci* **1997**, *64*, 1749-1754.
- [158] Chen, Y.; Jean, C. S. *Journal of Applied Polymer Science* **1997**, *64*, 1759-1768.
- [159] Delzenne, G. A.; Laridon, U. *36th Congress International De Chimie Industrielle* **1967**, *3*, 373.
- [160] Chujo, Y.; Sada, K.; Saegusa, T. *Macromolecules* **1990**, *23*, 2693-2697.
- [161] Chujo, Y.; Sada, K.; Saegusa, T. *Macromolecules* **1990**, *23*, 2636
- [162] Scheit, K. H. *Biochim. Biophys. Acta.* **1970**, *209*, 445-454.
- [163] Ni, X. et al. *J. Chin. Chem. Soc.* **2012**, *59*, 439-1445
- [164] Eisinger, J.; Lamola, A. A. *Methods Enzymol.* **1971**, *21*, 24-29.
- [165] Hiratsuka, T.; Uchida, K. *Biochim. Biophys. Acta.* **1973**, *320*, 635- 647.
- [166] Hiratsuka, T. *Biochim. Biophys. Acta.* **1983**, *742*, 496-508.
- [167] El-Sagheer, A. H.; Brown, T. *Chem. Soc. Rev.* **2010**, *39*, 1388-1405.
- [168] Seela, F.; Ingale, S. A. *J. Org. Chem.* **2010**, *75*, 284-295.
- [169] Seo, T. S.; Li, Z.; Ruparel, H.; Ju, J. *J. Org. Chem.* **2003**, *68*, 609-612.
- [170] Wenge, U.; Ehrenschwender, T.; Wagenknecht, H. A. *Bioconjugate Chem.* **2013**, *24*, 301-304.
- [171] Werder, S.; Malinovskii, V. L.; Haner, R. *Org. Lett.* **2008**, *10*, 2011-2014.
- [172] Ingale, S. A.; Pujari, S. S.; Sirivolu, V. R.; Ding, P.; Xiong, H.; Mei, H. *J. Org. Chem*, **2012**, *77*, 188-199.
- [173] Wang, Z.; You, T.; Xu, H. Y.; Haoxin, S. *Molecules* *1*, 68-73.
- [174] Udupi, R. H.; Kushnoor, A.; Bhat, A. R. *J. Indian. Chem. Soc.* **1999**, *76*, 461-464.
- [175] Tsukuda, T.; Shiratori, Y.; Watanabe, M. H.; Ontsuka, K.; Hattori, N. *Bioorg. Med. Chem. Lett.* **1998**, *8*, 1819-1824.

- [176] Hirpara, H. M.; Sodha, V. A.; Trivedi, A. M.; Khatri, B. L.; Parikh, A. R. *Indian J. Chem.* **2003**, *42*, 1756–1759.
- [177] Isloor, A. M.; Kalluraya, B.; Shetty, P. *Eur. J. Med. Chem.* **2009**, *44*: 3784–3787
- [178] Shivarama, H. B.; Narayana, P. K.; Sooryanarayana, R. B.; Shivananda, M. K. *Eur. J. Med Chem.* **2002**, *37*: 511–517.

## 7. List of Publications

1. Haque, M.; Sun, H.; Peng, X. *'Angewandte chemie. Int. ed. Engl.'*, "Photo-Switchable DNA Interstrand Cross-Link Formation by a Coumarin-Modified Nucleotide" **2014**, *53*, 7001–7005
2. . Haque, M.; Peng, X. *'Science China Chemistry'*: "DNA Associated Click Chemistry" **2014**, *57*, 215-231

## 8. Curriculum Vitae of Mohammad Mojibul Haque

---

### EDUCATION

**Doctors of Philosophy (PhD);** Major: Organic Chemistry; Minor: Physical Chemistry; GPA: 3.64/4.0

Chemistry and Biochemistry, University of Wisconsin-Milwaukee, WI, USA;

**Dissertation Title:** Modification of Pyrimidine and Purine Nucleotides by “Click” Chemistry: Design, Synthesis, and Properties Study

**Master of Science (M. S.)’ 2008;** Department of Chemistry, University of Dhaka, Bangladesh; Major: Physical Chemistry

**Thesis Title:** “Electrochemical behaviors analysis of Brilliant Red on glass electrode on cyclic voltammetry.”

**Bachelor of Science (B. S.)’ 2008,** Department of Chemistry, University of Dhaka, Bangladesh

### PROFESSIONAL SUMMARY AND TEACHING EXPERIENCE

#### 5 Years Teaching Experience:

5 years as graduate teaching assistant within Chemistry department, University of Wisconsin-Milwaukee, WI, USA.

#### Special Teacher’s Training Course:

- “Teaching and Learning in College: Reflection on Theory and Practice” at spring’ 2014, UWM, WI, USA.
- “Preparing Future Faculty (PFF)” faculty training course at Marquette University, WI, USA at spring’ 2013.
- “Leave Your Mark” professional leadership management course conducted at spring’ 2014 by UWM, WI, USA

#### Supervision of Undergraduate Research Projects:

Supervised 10 undergraduate students on different organic chemistry research projects throughout the last five years where I taught organic synthesis, DNA click chemistry, and characterization of a series of DNA nucleotides with different substituents, and DNA interstrand crosslinking study.

**Provided Tutoring to Undergraduate Chemistry Students:** Tutored undergraduate students and promoted learning by using a broad range of teaching techniques and methods in order to inspire and motivate students’ knowledge of chemistry.



**MAJOR COURSES COMPLETED IN MASTER'S & PHD STUDY**

- Modern Industrial Organic Chemistry
- Intermediate Chemical Thermodynamics
- Advance Organic Chemistry
- Medicinal Chemistry-1 and 2
- Advance Survey of Inorganic Chemistry
- Topics in Organic Heterocyclic Chemistry
- Topics in Organic Chemistry
- Organic Nanomaterials Chemistry
- Statistical Thermodynamics
- Introduction to Biochemistry
- Intermediate Analytical Chemistry
- Chemistry of Materials
- Polymer chemistry
- Advance photochemistry
- Advance Chemical Kinetics
- Chemistry of Atmospheric Environment
- Molecular Symmetry and Advance Spectroscopy

**SCHOLASTIC ACHIEVEMENTS: HONORS AND AFFILIATIONS**

- "Graduate Research Award": Department of Chemistry and Biochemistry, UWM, 2013
- Governance: Graduate Student Advisory Council (GSAC), UWM: January' 2013-December' 2013
- Mentor of Graduate student, Department of Chemistry and Biochemistry, UWM, 2012
- Chemistry and Biochemistry Graduate Councilor, Department of Chemistry and Biochemistry, UWM, 2013

**SELECTED PUBLICATIONS**

1. Haque, M.; Sun, H.; Peng, X. *'Angewandte chemie. Int. ed. Engl.'*, "Photo-Switchable DNA Interstrand Cross-Link Formation by a Coumarin-Modified Nucleotide" **2014**, *53*, 7001–7005
2. Haque, M.; Peng, X. *'Science China Chemistry'*: "DNA Associated Click Chemistry" **2014**, *57*, 215-231

**MOST RECENT PRESENTATIONS AND TRAININGS**

- Haque, M.; Peng, X. "Photoswitchable DNA Interstrand Cross-link Generation by Coumarin Modified Pyrimidine" 247<sup>th</sup> ACS National Meeting, Dallas, Texas. March'2014
- Haque, M.; Peng, X. "Click Modified Pyrimidine Provide Interstrand Crosslinking" 246<sup>th</sup> ACS National Meeting, Indianapolis, Indiana. September'2013
- Haque, M.; Peng, X. "Pyridine Modification and Interstrand Crosslinking Study" Annual Poster Competition, Chemistry and Biochemistry, University of Wisconsin- Milwaukee (UWM)
- Yeo, C.; Haque, M. M.; Peng, X. "Modification of Pyrimidine Nucleosides via "Click" Chemistry" UWM Poster Competition, Chemistry and Biochemistry UWM
- "Teaching and Learning in College: Reflection on Theory and Practice" conducted by UWM, WI
- Training "Preparing Future Faculty (PFF)" faculty training course provided by Marquette University, WI, USA
- Training "Leadership: Developing Communication Strategies" ACS national meeting, Indianapolis, Sep'2013
- Training "Collaborating Across Boundaries" ACS national meeting, Indianapolis, Sep'2013
- "Graduate Student Proposal Development Training" conducted by UWM in 2013
- "Keys to Successful Grant writing" Provided by UWM in 2013